2009

Synaptic Protein Profiling in the Mammalian Brain

Elizabeth Heller

Synaptic Protein Profiling in the Mammalian Brain

A Thesis Presented to the Faculty of

The Rockefeller University

in Partial Fulfillment of the Requirements for

the degree of Doctor of Philosophy

by

Elizabeth Heller

June 2009

Synaptic Protein Profiling in the Mammalian Brain

Elizabeth Heller, Ph.D.

The Rockefeller University 2009

The mammalian central nervous system (CNS) contains billions of neurons each receiving thousands of synaptic inputs. Synapses are specified in part through the precise localization of synaptic proteins, yet it has not previously been possible to analyze the protein content of an individual class of synapses. In order to achieve this, we have used the BAC (bacterial artificial chromosome) transgenic approach to target particular neurons for expression of a given neurotransmitter receptor fused to an affinity tag. Immunohistochemistry of fixed brain tissue confirmed the correct localization of each synaptic fusion protein to the appropriate cell type and morphological structure. In order to isolate the synaptic proteins of interest, we developed a novel method, in which a classically purified crude synaptosome fraction was subject to size exclusion chromatography to enrich for synaptic protein complexes. The tagged synaptic protein complexes were then purified by immobilization with antibody-coated magnetic beads and the eluate analyzed by mass spectrometry.

This novel method was used to profile proteins at two classes of synapses. First, we purified the parallel fiber to Purkinje cell synapse of the cerebellum. We identified ~60 post-synaptic proteins, including those involved in phospholipid metabolism and signaling, which are major unrecognized components of this synapse type. Second, we analyzed inhibitory synapses of layer V pyramidal cells of the cerebral cortex, thereby accomplishing the first successful *in vivo* purification of an inhibitory synaptic protein complex. We identified ~12 proteins, many of which have been implicated in inhibitory synapse structure and function *in vitro*, such as the scaffolding protein, gephyrin. The result of this work provides a novel approach for detailed investigations of the biochemical complexity of CNS synapse types.

Acknowledgements

First and foremost, I would like to thank my thesis advisor, Pr. Nathaniel Heintz, for his support and enthusiasm. He has let me develop as a scientist by providing continual encouragement and advice. It would not have been possible to complete this project without his continually optimistic and unique insights into my data.

Many thanks to all the members of the Heintz lab for making my graduate experience so rewarding. Thank you to Jie Xing for help with BAC modification, Wendy Yang for HEK293 cell trasnfections, Dr. Joe Doyle for help with gel filtration and antibody purification, Dr. Joe Dougherty for help with Protein G immunopurification and immunohistochemistry, and Prerana Shrestha for providing primers and shuttle vectors. A special thank you to Pinar Ayata, for a tireless effort to optimize our immunopurification strategy. Thank you to Dr. Shiaoching Gong for providing BACs and advice on modification. Thank you to Katie Casas, an invaluable technician and friend. Finally, I especially thank Betsy Gauthier for her tireless work in genotyping and maintaining the mouse colonies and providing general laboratory support.

Thank you to Pr. Chiye Aoki of New York University Center for Neural Science and the members of the Aoki Lab for help with the immuno-electron microscopy. I learned a tremendous amount in a short time under Pr. Aoki's mentorship and guidance, and I am so grateful to have had this collaboration.

Thank you to Pr. Brian Chait, Dr. Ileana Cristea, Dr. Wenzhu Zhang and Kelly Molloy of the Laboratory of Mass Spectrometry and Gaseous Ion Chemistry, for their collaboration on this project. Their efforts were crucial to our research and required a long-term effort that I am most grateful for.

I owe many thanks to my thesis committee members, Pr. Cori Bargmann and Pr. A. James Hudspeth for their advice and support. Their guidance throughout my thesis research was crucial for homing in on the best experimental strategies. In addition, their advice on matters of career path and choice of postdoctoral lab were invaluable. A special thank you to Pr. Mary Kennedy for coming all the way from the west coast to participate as my outside committee member.

Thank you to Dean Sidney Strickland, Assistant Dean Emily Harms, Kristen Cullen, Marta Delgado, Michelle Sherman and Cristian Rosario for making my time at Rockefeller as easy and comfortable as possible.

A very special thank you to Dr. Fekrije Selimi, for her friendship and guidance. She truly took me under her wing when I first joined the lab, and taught me a tremendous amount in terms of experimental design, strategy and technique. Her strength and encouragement have helped me make important experimental decisions, and to stick with the research even when it seemed unlikely to ever succeed.

I want to thank my family and friends for their love and support. They have enthusiastically let me share my work with them and that has made my experience at Rockefeller so much sweeter. Thank you to Yael Steren for a critical reading of this manuscript. Thank you to James Herman for review of the manuscript and help with the presentation. A special thanks to Dr. Ilana DeLuca, for her advice on all things scientific and otherwise. A very special thanks to my mom and dad. They have been my biggest source of strength and my most enthusiastic supporters from the beginning.

Table of Contents

List of Figures

List of Tables

CHAPTER I. INTRODUCTION

Synaptic structure

Information processing in the nervous system depends on the electrophysiological and pharmacological properties of neurons and neuronal elements. The release of neuroactive substances at a specialized locus, the synapse, is the most common method by which neurons influence one another. Neuronal activity at the synapse is classified by whether it increases (excitatory) or decreases (inhibitory) the membrane potential of the postsynaptic neuron. Synapses can be broadly divided into two distinct classes: Type I (asymmetric) or Type II (symmetric), based on the relative density of material on the pre- and postsynaptic neuronal membranes (Figure 1). Although there are many exceptions, neurons making type I synapses typically have excitatory actions, while those making type II synapses have inhibitory actions [15]. All neurons receive both excitatory and inhibitory inputs, however, the postsynaptic location of these inputs is distinct. Broadly speaking, excitatory synapses are made on dendritic shafts, usually on dendritic spines, and not on somata or axons, while inhibitory synapses are generally found on proximal dendritic shafts, somta and axon initial segments [13, 17].

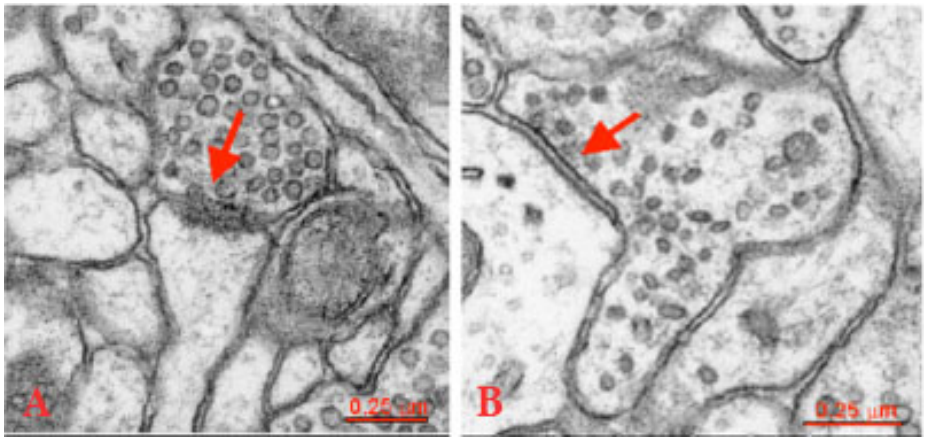

Figure 1. Gray's Type I and Type II synapses. (A) Type I (asymmetric; excitatory). The axons contain predominantly spherical vesicles and form synapses that are distinguished by a thickened, postsynaptic density. Scale bar = 0.22 µm. (B) Type II (symmetric; inhibitory) Axons contain clusters of vesicles that are predominantly flattened or elongated in their appearance. The pre-and postsynaptic membranes are more parallel than the surrounding non-synaptic membrane, and the synapse does not contain a prominent postsynaptic density [12]. Scale bar = 0.25 µm.

A large proportion of excitatory neurotransmission is due to pre-synaptic release of the neurotransmitter glutamate, an excitatory amino acid. Glutamate receptor (GluR) channels function in fast excitatory synaptic transmission, synaptic plasticity, and higher brain functions such as learning and memory [18-20]. Based on pharmacological and electrophysiological properties, GluR receptors have been classified into three major subtypes: α-amino-3-hydroxy-5-methyl-4-isozaxole propionic acid (AMPA), kainate, and N-methyl-D-aspartate (NMDA) receptors [15]. All these receptors are

components of tightly associated, multiprotein complexes. Components of these complexes regulate the synaptic targeting or removal from synaptic sites, local expression, signal transduction, and clustering of receptors [22].

Fast inhibitory neurotransmission is mediated by two different neurotransmitters in the nervous system: γ-aminobutyric acid (GABA) and glycine. GABA is the most abundant inhibitory neurotransmitter of the nervous system. Neurons that release this neurotransmitter form a diverse group that includes interneurons throughout the central nervous system (CNS). Inhibitory neurotransmission plays a key role in controlling neuronal activity. Accordingly, modulating the function of GABA receptors results in significant consequences for neuronal excitation [15]. In addition, these receptors are important for neural development and function, as demonstrated by gene deletion and mutation experiments [23]. GABA receptors are important therapeutic targets for a range of sedative, anxiolytic, and hypnotic agents, including a major class of anxiolytic molecules, the benzodiazepines. They are also involved in a number of CNS diseases, including sleep disturbances, anxiety, premenstrual syndrome, alcoholism, muscle spasms, Alzheimer's disease, chronic pain, schizophrenia, bipolar affective disorders, and epilepsy [24]. Given the importance of GABA receptors in the central nervous system it is noteworthy that their interacting

synaptic proteins have been exceedingly difficult to purify and identify. The molecular specialization at inhibitory synapses is an emerging field, and further work is likely to reveal novel therapeutics for treating a host of neurological and psychiatric conditions.

Study of synaptic proteins

Neurons interact with one another at the synapse, a specialized contact between the pre- and postsynaptic neuronal membranes. The postsynaptic membrane of excitatory synapses contains a highly organized structure called the postsynaptic density (PSD), which is composed of glutamate receptors, associated signaling proteins, scaffolding proteins, and cytoskeletal elements [25]. AMPA receptor-interacting proteins are located in the PSD, and analysis of this specialized structure is crucial to the study of synaptic specificity. In many neurons in the mammalian brain, including pyramidal neurons of the cerebral cortex and hippocampus and Purkinje cells of the cerebellum, the PSD is located on membrane protrusions called dendritic spines. The dimensions of the spine head are highly correlated with the size of the PSD and associated active zone, as well as synaptic strength [26]. Unlike excitatory synapses, inhibitory synapses lack a defined PSD and contacts are made on the dendritic shaft, the axon initial

segment, or soma [15]. Biochemical analysis of excitatory synaptic elements benefits from the ease of enrichment of PSD through several steps of centrifugation [27], while inhibitory synaptic complexes are not easily enriched [28, 29]. Because of this difference in synaptic structure the study of synaptic proteins has been largely biased in favor of excitatory synapses.

Classical PSD purification from the mammalian brain begins with homogenization followed by differential centrifugation and sucrose or Percoll gradient sedimentation to obtain synaptosomes [27, 30]. Synaptosomes are formed from the phospholipid layer of the cell membrane and synaptic proteins and they also contain the presynaptic machinery necessary for the uptake, storage, and release of neurotransmitters [27, 30]. Following synaptosome enrichment, the PSD is purified through extraction with nonionic detergents, such as Triton X-100 [27]. After purification, PSD proteins can be separated by SDS-PAGE (sodium dodecyl sulfate polyacrylamide gel electrophoresis) or two-dimensional gel electrophoresis, and major bands sequenced to identify abundant constituents such as postsynaptic density-95 (PSD-95), calcium/calmodulin-dependent protein kinase II (CaMKII), densin-180, synaptic GTPase-activating protein (SynGAP), and actin [31].

In recent years, large numbers of proteins in the PSD fraction or in immunoprecipitated GluR complexes have been detected by mass spectrometry (MS) methods, such as matrix-assisted laser desorption/ionization-time-of-flight (MALDI-TOF) MS and liquid chromatography (LC) coupled with tandem MS [32-38]. These experiments estimate the number of PSD proteins in the range of a few hundred to as many as one thousand. However, this number includes many potential contaminants, including mitochondrial and glial proteins. Furthermore, proteomic analysis of the PSD is likely to miss components that are in low abundance or only transiently associated with PSDs. Finally, MS data do not measure copy number of isolated proteins, which results in a misrepresentation of the structural importance of a given postsynaptic element. In order to address these issues, several experiments have aimed to accurately quantify the number of proteins in the PSD. For example, quantitative electron microscopy (EM) and immuno-EM were used to determine the size and molecular weight of the PSD, as well as protein stoichiometry and distribution within the PSD [39, 40]. Based on the accumulation of evidence from these studies it was possible to estimate the likely number of different proteins in the PSD. That is, if a PSD were composed solely of proteins of 100 kDa molecular mass, then there would

be 10,000 proteins, or 100 copies each of 100 different proteins, in an average PSD. This estimation reflects an important conclusion, based on EM combined with quantitative immunoblotting, that the average PSD contained 300 copies of the scaffold protein PSD-95 [41]. Thus, it is likely that the available MS data have misrepresented the protein complexity of the PSD due to false positives, false negatives, and the lack of stoichiometric analysis.

Estimates of the number of proteins in the PSD that rely on bulk separation from whole brain, even in the case of specific receptor co-immunoprecipitation, may falsely predict the protein complexity of the postsynaptic specialization. Because the results reflect only the total number and identity of all postsynaptic proteins, they might inaccurately depict the structure of the PSD. To improve the study of postsynaptic proteins it is crucial to enrich for only a subset of synapses, thus avoiding the additive effects of bulk separation. Targeting PSD analysis to particular synapses in only certain cell types or regions of the brain will result in more accurate and meaningful data. Moreover, a comprehensive approach, in which distinct PSDs are analyzed and then compared, will provide insight into the functional roles of such proteins, rather than simply brand them as generically postsynaptic. Single synapse-type analysis of the postsynaptic

specialization is necessary in order to uncover the nature and mechanisms of synaptic specificity.

Synaptic organization

In structuring a study of synaptic specificity, it is important to consider what is already known about neuronal circuitry.

Cerebral cortex

Classification of cerebral cortical neurons originated two centuries ago. Based on their appearance in Golgi-stained preparations, neurons were characterized according to their size, shape, and dendritic branching pattern [42]. The principal neuronal types of the cerebral cortex are the excitatory pyramidal cells, which project to distant targets, and the inhibitory non-pyramidal cells, which are the cortical interneurons. Excitatory neurons release glutamate as their neurotransmitter and exhibit a spiny dendritic morphology, while inhibitory neurons are smooth and release the neurotransmitter GABA. There are several types of spiny neurons including the pyramidal, star pyramidal, Betz, and spiny stellate cells [15]. Immunohistochemical analysis revealed further details of the different types of interneurons, generating a list of relatively simple but reliable markers

[43]. Projection neurons have been classified by the laminar position of their cell bodies, morphology, and electrophysiological characteristics [44], but there are relatively few neurochemical markers available for their identification. As illustrated in Figure 2, the laminar structure of the cortex depends largely on the distribution of these various cell types.

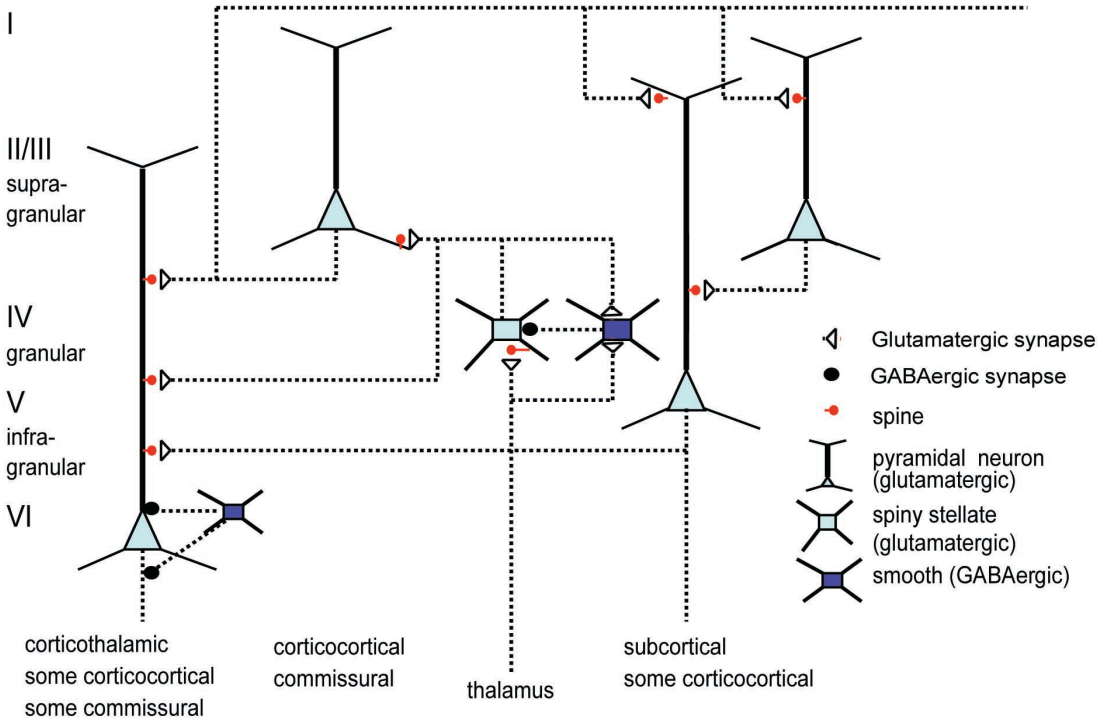

Figure 2. Canonical cortical circuitry. Afferent fibers originating from the thalamus terminate predominantly in layer IV. Here they glutamatergic spiny neurons, which are the main type of cortical input neuron, and GABAergic smooth neurons. Layer IV spiny neurons relay excitation to pyramidal cells in layer II/III. Within layer II/III, excitation is distributed laterally and vertically to other cortical layers, in particular to layer V. Layer II/III pyramidal neurons also contact each other. The output from the cortex is relayed from layer V to subcortical brain regions [13].

The major excitatory afferents to the cerebral cortex are from the dorsal thalamus, which is arranged in nuclei that correspond to single or multiple sensory modalities. The specific nuclei terminate mainly in layer IV and lower layers II/III, with a separate and less dense set of collaterals in upper layer VI. The non-specific (intralaminar) nuclei terminate densely in layers V and VI. Spiny stellate cells, the major cell type of layer IV, are the principal recipients of specific thalamocortical synapses. These cells in turn project to other layer IV spiny stellate cells and to layer II/III pyramidal cells [45]. The same cells that receive thalamic input are often projection neurons as well; these are usually pyramidal cells. The output from a pyramidal cell is specified by the layer in which the cell resides. The general rule of thumb is that cortico-cortical connections arise mainly from the superficial cortical layers and that subcortical projections arise from the deep layers [17, 46, 47]. Since the type of input to a cortical pyramidal neuron depends on its laminar location, synaptic molecules may be specific to the layer in which the postsynaptic cell is located. This laminar specificity would facilitate the process by which incoming afferents form synapses only on cells of a particular layer. A comparison of synaptic molecules based on the laminar location of the postsynaptic may provide insight into the molecular nature of such specificity.

Laminar specificity is only one marker of neuronal identity. Within a single cortical layer there exist distinct pyramidal cell populations. Genes that regulate the production of cortical cell types have been identified [48-50], but the molecular profile of a given neuronal cell type has remained largely unspecified. Because of both molecular and genetic properties, the pyramidal neurons of layer V prove particularly amenable to classification. The large size of layer V cell bodies facilitates electrophysiological studies, single cell RT-PCR, and cell filling to examine somatodendritic morphology [51]. Pyramidal neurons of layer V of the adult rodent cortex fall into two major classes, which can be distinguished by their projection site, morphology, and physiological properties. Type I cells project to the superior colliculus, spinal cord, or basal pons; they are characterized by thick tufted apical dendrites, and burst firing pattern. Type II layer V pyramidal neurons project to the contralateral hemisphere or to the ipsilateral striatum. Their apical dendrites are slender with fewer oblique branches that end without terminal tufts, usually in the upper part of layer II/III, and they do not exhibit burst firing [52]. Since these distinct projection neurons emerge sequentially within the very same layer, they constitute a unique model system to study cortical neuron specification [51].

Several techniques have been used to define protein markers of a given layer V pyramidal cell population. In one study, a population of back-labeled or GFP positive cell bodies from layer V transgenic lines was sorted and their gene expression profile was analyzed by microarray [53]. One marker of type I layer V pyramidal neurons, Otx1, is a transcription factor specifically expressed first in the ventricular zone and later in layer V and VI neurons [54]. Otx1 is required for the refinement of layer V connections to appropriate subcortical targets. In Otx1 null mice, the normally transient pattern of exuberant connections is retained into adulthood [55]. Comparison between several transcription factors reveals distinct subsets of pyramidal neurons within layer V, further subdividing Type I pyramidal neurons into distinct classes. For example, retrograde tracing showed that Er81 was expressed in corticospinal and corticocortical neurons, while Otx1 has been detected only in corticobulbar neurons [55]. The expression pattern of Otx1 exemplifies the use of genetic markers to define subpopulations of pyramidal neurons in cortex. In designing a study of synaptic specificity, it is useful to first target a genetically defined class of neurons. Analyzing only a particular synapse type within that class, which can be defined based on both synaptic morphology and the expression of particular synaptic markers, attains further specificity.

Cerebellum

The cerebellum is a widely studied neuronal structure that has undergone major elaboration throughout evolution and is essential for motor coordination [15]. The basic organization of the cerebellum is that of an interaction site between two distinct neuronal elements: the cerebellar nuclei and cortex. The cerebellar cortex receives afferents from the climbing and mossy fibers, while the main output is from the Purkinje cell (PC). Purkinje cell axons make inhibitory synapses on the projecting cells of the cerebellar nuclei [56].

The cerebellar cortex is divided into two distinct lamina: the molecular layer, which contains the Purkinje cells, and the granular layer. Climbing fiber afferents originate from a single brainstem nucleus, the inferior olive, and contact Purkinje cell dendritic spines in the molecular layer. Although each Purkinje cell receives only one climbing fiber input, each inferior olive cell axon branches to form several climbing fibers. The mossy fibers originate from a variety of CNS regions and synapse onto several granule cells, which increases the number of Purkinje cells stimulated by one mossy fiber axon. The granule cell axon projects towards the molecular layer where it branches to form a parallel fiber that contacts the dendrites of Purkinje cells. These fibers are found throughout the

molecular layer and synapse onto the Purkinje cell dendrites as well as the dendrites of all other cells in the cerebellum, excluding granule cells [14, 57].

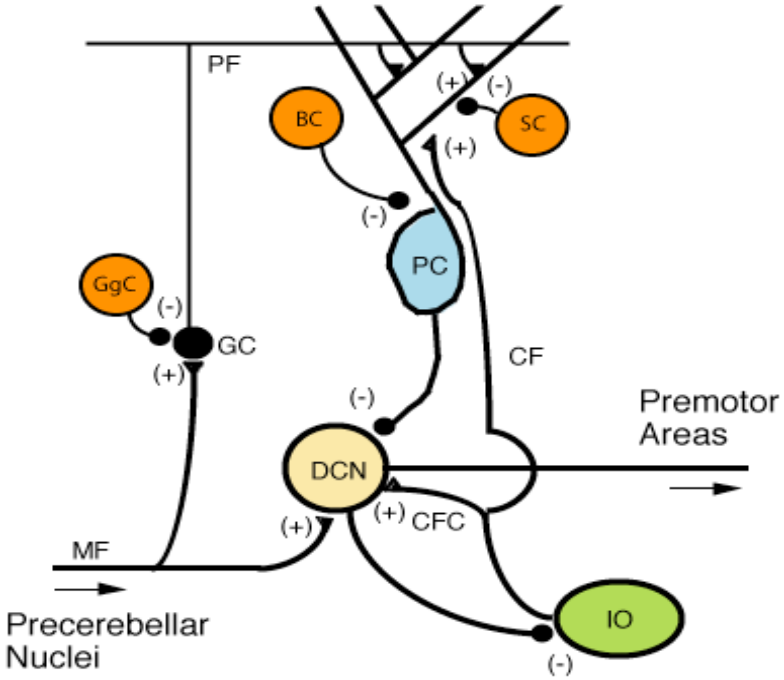

Figure 3. Diagram of the cerebellar circuitry. Climbing fibers, originating from the inferior olive, penetrate through the granular layer and make excitatory synapses onto Purkinje cell dendrites. Granule cell axons project through the Purkinje cell layer to form the parallel fibers in the molecular layer. Parallel fibers make excitatory contacts on the Purkinje cell dendrites. The basket and stellate cells make inhibitory synapses onto Purkinje cell bodies. Excitatory synapses are denoted by (+) and inhibitory synapses by (-). MF: Mossy fibers. DCN: Deep cerebellar nuclei. IO: Inferior Olive. CF: Climbing fiber. GC: Granule cell. PF: Parallel fiber. PC: Purkinje cell. GgC: Golgi cell. SC: Stellate cell. BC: Basket cell [14].

The cerebellum comprises several other cell types that can be distinguished in part based on their laminar specificity. The granular cell layer contains granule cells, which are contacted by mossy fiber axons, and Golgi cells, which form inhibitory synapses onto granule cells. The Purkinje cell layer contains basket cells, which make inhibitory synapses onto the somata and initial segments of Purkinje cells and spiny cells, which make inhibitory synapses onto Purkinje cell dendrites [56].

The architecture of climbing fiber and parallel fiber inputs demonstrates the disynaptic input to the Purkinje cell. Each Purkinje cell receives input from a single climbing fiber, whose afferents branch to "climb" along the entire dendritic tree, repeatedly contacting Purkinje cell dendritic spines. Morphologically, the presence of a climbing fiber synapse seems to exclude nearby parallel fiber-Purkinje cell contacts, thus dividing the dendrites into a central area covered by the climbing fibers, and a peripheral spiny portion that is contacted by parallel fibers. The distinct anatomy of these two excitatory inputs, as well as their molecular and functional differences (see below), make the Purkinje cell a useful model for the study of synaptic specificity.

Hippocampus

The hippocampus is located inside the medial temporal lobe of the cerebral cortex, forming part of the telencephalon (forebrain). It belongs to the limbic system and plays major roles in short term memory and spatial navigation [58]. As shown in part in Figure 4, the hippocampus and related areas comprise six distinct structures: entorhinal cortex (Ent), parasubiculum (PaS), presubiculum (PrS), subiculum proper (S), fields CA1-CA3 in Ammon's horn (Amn), and dentate gyrus (DG) [21, 58]. Neurons from layer two of the entorhinal cortex send afferents to the hippocampus via the perforant path, which terminate in the dentate gyrus and CA3. There is also a distinct pathway from layer 3 of the entorhinal cortex directly to CA1. Granule cells of the dentate gyrus send their axons, known as mossy fibers, to CA3. CA3 axons branch to form the Schaffer collateral, which contacts neurons of CA1. Pyramidal cells of CA1 send their axons to the subiculum and deep layers of the entorhinal cortex, thus completing the circuit. The hilus (h), also known as CA4, is a transition area between CA3 and the dentate gyrus and contains several types of pyramidal cells, including scattered mossy cells and basket cells. The mossy fibers make excitatory connections on the hilar basket cell neurons, which in turn form mainly inhibitory synapses on the granule cells. It has been suggested that the

reciprocal connection between granule cells and basket cells forms an inhibitory feedback circuit [59, 60].

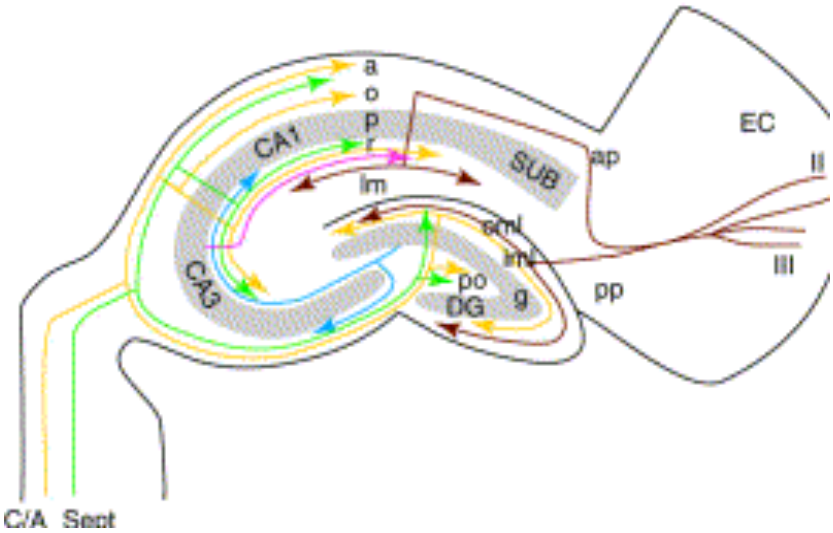

Figure 4. Connectivity in the hippocampus. Perforant path (pp) is shown in brown. Afferents from the entorhinal cortex (EC) innervate the outer molecular layer (oml) of the dentate gyrus (DG) and stratum lacunosum molecular (lm) layer of the cornu ammonis (CA). Mossy fiber (mf) pathway is shown in blue. These fibers connect DG with CA3. Schaffer collaterals (Sch) are shown in pink. Abbreviations: a, alveus; p, stratum pyramidale; SUB, subiculum. Circuitry diagram from review by T. Skutella and R. Nitsch [21].

In the hippocampus, as well as in the cerebellum and cerebral cortex, synaptic circuitry is further specified by the presence of particular neurotransmitter receptors. In particular, the properties and distribution of AMPA and GABA receptors is instructive to the study of synaptic specificity in these various brain regions.

Excitatory synapses: AMPA receptors

The glutamate receptor family comprises a diverse group of excitatory neurotransmitter receptors. Twenty-eight recombinant glutamate receptor (GluR) cDNAs plus a considerable number of splice variants thereof have been cloned. These 28 GluR genes include 22 members of the ionotropic subfamily as well as six metabotropic receptors [16]. A major class of glutamate receptors is the ionotropic AMPA receptor, which contains a cation-specific ion channel. The four AMPA receptor subunits, GluR1-GluR4, contain a large extracellular N-terminal domain, four hydrophobic membrane segments, and an intracellular C-terminus, as shown schematically in Figure 5 [61]. AMPA receptors are either homomeric or heteromeric oligomers composed of multiple subunits. Only two distinct subunits are usually found in a given receptor. Differences in the functional properties of native AMPA receptors result from variable assembly of these subunits. For example, all AMPA receptors are permeable to Na^+ and K^+, but homomeric receptors assembled from GluR2 subunits display little permeability to Ca^{++}, while heteromeric receptors assembled from GluR2, GluR3 or GluR4 are highly permeable to Ca^{++}. In this way, the GluR2 subunit is considered to regulate Ca^{++} permeability of the AMPA receptor [62].

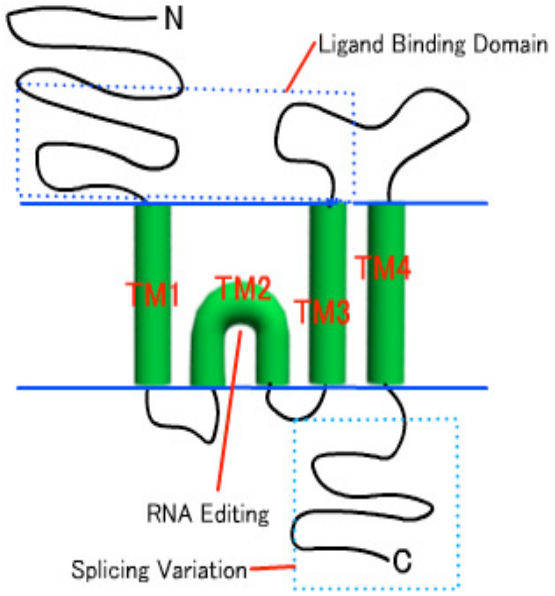

Figure 5. AMPAR subunit conformation. The four AMPA receptor subunits, GluR1-GluR4, contain a large extracellular N-terminal domain, four hydrophobic membrane segments, and an intracellular C-terminus. Variation in C-terminal sequences of the various subunits results in binding to differential interacting proteins [16].

Because differential subunit assembly results in distinct AMPA receptor functional properties it is of interest that each subunit is not uniformly expressed in all cortical laminae. Studies by *in situ* hybridization as well as immunohistochemistry have elucidated the expression patterns of GluR1-GluR4 subunits in the rodent brain, as summarized in Table 1 [7-9].

Differential receptor assembly will confer specific properties to the glutamatergic synapses in distinct areas of the brain.

Table 1. Distribution of AMPA receptor subunits.

region/cell type	GluR1	GluR2	GluR3	GluR4
cortex				
layer I		+++		++
layer II/III	+	+++	+	++
layer IV	+	+	+	
layer V	+	+++	+	
pyramidal n.	+	+++	++	
nonpyramidal n.	+++			
hippocampus				
CA1	+++	+++	+++	+
CA3	+++	+++	+++	+
DG				+++
striatum				
spiny n.	++	+++	+++	
aspiny n.	+++			
cerebellum				
purkinje cells		+++	+++	
granule cells		+++		++
golgi cells				
stellate/basket cells			+++	++
bergmann glia	+			++

Table 1: Distribution of AMPA receptor subunits. Immunohistochemical studies using antibodies against specific GluR subunits show that GluR1 and GluR3 expression is low in layers III and IV, while GluR4 expression is high in these layers. GluR2 is distributed uniformly. GluR1 immunoreactivity is low in layer IV, and GluR2/3/4c immunoreactivity is enriched highly in layers I, II, and III, low in layer IV, and enriched in deep layer V. Differences exist in other non-cortical structures as well [7-9].

GluRδ2

GluRδ was found as a novel member of GluR channel family by molecular cloning [63]. GluRδ2, the second member of the GluRδ subfamily, is selectively expressed in Purkinje cells of the cerebellum [64] and within cerebellar Purkinje cells (PCs), GluRδ2 is localized postsynaptically at parallel fiber-Purkinje cell synapses, but not at climbing fiber-Purkinje cell synapses [65]. With respect to the amino acid sequence identity, the GluRδ subtype is positioned between the NMDA and non-NMDA subtypes [64]. However, GluRδ2 has been referred to as an orphan receptor because it does not form functional glutamate-gated ion channels when expressed in transfected cells, either alone or with other GluRs, nor does it bind to glutamate analogs [64]. This receptor is predominantly expressed in Purkinje cells, and is crucial to cerebellar function. Mice that lack the gene that encodes GluRδ2 [66] display ataxia and impaired long-term depression (LTD), a putative cellular model of cerebellar information storage [67]. Despite their importance, the mechanisms by which GluRδ2 receptors participate in cerebellar function are not well understood.

AMPA receptor interacting proteins

The class of AMPA receptors present at a given synapse type is one determinant of synaptic specificity. Further refinement is achieved though the interactions of the receptor with postsynaptic molecules. Many AMPA receptor binding proteins have been discovered using the yeast-two hybrid system, confocal microscopy and electrophysiology. A description of a subset of such molecules follows below.

PSD95

The proteins found to interact with AMPA receptors can be roughly divided into two groups; those containing PDZ domains and those that interact through alternative sequences. The PDZ domain is a protein–protein interaction motif of approximately 90 amino acids [31]. The scaffolding function of PDZ domain-containing proteins is exemplified by PSD95. It contains three PDZ domains, an src-homology 3 (SH3) domain, and a guanylate kinase domain, which also acts as a protein interaction module. This multivalent structure allows PSD95 to arrange integral membrane proteins, including NMDA receptors, Shaker-type potassium channels, and the postsynaptic cell adhesion molecule, neuroligin. PSD95 also likely functions to recruit functional mediators such as synGAP and neuronal nitric oxide synthetase and anchoring proteins such as CRIPT [68]. PSD95

contains a number of domains to bring a variety of proteins into close proximity to each other, providing a means to cluster, anchor, and regulate receptors.

GRIP and APB

GRIP (glutamate receptor interacting protein) was the first protein shown to interact with AMPA receptors by the yeast two-hybrid system. Cloning of GRIP has demonstrated that it is a 130 kDa protein that contains seven PDZ domains, of which the fourth and fifth mediate binding to the C-termini of GluR2 and GluR3 [69, 70]. AMPA receptor binding protein (ABP) is related to GRIP in structure and shares 64–93% homology in the PDZ domains [71]. The functional implications of the interaction between GRIP and AMPA receptors remain unclear. GRIP was proposed to have a role in the clustering of AMPA receptors, even though not all clusters of AMPA receptors contain GRIP immunoreactivity [69]. In heterologous expression systems ABP and GRIP alone do not aggregate with GluR2 despite interacting strongly [71]. The fact that GRIP has multiple PDZ domains suggests that it may function in bringing proteins together which are important in synaptic localization and clustering, especially at certain times in development or activity.

Stargazin

The first transmembrane protein found to interact with AMPARs is stargazin, which is a member of a family of transmembrane AMPAR regulatory proteins (TARPs) that regulate the trafficking and physiology of AMPARs [72]. Stargazin is mutated in stargazer mice, which display absence epilepsy and lack functional AMPARs in cerebellar granule cells [73]. Stargazin plays two roles in trafficking AMPARs to synapses. First, stargazin can associate with all four AMPAR subunits and traffic them to the plasma membrane. Second, the extreme COOH terminus of stargazin can bind to PSD-95 and other PDZ proteins to mediate synaptic clustering of AMPARs [74]. The expression patterns for TARP family proteins in the central nervous system appear to cover all populations of neurons and glia that express AMPA receptors, suggesting a general role for this regulatory mechanism.

Homer

Homer acts as a postsynaptic adaptor protein that links multiple targets, including proteins involved in glutamate receptor signaling [75]. Alternative splicing results in two predominant forms of the Homer protein. The short Homer forms lack the carboxy-terminal domain and are expressed in an activity-dependent manner [76]. The long forms are constitutively

expressed and consist of two major domains: the amino-terminal target-binding domain, which includes an Enabled/vasodilator-stimulated phosphoprotein (Ena/VASP) homology 1 (EVH1) domain, and the carboxy-terminal self-assembly domain containing a coiled-coil structure and leucine zipper motif. These long Homer proteins form multimers that are thought to cluster other synaptic proteins, a process that may be required for synaptic function [77].

Shank

ProSAP/Shank molecules are early components of postsynaptic specializations present during synaptogenesis. They are efficiently targeted to synaptic sites and contain several protein-protein interaction domains, namely ankyrin repeats, an SH3 and PDZ domain, proline-rich stretches, and a SAM (sterile alpha motif) domain [78]. The AMPA receptor GluR1 subunit has recently been reported to interact directly with the PDZ domain of Shank [79] attaching the AMPAR complex to the other GluR complexes. GluRδ2 has been shown to interact with Shank protein by a yeast two-hybrid screen and this interaction was confirmed with co-immunoprecipitation experiments from synaptosomal plasma membrane (SPM) fractions collected from mouse cerebella [80].

The function of Shank protein in the cerebellum is likely related to the fact that it binds to Homer and GRIP [81]. It is known that Homer binds mGluR1α [82], whereas GRIP interacts with GluRδ2 [69]. Thus, Shank may organize mGluR1 and ionotropic AMPA receptors into a complex that is critical for cerebellar LTD induction. Immunoprecipitation experiments with SPM fractions of cerebella showed that GluRδ2 indeed forms a protein complex with Homer and mGluR1α *in vivo* [80]. These results suggest that GluRδ2 regulates cerebellar synapse dynamics through the interaction with Shank proteins.

Insertion of AMPA receptors into the synapse

The type and number of AMPA receptor subunits present at a given synapse is variable, and depends on experience and age of the organism [83]. AMPARs are characterized by their ability to move into and out of the postsynaptic membrane in a subunit-dependent fashion [84]. This AMPAR trafficking, which requires regulated endo- and exocytosis, depends not only upon receptor subunits and interacting proteins, but also upon the nature of synaptic stimulation or neuronal cell types [85]. It has been reported that receptors containing the GluR1-subunit are added to hippocampal synapses in an activity-dependant manner, a process that requires interactions between

GluR1 and group I PDZ domain proteins [86]. In contrast, GluR2/GluR3 receptors replace existing synaptic receptors in a constitutive manner dependent on interactions by GluR2 with NSF and group II PDZ domain proteins [87]. Experiments in the mouse barrel cortex demonstrated this process *in vivo*. Experience-dependent increases in synaptic strength at layer IV to II/III synapses were prevented by expression of a peptide that inhibits protein interactions with the intracellular C-terminal tail of GluR1 [88]. These findings suggest crucial differences in the regulation of AMPAR subunit delivery to synapses.

Differences in domain organization of GluR1 and GluR2 subunits can partially account for differences in their regulation. Two distinct C-terminal interaction domains on GluR2 have been characterized: an N-ethylmaleimide-sensitive fusion factor (NSF)-binding site and an extreme C-terminal PDZ-binding motif (ct-GluR2/3 PDZ). The PDZ-binding motif has namely, GRIP, ABP, and protein interacting with C-kinase 1 (PICK1) [89, 90]. GluR1, GluR3 and GluR4 do not interact with NSF, which has been shown to be involved in various membrane fusion events, such as exocytosis of synaptic vesicles.

The above examples illustrate differences in interacting proteins of the various AMPA receptor subunits; however, most studies to date have been

limited to a particular subunit in a particular cell type. Furthermore, with the exception of the TARPs, most interacting proteins have been characterized with respect to trafficking of receptor subunits, rather than their channel or signaling functions. While such studies suggest the existence of significant differences between the interacting proteins of individual subunits, a comprehensive approach to characterize such differences has not been carried out. By isolating distinct populations of GluR-containing synapses from the intact brain and analyzing their protein content, it will be possible to elucidate such differences on a larger scale.

Inhibitory synapses: $GABA_A$ receptors

The $GABA_A$ receptor is a ligand-gated chloride ion channel, comprising five subunits selected from a pool of 19 distinct gene products [91]. Subunit rules for $GABA_A$ receptor assembly have emerged, with the largest group of $GABA_A$ receptors being made up of $\alpha 1 \gamma 2$- and a β-subunit [10]. GABA neurotransmitter acts as an agonist, binding extracellulary between the α and β subunits and inducing a conformational change that increases permeability to chloride ions. Each subunit consists of a short extracellular C-terminus, a large extracellular N-terminus, four transmembrane domains (TM1-TM4) and a large variable-sized cytoplasmic loop between TM3 and TM4, as

illustrated in Figure 6. The intracellular loop contributes most of the cytoplasmic domain of the $GABA_A$ receptor and includes multiple protein-protein interaction sites for trafficking and postsynaptic scaffold proteins and phosphorylation sites for diverse serine, threonine and tyrosine kinases [11]. The amphiphilic TM2 domain provides the lining of the ion pore within the pentameric structure [10].

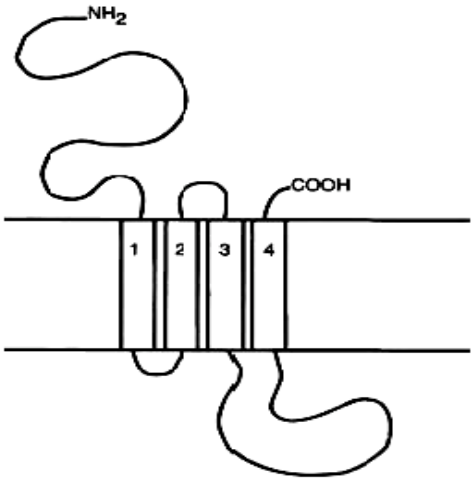

Figure 6. $GABA_A$ receptor subunit composition. Receptor subunits consist of four hydrophobic transmembrane domains (TM1-4), where TM2 is believed to line the pore of the channel. The large extracellular N-terminus is the site for ligand binding as well as the site of action of various drugs. Each receptor subunit also contains a large intracellular domain between TM3 and TM4, which is the site for various protein-protein interactions as well as the site for post-translational modifications that modulate receptor activity [10, 11].

Many substances act as modulators of $GABA_A$ receptors. Benzodiazepines are characterized by their anxiolytic, anticonvulsant, sedative, and amnesic effects. They enhance the GABA-induced chloride current by allosteric modulation, increasing the frequency of chloride channel opening. Barbiturates, on the other hand, prolong the duration of chloride channel opening [92]. The particular subunit composition of the receptor influences its pharmacological properties. For example, receptors composed of α1 or α2γ2β subunits respond to benzodiazepine and nonbenzodiazepine anxiolytics. In contrast, receptors lacking γ subunits, or those γ-subunits combined with α4 or α6, are generally insensitive to the benzodiazepines and related drugs [93].

The expression of $GABA_A$ receptor subtypes is spatially, regionally, and developmentally regulated, with individual subunits having distinct but overlapping expression patterns, as summarized in Table 2 [1-4]. In addition to differential subunit expression throughout brain regions, the $GABA_A$ receptor subunit composition varies between cell types and undergoes differential subcellular targeting. The α4, 5, 6, and δ-containing subunits are located extrasynaptically and are responsible for the tonic inhibitory current (persistent: long-term $GABA_A$ exposure at low concentrations), while all of the other $GABA_A$ receptor subunits—especially the γ2-subunit

containing $GABA_A$ receptors—are preferentially expressed on the synaptic site and are involved in phasic inhibition (transient: short-term GABA exposure at high concentrations) [94].

Table 2. Immunohistochemical distribution of GABA receptor subunits throughout the mammalian brain [1-4].

$GABA_AR$ Subunit	Cerebral Cortex	Cerebellum (PC layer)	Cerebellum (Mol. Layer)	Hippo-campus (CA1)	Hippo-campus (CA3)
α1	+++		+++	+++	+++
α2	++		++	++	+++
α3	+				+
α4	++			++	++
α5	+	+	++	+++	+++
α6			++		
β1	++	+	+	++	+++
β2	+++		+	+++	+++
β3	+++			+++	+++
γ1		+			
γ2	+++		+	+++	+++
γ3	+	++	++	+	+
δ	+++			+	+

The significance of the structural diversity of $GABA_A$ receptors remains unknown. One intriguing possibility is that the diversity in $GABA_A$ receptor subunits is important for mediating subcellular localization. Differential subcellular targeting of $GABA_A$ receptors is best documented in hippocampal pyramidal neurons. Here, receptors that contain α1 subunits seem to be equally distributed at all inhibitory synapses on the neuronal

somata, the proximal and distal dendrites, the spines, and the axon initial segments. By contrast, receptors that contain α2 subunits are preferentially localized at axo-axonic synapses on the axon initial segments [95, 96]. The subunit-specific targeting of $GABA_A$ receptors has also been analyzed in cerebellar granule cells, which express a range of subunits, including α1, α6, β2, β3, γ2 and δ; these subunits can assemble as α1/β2/3γ2 or α6/β2/3δ combinations [4]. Receptors that contain δ subunits are specifically targeted to extrasynaptic domains [97, 98], whereas receptors that contain the γ2 subunit are localized to synaptic sites on granule cells [99]. In addition to differential subcellular trafficking of the various GABA receptor subunits, receptor diversity likely confers specificity of GABA receptor interacting proteins.

$GABA_A$ receptor interacting proteins

While the structure and pharmacology of the $GABA_A$ receptors has been widely studied, analysis of the protein components of inhibitory synapses has been limited. Studies to identify $GABA_A$ receptor interacting proteins have relied heavily on *in vitro* methods, such as the yeast two-hybrid system and heterologous cell expression systems. A summary of some of the major interacting partners follows below.

GABARAP

GABARAP is a $GABA_A$ receptor-associated and microtubule-associated protein originally found in a yeast two-hybrid system using the intracellular loop of γ2 as bait [100]. GABARAP is enriched predominantly in intracellular membranes including the Golgi apparatus and postsynaptic cisternae. It is not found at significant levels within inhibitory synapses [101, 102]. Functionally, GABARAP acts as a linker protein between the microtubule protein tubulin and the intracellular loop of the γ2 subunit, which promotes the clustering of γ2-subunit containing $GABA_A$ receptors [100]. In addition, GABARAP has a basic N-terminus that can bind to tubulin and an ubiquitin-like C-terminal γ2 subunit-binding region. Additional binding partners of this multifunctional adapter molecule include gephyrin, GRIF-1, NSF, PRIP-1, and ULK1 [103, 104].

Gephyrin

Gephyrin was originally found to anchor glycine receptors to the postsynaptic cytoskeleton [105]. Like GABARAP, gephyrin is a tubulin-binding protein, and is involved in organizing postsynaptic $GABA_A$ receptors at inhibitory GABAergic synapses [28, 106]. Gephyrin is concentrated in the postsynaptic membrane at many inhibitory synapses and has been shown to colocalize with $GABA_A$ receptors [98], but a direct

interaction by co-immunopurification has not been demonstrated [107]. GABARAP binds gephyrin and $GABA_A$ receptors directly, suggesting that GABARAP might function as the adaptor for the association of these two proteins. Studies of the mechanisms for clustering of major $GABA_A$ receptor subclasses at GABA-dependent synapses have demonstrated that both the γ2 subunit of $GABA_A$ receptors and gephyrin are involved in receptor clustering, targeting and localization [108]. One study also revealed that synaptic $GABA_A$ receptors have lower levels of lateral mobility as compared to their extrasynaptic counterparts, and suggests a specific role for gephyrin in reducing the diffusion of $GABA_A$ receptors, facilitating their anchoring at inhibitory synapses [109]. Gephyrin is not required for clustering of all GABAR subunits, as demonstrated by a study of receptor localization in neurons of gephyrin deficient mice [110]. The punctate staining of $GABA_A$ receptor α1 and α5 subunits was unaltered in mutant mice, whereas the numbers of α2-, α3-, β2/3-, and γ2-subunit-immunoreactive synaptic sites were significantly reduced. This result demonstrates that additional mechanisms for $GABA_A$ receptor clustering may be revealed by studies of subunit-specific interacting proteins.

Profilin and mENA/VASP

Neuronal gephyrin has also been shown to interact directly with key regulators of microfilament dynamics, such as profilins I and IIa, and with microfilament adaptors of the mammalian enabled (mENA)/vasodilator stimulated phosphoprotein (VASP) family, including neuronal mENA. Profilin and mENA/VASP coprecipitate with gephyrin from brain tissue and cultured cells. Gephyrin, profilin, and Mena/VASP colocalize at synapses of rat spinal cord and cultivated neurons and in gephyrin clusters expressed in transfected cells [111]. Thus, mENA/VASP and profilin can contribute to the postulated linkage between receptors, gephyrin scaffolds, and the microfilament system and may regulate the microfilament-dependent receptor packing density and dynamics at inhibitory synapses.

GRIP-1

GRIP-1, which was first found in the glutamatergic system, also interacts with the γ2 subunit of $GABA_A$ receptors [69]. It exists in various splice forms, which localize differently in the intact brain. It has been reported that GRIP1a/b localized to both GABAergic and glutamatergic synapses in cultured hippocampal neurons [69, 70], but not to GABAergic synapses in the intact brain [70]. GRIP1c is found to be present at excitatory synapses in both cultured neurons and intact brain as demonstrated by

immunofluorescence and electron microscopy. Contrary to the other GRIP isoforms, it also localizes to GABAergic synapses, suggesting a possible role in GABAergic transmission. GRIP1c does not co-immunoprecipitate with any $GABA_A$ receptors from brain extract, but rather with AMPA receptors [112]. GRIP1c might interact with $GABA_A$ receptors through GABARAP or other $GABA_A$ receptor associated proteins to participate in $GABA_A$ receptor trafficking and clustering. Its exact role at inhibitory synapses remains unknown, although its ability to interact with GABARAP suggests that it may be involved in the synaptogenesis of inhibitory synapses or in the regulation of $GABA_A$ receptor function [104].

PRIP-1

PRIP-1 (Phospholipase-C related catalytically inactive protein type-1) is an inositol 1,4,5-trisphosphate-binding protein similar in domain organization to phospholipase C-δ1 but lacking PLC activity. PRIP-1 competitively inhibits the binding of the γ2 subunit of $GABA_A$ receptors to GABARAP, suggesting that this protein participates in $GABA_A$ receptor assembly and transport to the cell surface [113].

PLIC-1

Plic-1, is associated with the ubiquitination-degradation machinery (proteasome/ubiquitin-ligase), and contains a ubiquitin-like N-terminus that

is 33% identical to ubiquitin [114]. It also contains a carboxy-terminal ubiquitin-associated domain that interacts directly with the intracellular loop of the α- and β-subunit containing $GABA_A$ receptors. Functionally, Plic-1 facilitates $GABA_A$ receptor membrane insertion by increasing the half-life of intracellular receptor pools without modifying receptor endocytosis [114].

GRIF-1

GRIF-1 ($GABA_A$ receptor interacting factor-1) is a member of a coiled-coil domain family of proteins thought to function as adaptors in the anterograde trafficking of organelles utilizing the kinesin-1 motor proteins to synapses. GRIF-1, has been shown to interact with the intracellular loop of the β2 $GABA_A$ receptor subunit [115].

GODZ

The large intracellular loop of the γ2 subunit is rich in cysteine residues, which are absent from the equivalent domain of all the other subunits [24], suggesting that it might be a candidate for palmitoylation. Recent work demonstrated that the γ2 subunit is palmitoylated on five cysteine residues in the large intracellular loop [116, 117]. Palmitoylation is required for controlling both $GABA_A$ receptor clustering at synaptic sites and for the cell surface stability of these proteins in neurons. GODZ (Golgi-specific DHHC zinc finger protein) is a $GABA_A$ receptor interacting protein, which acts as a

neuron-specific thioacyltransferase that palmitoylates the intracellular loop of the γ2-subunit containing $GABA_A$ receptor [116].

AP2

Dynamin-dependent endocytosis is important in the regulation of cell surface levels of a number of integral membrane proteins and involves their recruitment into clathrin-coated pits by adaptor proteins. Internalization of $GABA_A$ receptors is mediated by clathrin-dependent endocytosis. Recent studies have demonstrated that $GABA_A$ receptors associate with the adaptin complex protein, AP2, and colocalize with AP2 in cultured hippocampal neurons [118]. This interaction is mediated by the $GABA_A$ receptor γ2 subunit, at a site specific for tyrosine phosphorylation [119], and the μ2 subunit of AP2 [120].

The above examples of GABAR- and AMPAR-interacting proteins demonstrate the importance of neurotransmitter receptor-interacting proteins in synaptic specificity and function. In addition, there are many proteins present at the synapse that do not directly interact with receptors, such as the neuroligin family of cell adhesion molecules. Further study of synaptic proteins will be crucial to broadening our understanding of the nervous system.

Synaptic specificity

The mechanism by which billions of neurons accurately form complex circuitries remains an area of intense study. It is clear that developmental genetic programs play a key role in establishing synaptic circuitry. Many molecules involved in axon guidance and synaptogenesis have been identified and their functions described [121, 122]. However, most of these molecules are found ubiquitously throughout the nervous system and are generic components of synapse formation, rather than markers of specific synaptic connections.

One feature necessary for synaptic heterogeneity is cell-type specific expression of a protein, and targeting of that protein to all presynaptic or postsynaptic sites made by a cell. On the presynaptic side, neurotransmitter synthetic enzymes and vesicular and plasma membrane transporters that determine the chemical nature of a synapse generally fall into this category. For example, the GABA synthetic enzyme glutamic acid decarboxylase (GAD65 and GAD67), the vesicular inhibitory amino acid transporter responsible for loading GABA into vesicles (VIAAT/VGAT), and the major plasma membrane transporter responsible for reuptake of GABA (GAT-1) are found at symmetric but not asymmetric synapses [123-126]. *In situ* hybridization studies indicate this is due primarily to expression by

GABAergic but not glutamatergic neurons [127, 128]. Thus, expression of a small number of genes or even a single gene can determine presynaptic transmitter phenotype.

In addition to genetic determinants, morphological constraints can direct specific synapse formation. Certain subcellular domains can be permissive for specific synapse types and even selective for particular receptors. For example, the axon initial segment of hippocampal pyramidal cells is permissive (or perhaps instructive) for formation of GABAergic but not glutamatergic postsynaptic sites [129]. Furthermore, GABAergic synapses on the axon initial segment have a higher density of the $GABA_A$ receptor $\alpha 2$ subunit than do GABAergic synapses on dendrites of the same cell, whereas the $\alpha 1$ subunit is more uniformly targeted to both somatodendritic and axon initial segment GABAergic synapses. The results demonstrate that granule cells receiving GABAergic synapses at a restricted location on their distal dendrites exhibit a highly compartmentalized distribution of $GABA_A$ receptor in their plasma membrane [130]. The mechanism by which this differential subunit distribution is maintained could be uncovered by subunit-specific co-immunoprecipitation from hippocampal pyramidal neurons, followed by mass spectrometric analysis to identify unique interacting partners.

Another excellent example of specific localization of inhibitory inputs is found in the Purkinje cells of the cerebellum. These neurons receive two sets of GABAergic inputs: the basket and stellate interneurons. The stellate cells selectively innervate Purkinje cell dendrites, while the basket cells project to the axon initial segment, forming the so-called 'pinceau synapses.' Using BAC transgenic mice in which basket cells were labeled throughout their development, pinceau synapse targeting was found to be achieved through multiple steps [131]. Basket axons first contact the Purkinje cell soma and subsequently migrate down towards the axon initial segment. This migration was found to be dependant on a gradient of neurofascin, a member of the L1 subfamily of immunoglobulin proteins, which was found to emanate from the AIS towards the soma and dendrite. The specificity of basket cell innervation demonstrates the subcellular targeting of inhibitory terminals and the role of guidance cues in development of synaptic specificity.

Even within a single class of synapse (a single presynaptic cell type making synapses onto a single postsynaptic cell type), there exists a heterogeneity of features. As in the case of $GABA_A$ receptor subunit distribution, differential GluR subunit distribution also contributes to synaptic specificity. One example is the variability in postsynaptic AMPA

type glutamate receptor content in hippocampal pyramidal neurons. Quantitative electron microscopy studies of CA3 Schaeffer collateral synapses onto CA1 neurons found 19% of synapses strongly immunoreactive, 67% moderately immunoreactive, and 17% immunonegative for AMPA receptors [132]. Immunonegative synapses were exclusively the smaller synapses [133]. Because every Schaeffer collateral synapse onto CA1 pyramidal cell spines contains NMDA receptors [133, 134], a subset of these synapses express only NMDA receptors and could correspond to the anatomical substrate for the electrophysiologically defined 'silent synapses' [135]. These observations suggest that the targeting mechanisms and the regulation of cell surface expression of these two types of glutamate receptors follow different rules. Indeed, recent studies indicate that, unlike NMDA receptors, AMPA receptors are highly mobile in a short time scale and that these dynamic properties are relevant for the observed heterogeneity in AMPA receptor synapse composition and could have an important part in mediating different forms of synaptic plasticity.

Although there are limited examples of non-receptor molecules for synaptic specificity in the mammalian nervous system, one important family of cell adhesion molecules, the neuroligins (NLs) have been shown to possess some differential synaptic expression. *In vitro* functional studies

indicate that an interaction between β-neurexin and neuroligins can trigger synapse initiation. Axons from pontine explants form presynaptic vesicle clusters when they come into contact with non-neuronal cells that express neuroligin-1 or neuroligin-2 [136]. Neuroligin family members are differentially spliced, an observation that gave rise to the idea that differential localization and binding between them could serve to specify synapses. For example, neuroligin-2 (NL-2) is a postsynaptic adhesion molecule that localizes at GABAergic synapses and triggers synapse formation by interacting with presynaptic neurexins [137, 138], while neuroligin-1 (NL-1) is targeted to glutamatergic synapses [136, 139]. This differential expression may play an important role in specifying distinct types of synapses and in determining a balance between neuronal excitation and inhibition [140]. The mechanisms responsible for the differential targeting of NL-1 to glutamatergic synapses and NL-2 to GABAergic synapses are unclear, although there is evidence that such specificity could arise from intracellular interactions with postsynaptic scaffolds [140]. However, the binding partners of NL-2 at GABA synapses are not known.

Further evidence for the role of synaptic adhesion molecules has proven elusive, even though Sperry's 1963 Chemoaffinity Hypothesis proposed their function in specifying synapses [141]. Recent work

identified SYG-1 in a genetic screen for *Caenorhabditis elegans* mutants defective in synaptic positioning [142]. In SYG-1 mutants, the neurons that synapse on vulval muscles fail to cluster synaptic vesicles at their normal sites of synaptic contact; instead, vesicles are clustered at several ectopic sites. Vesicle clustering (and thus presumably synapse formation) at the correct location requires SYG-1-dependent contact with vulval epithelial guidepost cells, which may express specific receptors for SYG-1. SYG-1 is likely to be the *C. elegans* orthologue of vertebrate NEPH1 [143], which are expressed in the CNS [144] and could play roles in synaptogenesis.

The experiments described above exemplify recent approaches to the study of synaptic specificity, a crucial area in the field of neurobiology. In order to elucidate the mechanism by which neurons form and maintain appropriate contacts it will be necessary to expand our understanding of synaptic proteins beyond neurotransmitter receptors and other ubiquitous components. Furthermore, neurobiological disease often results from cell- or synapse-specific dysfunction [67, 145], necessitating an experimental approach that can target only the relevant structures. In light of these issues, we have designed a novel approach to the study of the postsynaptic specialization in the adult mammalian CNS.

A novel approach to the study of synaptic specificity

Previous studies into the complexity of the postsynaptic specialization and the methods of generating synaptic specificity are limited in scope. A comprehensive approach to the nature of synaptic specificity in the mammalian brain has yet to be developed. To address this issue, we have developed a novel approach that is schematically outlined in Figure 7.

Cell-specific expression of a synaptic affinity tag

In order to purify a single class of synapse, it was necessary to first identify a transmembrane protein with synapse specific expression. As discussed above, this is likely to be a particular neurotransmitter receptor, as in the case of the cerebellar Purkinje cell molecule, GluRδ2, which is found only at the parallel fiber-Purkinje cell synapse. The cDNA for a particular receptor subunit was N-terminally fused to cDNA for an affinity tag, Venus, a YFP variant. Several groups have demonstrated that such a fusion protein, with GluR2 for example, is efficiently translated and inserted into the synaptic membrane as a functional receptor [83, 90]. The constructs were analyzed for expression and insertion into the membrane by transformation in heterologous cells followed by immunocytochemistry and immunoblotting.

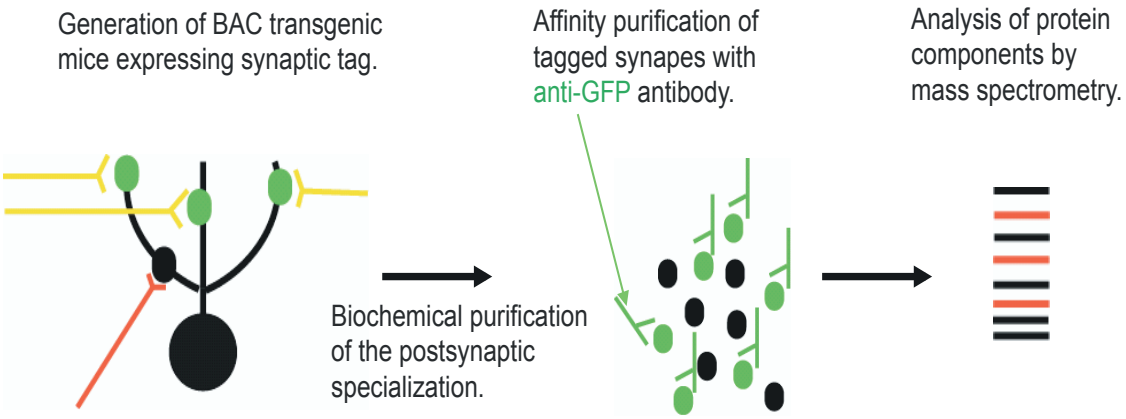

Figure 7. Novel scheme for tagging and isolation of particular synapses. Through a BAC transgenic approach, mice are generated that express a receptor-GFP fusion protein targeted to a single synapse type in a single cell type. After biochemical purification of the postsynaptic specialization, the tagged synaptic complexes are affinity purified using an anti-GFP antibody. Protein components are identified by mass spectrometry.

To generate transgenic mice with cell-specific expression of a given Venus-receptor fusion protein, we relied on the bacterial artificial chromosome (BAC) transgenic approach [6, 146]. In this system, the fusion construct is inserted into the BAC downstream of the complete regulatory elements of a gene endogenously expressed in the neurons of interest. The GENSAT [5] project has generated thousands of BAC lines that express

GFP alone. An analysis of the expression patterns of such lines was used to select BACs that drive expression only in neuronal subpopulations of interest. Figure 8 shows several of the BAC lines selected, and the particular cell types targeted by that line [5].

We relied on SDS-PAGE and immunoblotting of whole brain extract as well as immunohistochemistry of fixed brain sections to verify expression of the receptor-Venus fusion protein in the transgenic animal. In some cases immuno-electron microscopy was used to validate appropriate subcellular targeting of the receptor fusion protein to the correct synapse type. Once expression of the fusion protein in a given transgenic line was confirmed, we went on to biochemically purify the tagged synaptic protein complexes.

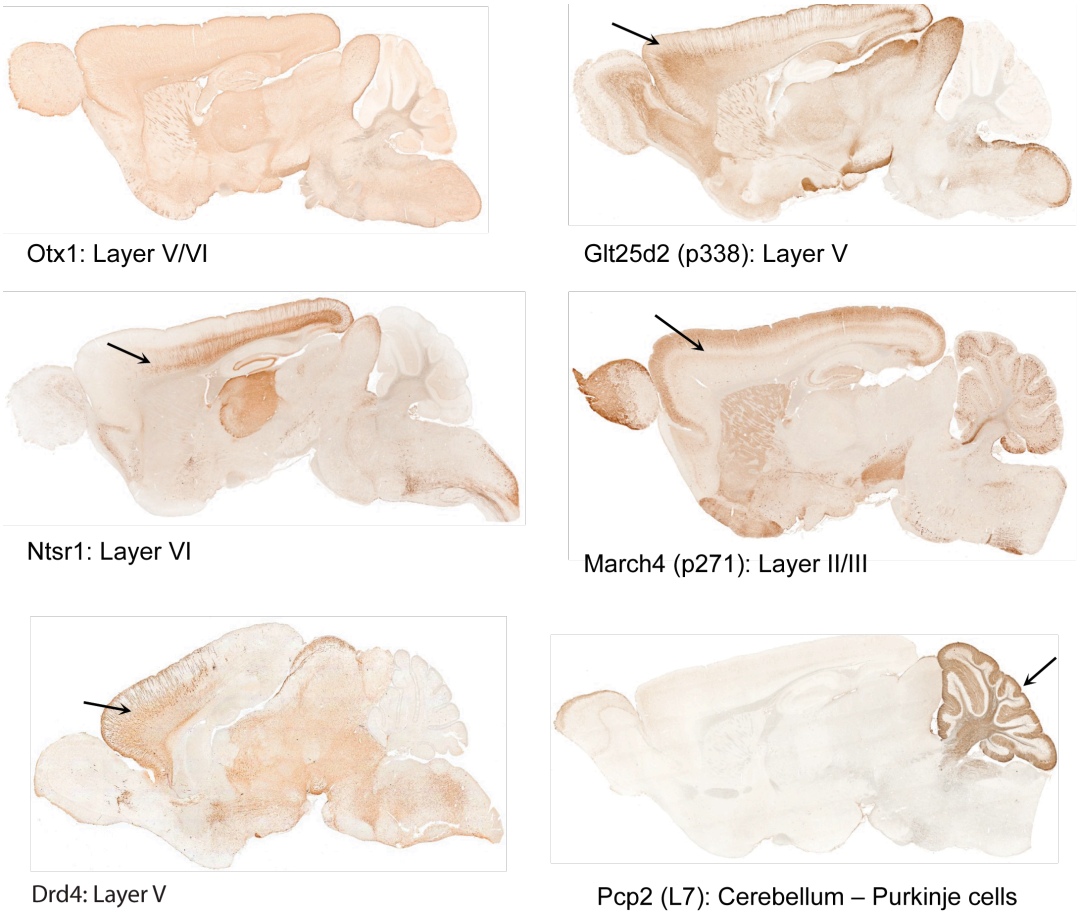

Figure 8. Selection of BAC drivers for cell type specific expression. Each BAC transgenic line expresses GFP in a particular cell type (arrow). By replacing the GFP coding region with that for a given protein of interest it is possible to target transgene expression to a particular neuronal cell population [5, 6].

Purification of targeted postsynaptic protein complex

In order to identify proteins at the synapse, rather than other subcellular compartments in which our fusion protein is localized, it was necessary to first enrich for the postsynaptic specialization. We relied on both classical methods of synaptosome and PSD enrichment [27, 147] and a novel method in which a crude synaptosome fraction was detergent solubilized and separated by gel filtration. An anti-GFP antibody immobilized on magnetic beads was used to affinity purify the tagged postsynaptic protein complex [148, 149]. The specificity of the isolated protein complex was verified by immunoblotting for known synaptic proteins (positive controls) and contaminants (negative controls). Once the specificity of the approach was confirmed, we relied on mass spectrometric analysis to identify the specific postsynaptic protein components.

Identification of synaptic proteins by mass spectrometry

Mass spectrometric analysis was done in collaboration with members of the Laboratory of Mass Spectrometry and Gaseous Ion Chemistry at The Rockefeller University. Synaptic protein samples were separated by SDS-PAGE and stained with MS compatible staining methods, such as Coomassie blue or zinc staining. Individual protein bands were excised,

reduced, alkylated and digested with trypsin. The peptide mixtures were analyzed by various MS techniques, such as single stage (*e.g.* MALDI-QqToF or MALDI-ToF), multiple stage (*e.g.* MALDI or ESI-IT) mass spectrometry, and on-line liquid chromatography tandem mass spectrometry (LC-MS/MS) to generate peptide sequence information [150, 151]. Such an approach has proved successful for analysis of the protein complex associated with the glutamate receptor, N-methyl-D-aspartate (NMDA) [32].

Isolation of specific synapses for a comparative study

The value of such a novel approach for discovering determinants of synaptic specificity lies in the fact that it enables the targeting of many different synapse types. In order to decipher which proteins are functionally important, it is crucial to make useful comparisons between different synaptic populations.

One such comparison is between excitatory and inhibitory synapses in the same cell type. We expect there to be a considerable number of distinguishing proteins between these two types of synapses since they are functionally distinct, their receptors are genetically unrelated, they occupy distinct cytochemical locations on the postsynaptic neuron and they arise from distinct presynaptic cell types. To discover such differences one could

examine the protein profiles of AMPAR-containing and GABAR-containing synapses in the same neurons (i.e. expressed under the same BAC control elements). Any general determinants of inhibitory versus excitatory synapse specificity should be found in several types of either excitatory or inhibitory synapses, but not both. Furthermore, such an experiment would result in the first successful biochemical purification of an inhibitory postsynaptic specialization, and would provide important insights into the nature and complexity of inhibitory synaptic structure.

Another interesting comparison is between excitatory synapses themselves. As summarized above, studies on AMPA receptor subunit localization in the mammalian CNS have demonstrated striking differences in the expression profiles of individual subunits. Inputs to the Purkinje cell (PC) of the cerebellum exemplify synaptic specificity, since all excitatory inputs to Purkinje cells contain the AMPA receptor GluR2 subunit, but only the parallel fiber to Purkinje cell (PF/PC) synapses contain the GluRδ2 receptor. Purification of the PF/PC synapse would uncover the molecules responsible for its unique structure and function. Another example of excitatory synaptic specificity lies in the laminar organization of AMPARs in the cerebral cortex. Pyramidal cells in the various cortical laminae receive distinct afferents and express unique but overlapping AMPAR

subunits. Furthermore, pyramidal cells within a given layer can be subdivided into genetically and developmentally distinct populations. A study to identify AMPAR interacting proteins specific to a given pyramidal cell population is possible due to the availability of BAC transgenic lines specific for pyramidal cell laminar expression (Figure 8). Purification and identification of such molecules will expand our understanding of such cell populations, and prove useful in defining CNS cell and synapse types.

We have successfully generated multiple BAC transgenic mouse lines, each expressing a receptor-Venus fusion protein in a cell type of interest. In addition, we have determined the technical limits of fusion protein expression in the adult mammalian CNS. Using a novel approach to study the postsynaptic specialization we have successfully purified both excitatory and inhibitory synaptic protein complexes from distinct cell types. A comprehensive analysis at the results of this work follows.

CHAPTER II. MATERIALS AND METHODS

Animals

All experiments using animals were performed according to protocols approved by the Institutional Animal Care and Use Committee at the Rockefeller University. All BAC transgenics were bred on the FVB background and littermates were used as wild-type controls.

Antibodies

The following antibodies were used at the indicated dilutions:

rabbit anti-GFP, Abcam #ab6556 (1/5000 for immunoblotting; 1/500 for immuno-electron microscopy); rabbit anti-GluRδ2, Millipore #AB1514 (1/2000); rabbit anti-GluR1, Abcam #ab31232 (1/1000); mouse anti-GluR2, Millipore #MAB397 (1/500); mouse anti-PSD95, Affinity Bioreagents #MA1-046 (1/2000); rabbit anti-PSD93 Millipore #AB5168 (1/100); mouse anti-NR2A, Millipore #MAB5216 (1/500); mouse anti-Gephyrin, BD transduction Laboratories #610584 (1/250); mouse anti-GABA(A) receptor β2/3, Upstate #05-474 (1/1000); rabbit anti- GABA(A) receptor α1, Upstate #06-868 (1/1000); rabbit anti- GABA(A) receptor α1, SantaCruz; rabbit anti- GABA(A) receptor α6, Millipore #AB5610 (1/2500); rabbit anti-GABA(A) receptor γ2, Millipore #AB6954 (1/1000); rabbit anti-Homer (H-

342), Santa Cruz #sc-15321 (1/200); mouse anti-BiP/GRP78, BD transduction Laboratories #610978 (1/500); mouse anti-COX (cytochrome oxidase subunit I), Molecular Probes #A6403 (1/20000); rabbit anti-RPTPmu, Abcam #ab23820; goat anti-BAIAP2, Abcam #ab15697; rabbit anti-delta2 Catenin, Abcam # ab11352; rabbit anti-mGluR1, Abcam #ab6439 (1/1000); guinea pig anti-VgluT1, Millipore (1/3000); guinea pig anti-VgluT2, Millipore (1/3000); mouse anti-GAD65/67, Stressgen bioreagents #MSA-225 (1/500); rabbit anti-GAD65/67, Millipore #AB1511 (1/400); mouse anti-Gephyrin, BD trasnsduction Laboratories #610585 (1/1000); rabbit anti-Gephyrin, Millipore #AB5725 (1/1000); goat anti-Neuroligin-2, Santa Cruz #sc-14089 (1/50); mouse anti-GRIP (1/500), BD transduction laboratories #611318.

Rabbit anti-Neph1 was a generous gift from Pr. Sumant Chugh.

The polyclonal anti-Gm941 antiserum was custom-generated by injection into rabbits of peptide #1, LKEGDEEIKSDIYTLC, and peptide#2, PLKVERAPAPHGPC. Bleeds were purified using protein G and then affinity-purified against peptide #2 (Green Mountain Antibodies, Burlington).

The polyclonal anti-MRCK gamma antibody was custom-generated by injection into rabbits of the following peptide: SERPRSLPPDPESESSPC. Bleeds were purified using protein G and then affinity-purified against the peptide (Green Mountain Antibodies, Burlington).

The goat anti-GFP antiserum was generated by injection in a goat of the full-length GFP (Green Mountain Antibodies) and was affinity-purified using a column made of Sepharose-4B resin coupled to full-length GFP.

The monoclonal anti-EGFP antibody (clone 19F7) was generated by immunizing mice with purified GST-EGFP fusion protein (Monoclonal Antibody Core Facility at Memorial Sloan-Kettering Cancer Center, New York). Several rounds of screening were performed to identify clones that functioned well in immunoprecipitation assays. Initially, monoclonal supernatants were tested by ELISA using 96 well plates coated with EGFP purified from transiently transfected 293T cells. Next, positive clones were screened in immunoprecipitation assays, again using the EGFP purified from transfected 293T cells. Finally, we identified four positive clones which strongly immunoprecipitated EGFP from cerebellar lysates from a transgenic mouse line expressing EGFP under the Pcp2 BAC driver.

BAC modification and transgenic mice

Pcp2-VGluRδ2

The cDNA encoding GluRδ2 together with the 3'UTR was amplified from cerebellar RNA, and placed in frame with a preprotrypsin signal sequence and Venus in a building vector based on eGFP-C2 (Clontech, Mountain View). The sequence encoding the tagged VGluRδ2 and the SV40 polyadenylation signal from the building vector were subcloned into the PL53.SC-AB shuttle vector. The Pcp2 containing BAC RP23-192G13 was then modified by homologous recombination using this shuttle vector and the two-step method [152]. Recombination boxes of 1kb were amplified from the BAC genomic DNA using the following primers: for box A, 5'TTGGCGCGCCGGTTCCACCCTCATGTTG3' AND 5'AGCTTTGTTTAAACCCGATCGCCCTGCACGTGGGG3'; for box B, 5'ATAAGAATGCGGCCGCCGGCTTTCTGGGTTCTGGC3' and 5'ATAAGAATGCGGCCGCGTTTAAGCCAGGTGTGGG3'. These recombination boxes allow the replacement of the Pcp2 ATG by the cDNA construct. Correct modification of the Pcp2 BAC was visualized by southern blot on BAC DNA digested by EcoRI, separated on 0.8% agarose gel and probed with P^{32}dATP-labeled box A. Pulsed-field gel electrophoresis was performed on BAC DNA digested by SpeI.

Otx1-VGABA$_A$ Rα1 and Otx1-VGluR1

The cDNA encoding GABA$_A$ α1 or GluR1 together with the 3'UTR was amplified from cortical RNA, and placed in frame with a preprotrypsin signal sequence and Venus in a building vector based on eGFP-C2 (Clontech, Mountain View, USA). The sequence encoding the tagged VGABA$_A$ α1 or VGluR1 and the SV40 polyadenylation signal from the building vector were subcloned into the PL53.SC-AB shuttle vector.

The Otx1 containing BAC RP23-106C14 was modified by homologous recombination using this shuttle vector and the two-step method [152]. Recombination boxes of 1kb were amplified from the BAC genomic DNA using the following primers: for box A, 5'AGCTTTGTTTAAACGCTAACAGCCGGGTGGAGGT3' and 5'TTGGCGCGCCGGCCTTCCAAAATCCCTAGA3'; for box B, 5'AAGGAAAAAAGCGGCCGCCTGAGGGGACATGCGAGA3' and 5'CGACGCGTACCTCAAACAACCCCCATAC3'. These recombination boxes allow the replacement of the Otx1 ATG by the cDNA construct.

Additional BACs modified with VGluR1

Several additional BACs were modified with Venus-GluR1. The sequence encoding VGluR1 and the SV40 polyadenylation signal from the eGFP-C2

building vector were subcloned into the pLD53.SC2 shuttle vector. The BAC was then modified by homologous recombination via a single 1kb box following previously published methods [146]. Using this modified shuttle vector it is not necessary to resolve the intervening sequences before injecting the modified BAC into oocytes for generation of transgenic mice.

March4 (RP23-216L22)

Box A 5'AGCTTTGTTTAAACCCCTCCAAGCAGCAAATA3'

5'TTGGCGCGCCGTCTTCTACCCCCACCCAAT3'

Glt25d2 (RP23-160M1)

Box A 5'AGCTTTGTTTAAACGTTCCGTAGCCGGCGGGAGG3'

5'TTGGCGCGCCTGTGCTGATCTTCCCACTCT3'

Ntsr1 RP23-314D14

BoxA 5'GCATCGTCTCCAGTCCGAACTGTGGATGTGG3'

5' CAGGTTGAACTGCTGATCAACAGATC3'

Drd4 RP23-134L4

BoxA 5'GATTCTGGCCCACGCCCGGCCAAC3'

5'CAGGTTGAACTGCTGATCAACAGATC3'

Correct modification of the each BAC was visualized by southern blot on BAC DNA digested by EcoRI, separated on 0.8% agarose gel and probed with P^{32}dATP-labeled box A.

A correctly modified BAC was purified by cesium chloride and DNA was then dialyzed in oocyte injection buffer for generation of transgenic mice. Integration of the BAC in the mouse genome was visualized by Southern blot using genomic DNA digested by EcoRI and box A as a probe.

Preparation of synaptic protein complexes and affinity purification

Pcp2-VGluRδ2 and Pcp2-EGFP

Ten cerebella from adult mice were used for the preparation of a crude synaptosome fraction P2 (based on previously published protocols [147]). The solution used as a homogenization and resuspension buffer contained 0.32M sucrose, 5mM HEPES, 0.1mM EDTA, pH=7.3 and a protease inhibitor cocktail (Sigma, Saint Louis). P2 was then solubilized 30 minutes at 4°C using a final concentration of 0.5% Triton X-100. The cleared solubilized fraction was separated by gravity flow on a gel-filtration column (Sephacryl S1000 Superfine, GE Healthcare) prepared using a solution containing 2mM $CaCl_2$, 132mM NaCl, 3mM KCl, 2mM $MgSO_4$, 1.2 mM NaH_2PO_4, 10mM HEPES and 0.5% Triton X-100, pH=7.4. 2 ml fractions were collected and aliquots were used for protein dosage using the BCA Protein assay kit (Pierce, Rockford). Calibration of the gel-filtration column was performed using the gel filtration HMW calibration kit (GE Healthcare).

Pooled fractions from the column were used for affinity-purification of tagged PSDs. Dynabeads M-270 epoxy beads (Dynal, Oslo) were conjugated using 15 mg of affinity-purified goat anti-GFP antibody per mg of beads [153]. 6 mg of beads were used for affinity-purification of pooled synaptic fractions from 10 cerebella during one hour at 4°C. Beads were then washed in 2mM $CaCl_2$, 300mM NaCl, 3mM KCl, 2mM $MgSO_4$, 1.2 mM NaH_2PO_4, 10mM HEPES and 0.5% Triton X-100. Purified complexes were eluted in 0.5N NH_4OH, 0.5mM EDTA for 20 minutes, dried and resuspended in the desired volume of protein electrophoresis sample buffer. Biochemical preparations and affinity-purifications were performed in parallel for each genotype starting with 10 cerebella each. For mass spectrometry analysis, samples from several successive experiments were pooled.

Otx1-VGABA$_A$Rα1 and Otx1-GFP

Five cortices from adult mice were used for the preparation of a crude synaptosome fraction P2 (based on previously published protocols [147]. The solution used as a homogenization and resuspension buffer contained 0.32M sucrose, 5mM HEPES, 0.1mM EDTA, pH=7.3 and a protease inhibitor cocktail (Sigma, Saint Louis). P2 was then solubilized 30 minutes

at 4°C using a final concentration of 0.1% Triton X-100. The cleared solubilized fraction was separated by gravity flow on a gel-filtration column (Sephacryl S1000 Superfine, GE Healthcare) prepared using a solution containing 2mM $CaCl_2$, 132mM NaCl, 3mM KCl, 2mM $MgSO_4$, 1.2 mM NaH_2PO_4, 10mM HEPES and 0.1% Triton X-100, pH=7.4. 2 ml fractions were collected and aliquots were used for protein dosage using the BCA Protein assay kit (Pierce, Rockford). Calibration of the gel-filtration column was performed using the gel filtration HMW calibration kit (GE Healthcare).

Pooled fractions from the column were used for affinity-purification of tagged inhibitory synaptic protein complexes. Dynabeads Protein G beads (Dynal, Oslo) were conjugated in 0.15M KCl for 2 hours at room temperature using 0.88 mg of mouse monoclonal anti-EGFP antibody per 1mL of beads. Following conjugation, the antibody was crosslinked to ProteinG with 20mM Dimethyl pimelimidate•2 HCl (Pierce, Rockford, IL) in 0.2 M triethanolamine, pH 8.0. The crosslinking reaction was stopped with 50mM Tris pH 8.0. 5mL of beads were used for affinity-purification of pooled synaptic fractions from 5 cortices during forty-five minutes at 4°C. Beads were then washed in 2mM $CaCl_2$, 300mM NaCl, 3mM KCl, 2mM $MgSO_4$, 1.2mM NaH_2PO_4, 10mM HEPES and 0.1% Triton X-100. Purified complexes were finally eluted in 1.0N NH_4OH, 0.5mM EDTA for 20

minutes, dried and resuspended in the desired volume of protein electrophoresis sample buffer. Biochemical preparations and affinity-purifications were performed in parallel for each genotype starting with 5 cortices each. For mass spectrometry analysis, samples from several successive experiments were pooled.

Otx1-VGluR1 and p338-VGluR1

Between three and five cortices or ten hippocampi from adult mice were subject to biochemical purification of PSDs as described above for Pcp2-VGluRδ2, the only difference was that the final concentration of Triton X-100 was 1.0%. for cortex and 0.1% for hippocampus. This percentage Triton X-100 was used for solubilization of the crude synaptosome fraction and in the gel filtration buffer. Pooled fractions from the column were used for affinity purification as described above for Otx1-VGABA$_A$ α1.

Protein extracts for expression analysis

Total protein extracts from cerebellum, hippocampus or cerebral cortex were prepared by homogenizing the tissue and incubating for 30 minutes at 4°C in a buffer containing 50 mM Tris-Cl, 150mM NaCl, 0.1% SDS, 0.5% sodium deoxycholate and 1% NP-40 complemented with a protease inhibitor

cocktail. The homogenate was then sonicated and centrifuged 30 minutes at maximum speed to provide the supernatant for western blot analysis.

For immunoprecipitation experiments, the homogenate was incubated in 50 mM Tris-Cl, pH=7.4, containing 1% Triton X-100 final for 30 minutes and then centrifuged at maximum speed. The supernatant was affinity-purified using anti-GFP coated dynabeads for one hour at 4°C. Beads were washed with 50 mM Tris-Cl, pH=7.4, containing 1% Triton X-100 and immunocomplexes eluted for western blot analysis.

Immunoblotting

Protein samples (dissolved in NuPAGE LDS sample buffer, Invitrogen, Carlsbad) were separated on 4-12% NuPAGE Bis-Tris gels (Invitrogen). Proteins were then transferred using the semi-dry method (SD transfer cell, Biorad, Hercules) on Immobilon-P PVDF membrane (Millipore, Bedford). Antibodies were diluted in 5% milk/PBS/0.2% Tween-20. Secondary antibodies were conjugated to horseradish peroxidase (Pierce) and detection performed using a chemoluminescent substrate.

Immunofluorescence

Mice were perfused transcardiacally using 4% paraformaldehyde in phosphate buffer saline pH=7.4 (PBS), then 10% sucrose in PBS. Brains were incubated for 3 days in 30% sucrose in PBS. 25 mm-thick cerebellar or whole brain saggittal sections were cut using a freezing sliding microtome.

For detection of VGluRδ2 or VGluR1, sections were incubated in 0.3% H_2O_2 in PBS at 4°C, washed in PBS and preincubated in 4% normal donkey serum in PBS. Incubation with the goat anti-GFP antibody (diluted 1/25000 in 1% normal donkey serum/PBS/1% Triton X-100/0.1%fish gelatin) was performed overnight at 4°C. Immunolabeling was detected using a biotinylated anti-goat secondary antibody (1/5000 in PBS/1% Triton X-100/0.1% fish gelatin) followed by amplification using streptavidin-HRP (1/500) and TSA-FITC (Perkin Elmer, Waltham, USA). All washes were performed in PBS/1% Triton X-100.

For detection of the other antigens by immunofluorescence, sections were incubated overnight with the corresponding antibodies and mouse anti-calbindin (1/5000, Swant, Bellinzona) diluted in 1.0% normal donkey serum/PBS/0.2% Triton X-100. Immunolabeling was detected using an Alexa-488 conjugated anti-rabbit or anti-goat and a Rhodamine-RedX

conjugated anti-mouse or Cy3 conjugated anti-guinea pig. All washes were performed in PBS/0.2% Triton X-100. Pictures were taken using a LSM 510 laser scanning confocal microscope (Carl Zeiss, Thornwood, USA).

Immuno-electron microscopy of Otx1-VGABA$_A$Rα1

Preparation of brain tissue for light and electron microscopy

Transcardial perfusion was achieved by using a peristaltic pump to control the flow-rate of the perfusates to 10 ml/min. The perfusates were the following: (1) 10 - 50 ml of saline containing heparin (1000 U/ml), over a 1-min period; (2) 200 ml of 0.1 % glutaraldehyde, mixed with 4.0% paraformaldehyde in 0.1M phosphate buffer (pH 7.4). During the subsequent hours, the brain was cut into 40 mm-thick sections using a vibratome. On the 5th hour following the perfusion, the sections were immersed in PBS containing 1.0% sodium borohydride, so as to terminate residual cross-linking activities of glutaraldehyde.

GAD65/67 and GFP Double Immunocytochemistry

Double labeling using 3,3-diaminobenzidine HCl (DAB) and silver-intensified colloidal gold (SIG) immunolabeling techniques were employed to mark the colocalization of Venus-GABA$_A$ α1 and GAD 65/67 [154].

Cortical sections were incubated for 30 min in PBS-azide containing 1% bovine serum albumin (BSA) (Sigma Chemicals, Saint Louis) to block any nonspecific immunolabeling. These sections were then incubated on a shaker for 3 days at room temperature in PBS-BSA-azide containing primary antibodies, goat anti-GFP (1:500) to recognize Venus-$GABA_A$ α1, and rabbit anti-GAD65/67 (1:400). This and all subsequent incubation steps were followed by 3 rinses in PBS (pH 7.4).

For immunolabeling with DAB, sections were incubated in biotinylated rabbit anti-goat IgG, recognizing the anti-GFP antibody, or in goat anti-rabbit IgG, recognizing the anti-GAD antibody (Vector Laboratories, Burlingame), both at dilutions of 1:100 (15 mg/ml) for 1 hour at room temperature. Sections were then incubated in the ABC solution (Elite Kit, Vector Laboratories, Burlingame) for 30 min and immersed in PBS (pH 7.4) containing 0.3% DAB with 0.03% hydrogen peroxide (H_2O_2) . Reaction time was approximately 10 minutes for all sections. The peroxidase reaction was terminated by immersing sections in PBS. This ICC reaction was followed by multiple postfixation steps to preserve ultrastructure: 1.0% glutaraldehyde with PBS (pH 7.4) for 10 min; 0.1% osmium tetroxide (in 0.1 M PB) for 30 minutes; and 1.0% uranyl acetate in 70% ethanol, overnight.

For Venus-$GABA_AR\alpha1$ immunolabeling with SIG, sections were incubated for 16 hour in ultrasmall (0.8 nm) gold-conjugated rabbit anti-goat IgG (Electron Microscopy Sciences, Washington) at a dilution of 1:100 in PBS--BSA (pH 7.6). Sections were then postfixed in 1.0% glutaraldehyde with PBS (pH 7.4) for 10 min to cross-link antibodies to antigenic sites prior to silver intensification. To prepare sections for silver intensification, sections were rinsed for 1 min in 0.2 M citrate buffer (pH 7.4). These sections were immersed into the silver intensification reagent (Silver IntensEM Kit, Amersham, Buckinghamshire) at room temperature for 12 min. The duration of the silver intensification step differed by no more than 10 s among the samples. Silver intensification was terminated by rinsing sections in citrate buffer. These sections were stored in PBS overnight. On the following day, sections were incubated in 0.1% osmium tetroxide (in 0.1 M PB) for 30 minutes; and 1.0% uranyl acetate in 70% ethanol, overnight.

Images used for were captured digitally using a CCD camera attached to a JEOL 1200XL electron microscope at a magnification of 40,000-60,000x and spanning and area of 29 mm^2.

Mass spectrometry analysis

Pcp2-VGluRδ2 and Pcp2-EGFP

Following immunopurifications, the isolated proteins were resolved by 1-D SDS-PAGE and stained with Coomassie Blue (GelCode Blue, Pierce). Each entire gel lane (from the 30 and 50 mice preparations) was cut into 1mm sections, and proteins were digested with 12.5ng/μL sequencing grade modified trypsin (Promega, WI, USA). The resulting peptides were extracted on reverse phase resin (Poros 20 R2, PerSeptive Biosystems), eluted with 50% (v/v) methanol, 20% (v/v) acetonitrile and 0.1% (v/v) trifluoroacetic acid, and subjected to MALDI QqTOF MS and MALDI ion trap MS/MS analyses as described [155, 156].

Otx1-VGABA$_A$ α1 and Otx1-EGFP

Following immunopurifications, the isolated proteins were subject to analysis by LC-MS/MS based on previously published protocols [157]. Immunopurified proteins were resolved by 1-dimensional SDS-PAGE and stained with E-Zinc™ Reversible Stain Kit (Thermo Scientific, Rockford, IL). Each gel lane was divided into two sub-samples. One sub-sample contained all visible gel bands, and the other contained the gel regions between the bands. Proteins in each sub-sample were subjected to in-gel

digestion by incubating with Trypsin (Roche, Indianapolis). The resulting peptides were extracted onto POROS 20 beads (20 um C18 particles) (Applied Biosystem, Foster City). For liquid chromatography-tandem mass spectrometry analysis, peptides were eluted and loaded onto a 360 μm o.d. x 75 μm i.d. analytical column (6 cm long) packed with C18 5 μm sized resin (YMC Co., Kyoto) constructed with an integrated electrospray emitter tip (New Objective, Woburn). Peptides were then eluted from the analytical column directly into a LTQ-Orbitrap mass spectrometer (Thermo Scientific, Waltham) using a HPLC solvent delivery system at a flow rate of 300nl/min.

The acquired LC-MS/MS data were used to identify proteins present in each sub-sample by searching a mouse protein sequence database using the GPM database search program(http://prowl.rockefeller.edu /tandem/thegpm_tandem.html). Mass tolerances used in the database searching were 15 ppm and 0.4 Da, respectively, for measured masses of peptide ions and for fragmentation ions. The cut-off score (the logarithm of E-value) of -4 is used for identified proteins. Combining two lists of proteins from the two sub-samples of each IP sample, we generated a list of proteins present in the IP sample. To obtain proteins uniquely present in the fusion protein IP sample, we subtracted proteins found in control IP sample from the list of proteins found in the fusion protein IP sample.

CHAPTER III. PROTEIN PROFILE OF THE PARALLEL FIBER-PURKINJE CELL SYNAPSE

Introduction

The Purkinje cell (PC) is the major output neuron of the cerebellum, and its function is crucial for motor development and learning [56, 158]. The major excitatory afferents to PCs are from the granule cell (GC) axons, as they branch to form the parallel fibers (PFs), and from the climbing fibers (CFs), whose axons originate from the inferior olive. Purkinje cells selectively express GluRδ2, a glutamate receptor subtype. Although GluRδ2 protein is initially found at spines at CF/PC and PF/PC synapses, it localizes to PF/PC synapses after approximately P21 [65]. Because PFs form synapses on distal dendrites of Purkinje cells, a unique sorting mechanism must be necessary for GluRδ2 to bypass CF synapses, which are located at proximal dendrites. The mechanism of such a sorting mechanism remains unknown, as it has not previously been possible to molecularly dissect the two synapse types.

Dysfunction of the cerebellum typically manifests as motor discoordination, or ataxia, a common symptom of various neurological disorders in mice and humans. Recent studies have also demonstrated the involvement of the cerebellum in non-motor functions and in

neuropsychiatric disorders such as dyslexia, autism, and attention deficit hyperactivity disorder [159-161]. The lack of specific pharmacological tools with which to manipulate GluRδ2 has hampered studies to determine its function. However, studies of mutant mice, such as GluRδ2$^{-/-}$ and *hotfoot*, in which the receptor fails to traffic to the PC surface, have provided some clues to the function of GluRδ2 in Purkinje cells. Ataxia is easily recognized as the phenotype of these mutations, but it is not accompanied by a macroscopic morphological anomaly in the cerebellum [66]. LTD of Purkinje cells from these mice is impaired *in vitro*, and they perform poorly on tasks that measure behavioral plasticity [161, 162].

The factor(s) that activates GluRδ2 receptors, a ligand, a receptor subunit or associated messengers have yet to be found. A better understanding of GluRδ2 function may provide key insights into normal and abnormal cerebellar functions and thus permit the development of novel approaches for therapy of particular neurological disorders. To this end we targeted the parallel fiber-Purkinje cell (PF/PC) synapse for affinity purification and protein analysis by mass spectrometry using our novel approach.

Results

Generation of mice with tagged parallel fiber – Purkinje cell synapses

In order to specifically purify PF/PC synapses, we used molecular cloning to generate a synaptic tag consisting of GluRδ2 fused to an N-terminal affinity tag, Venus (a YFP variant). This fusion protein was tested for proper expression and trafficking to cell surface in transfected HEK293 cells (Figure 9A). Immunoblot analysis of protein extract obtained from transfected HEK293 cells shows that an anti-GluRδ2 antibody recognizes the fusion protein at the expected size, approximately 140 kDa, and that it is absent from cells transfected with Venus alone. The GluRδ2 antibody recognizes the wild-type protein in cerebellar protein extract at a size smaller than the fusion protein by the expected 27 kDa. Immunocytochemistry using an anti-GFP antibody shows surface expression of the Venus-GluRδ2 (VGluRδ2) fusion protein in transfected HEK293 cells under non-permeabilizing conditions, with the N-terminal Venus was localized extracellularly.

In order to express VGluRδ2 selectively in Purkinje cells of the cerebellum we relied on the BAC transgenic approach [6]. Homologous recombination was used to insert the transgene cDNA into the Pcp2 BAC [5], which contains the regulatory sequences for Purkinje

Figure 9. Construction of a fusion between Venus and GluRδ2 (VGluRδ2). (A) Venus was fused on the N-terminal extracellular part of GluRδ2 (top left panel). A GluRδ2 positive band was detected in protein extracts from VGluRδ2 transfected HEK293 cells, but not in extracts from Venus-transfected cells (bottom left panel). The band was at the expected size (about 140 kDa), larger than the endogenous GluRδ2 detected in cerebellar extracts. Immunofluorescence using an anti-GFP antibody detected the extracellular Venus in VGluRδ2 transfected cells in non-permeabilizing conditions (red, right panels), showing the proper topography of the tagged receptor. (B) The correct modification of the Pcp2 BAC with the VGluRδ2 construct was checked by Southern blot (left panel, probe shown in C, BAC DNA digested with EcoRI) and pulsed-field gel electrophoresis (right panel, BAC DNA digested with SpeI), before injection in mouse oocytes. (C) Schematic diagram of the BAC containing the Pcp2 gene, which is expressed specifically in Purkinje cells. The VGluRδ2 cDNA was placed at the level of the Pcp2 ATG. The arrow indicates the regulatory region. Scale bar = 0.5 Kb.

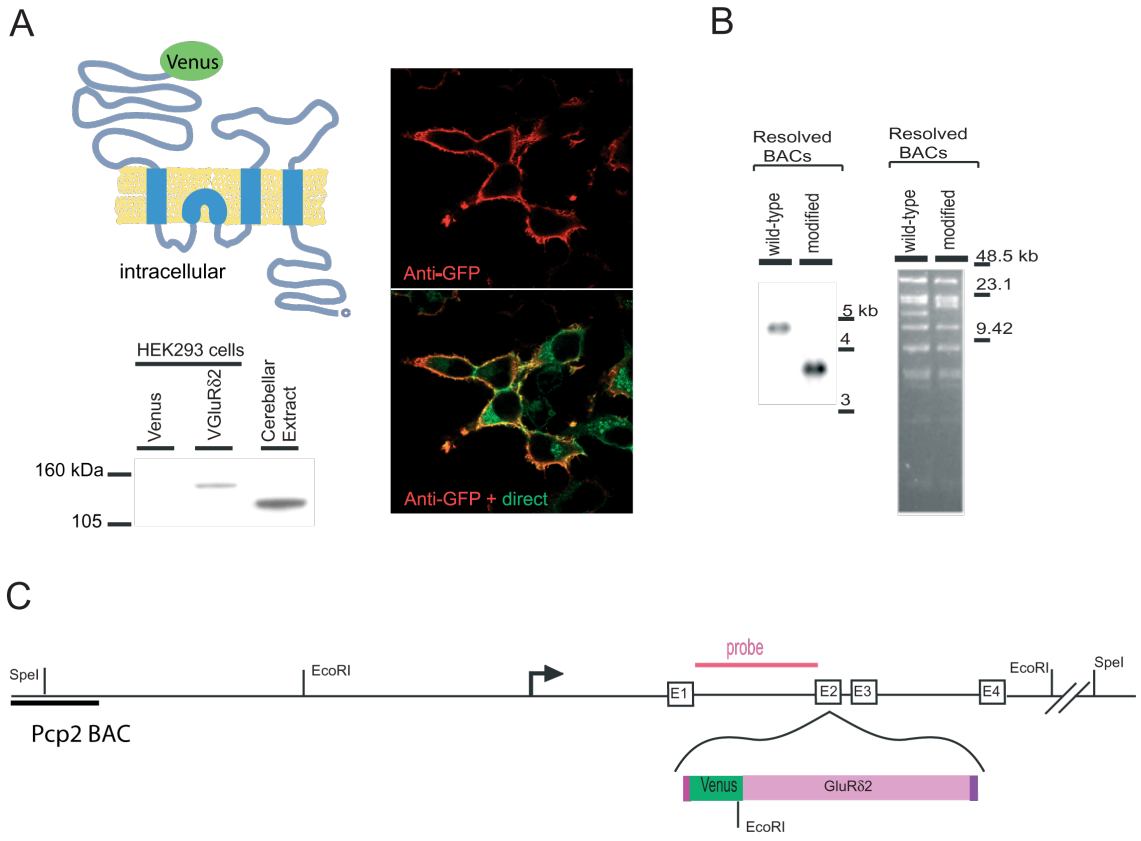

Figure 9. Construction of a fusion between Venus and GluRδ2 (VGluRδ2).

cell specific expression (Figure 9C). Pulsed-field gel electrophoresis (PFGE) and Southern blotting (Figure 9B, left panel) were used to verify correct modification of the Pcp2 BAC. The VGluRδ2 cDNA was placed at the level of the Pcp2 ATG, to disrupt expression of the endogenous BAC Pcp2 protein (Figure 9C).

We next generated transgenic mice containing the Pcp2-VGluRδ2 construct, by surgical implantation of injected fertilized oocytes into a pseudopregnant female. PCR screening and Southern blot analysis was used to determine both the presence and copy number of transgene insertion into the genome (Figure 10A). The VGluRδ2 construct contains an additional EcoR1 restriction site, which enables the probe to distinguish the wild-type Pcp2 sequence from that contained within the BAC transgene. Using this probe against whole genome DNA digested with EcoR1 reveals a second band present only in the transgenic mice that corresponds to the Pcp2-VGluRδ2 transgene.

Figure 10. Tagging the parallel fiber/ Purkinje cell synapse in transgenic mice. (A) Southern blot was used to identify transgenic mice having integrated the Pcp2 BAC containing VGluRδ2. (B) VGluRδ2 expression was detected using an anti-GFP antibody that recognizes Venus, on immunoblots from total protein extracts of transgenic (Tg) versus wild-type (Wt) cerebella. * indicates a non-specific band. (C) Both VGluRδ2 and GFP were affinity-purified using a goat anti-GFP antibody from 1.0% Triton X-100 cerebellar extracts from wild-type (Wt), Pcp2/VGluRδ2 (Vδ2) and Pcp2/EGFP control (GFP) mice, as shown by probing the immunoblots with an anti-GFP antibody (left). VGluRδ2 specifically copurified the endogenous GluRδ2, as shown by probing the same blot with an anti-GluRδ2 antibody (right). (D) Immunofluorescence on cerebellar sections using an anti-GFP antibody shows the specific localization of VGluRδ2 in the molecular layer (ml) and somata of Purkinje cells (Pcl) of Pcp2/VGluRδ2 mice. Soluble GFP is detected in the molecular layer, dendrites, somata and axons of Purkinje cells in sections from Pcp2/EGFP mice. Abbreviations: ml, molecular layer; Pcl, purkinje cell layer; gcl, granule cell layer. Scale bars: upper panels= 200 μm; lower panels= 50 μm.

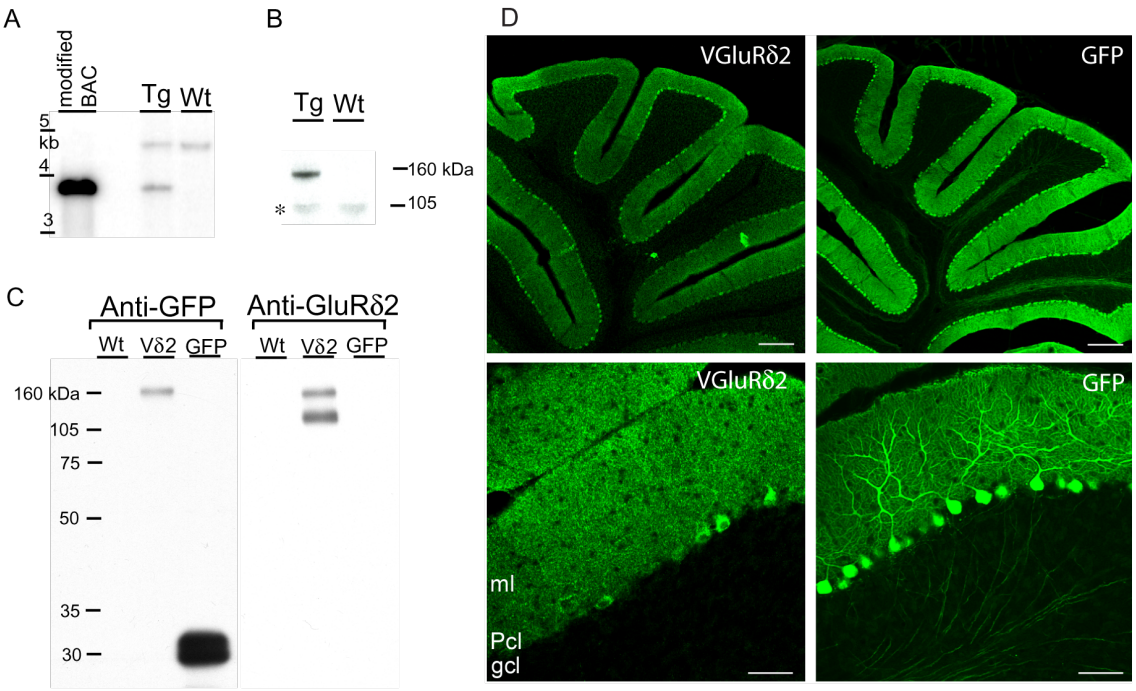

Figure 10. Tagging the parallel fiber to Purkinje cell synapse in transgenic mice.

To confirm expression of the VGluRδ2 transgene, we collected cerebellar protein extract from both wild-type and Pcp2-VGluRδ2 transgenic mice. SDS-PAGE followed by immunoblotting with anti-GFP antibody revealed the presence of the fusion protein at the expected size only in the transgenic mouse (Figure 10B). The VGluRδ2 fusion protein was successfully affinity purified from cerebellar protein extract using a goat anti-GFP antibody (Figure 10C). SDS-PAGE followed by immunoblotting with an anti-GFP antibody of the affinity-purified material from Pcp2/VGluRδ2 mice showed

the fusion protein present at the correct size. This band was absent from material purified from wild-type mice. In addition, we used a mouse expressing soluble GFP in Purkinje cells under the same Pcp2 BAC as a positive control for the affinity purification conditions. The band corresponding to VGluRδ2 is absent, while the soluble GFP band is present at the expected size. Immunoblotting of this same material with an anti-GluRδ2 antibody reveals both the VGluRδ2 fusion protein and the wild-type GluRδ2 protein, demonstrating their successful oligomerization. Neither GluRδ2 nor VGluRδ2 co-purified from the wild-type or Pcp2-GFP extract, demonstrating the specificity of the affinity purification method (Figure 10C, right). Immunohistochemistry on fixed cerebellar brain tissue confirmed correct expression and localization of VGluRδ2 in Pcp2/VGluRδ2 mice (Figure 10D). Immunofluoresence using an anti-GFP antibody shows the expected localization of VGluRδ2 in the molecular layer and somata of Purkinje cells. The expression pattern in Pcp2/VGluRδ2 shows soluble GFP present in all layers of the cerebellum, including Purkinje cell dendrites and axons (Figure 10D, right).

Biochemical purification of tagged parallel fiber – Purkinje cell synapses

In order to verify the presence of VGluRδ2 in the synaptic fraction from cerebellar extract, we used a previously published synaptosome enrichment method, which relies on centrifugation of homogenized cerebellar material through a discontinuous Percoll gradient [147]. The synaptosome fraction was enriched in endogenous synaptic proteins such as GluRδ2, $GABA_AR$ α1, and PSD95 (Figure 11, left panel), while BIP, an endoplasmic reticulum marker, and COX, a mitochondrial marker, were selectively absent. VGluRδ2 was detected in the synaptosome-enriched fraction and was distributed amongst the different fractions in the same manner as wild-type GluRδ2. Finally, electron microscopy of the synaptic fraction (3) showed enrichment for synaptosomes.

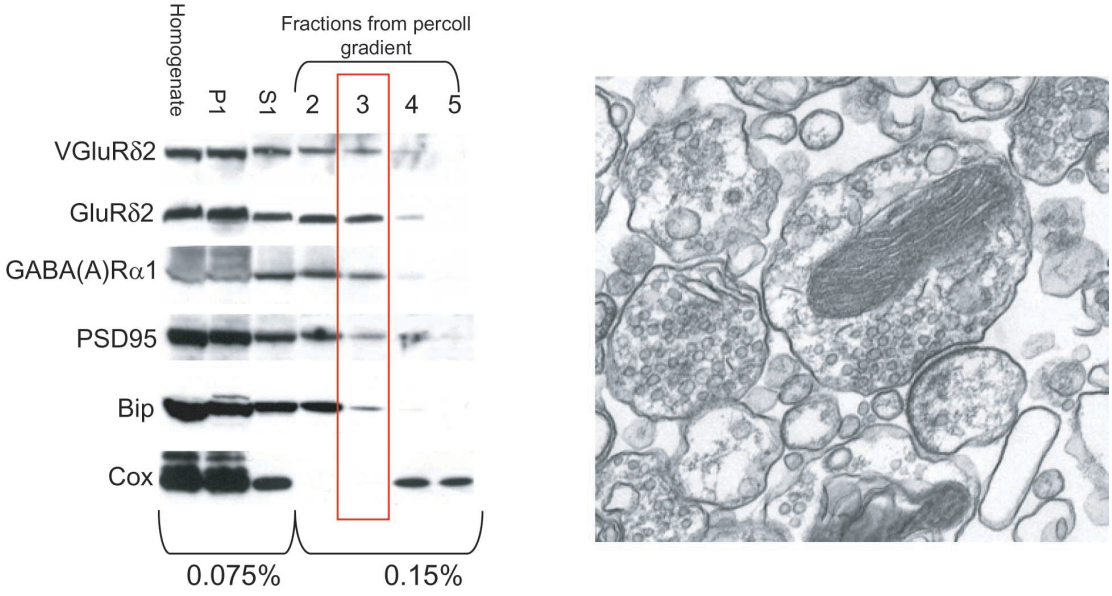

Figure 11. Synaptosome preparation from VGluRδ2 cerebella using the Percoll gradient method. Fractions were probed for excitatory synapse markers (GRID2, PSD95), the inhibitory synapse marker GABA(A)Ra1, the endoplasmic reticulum marker BIP and the mitochondrial marker COX. VGluRδ2 was detected using an anti-GFP antibody. The right panel shows an electron micrograph from fraction 3 enriched in synaptosomes.

Using the classical purification approach we successfully isolated the tagged parallel fiber to Purkinje cell synapse. However, the material losses from this method were substantial. In order to more efficiently enrich for the postsynaptic density (PSD) we developed a novel method based on solubilization of a crude synaptosome fraction followed by size exclusion chromatography to enrich for the PSD protein complex (Figure 12).

Figure 12. VGluRδ2 is detected in excitatory synaptic fractions using a new purification method. **(A)** We prepared a crude synaptosome P2 fraction that was solubilized in 0.5% Triton X-100. The extract was then separated on a Sephacryl S1000 gel filtration column. Calibration of the column indicated that protein complexes smaller than 669 kDa (arrow in B) were resolved after fraction 10.
(B) Protein concentration was measured for every fraction collected. **(C)** 0.1% in volume of every fraction was assayed for the presence of excitatory synapse markers (GluRδ2, GLUR2, PSD95, NR2A), inhibitory synapse markers (GABA(A)Rβ, GABA(A)Rα1), the endoplasmic reticulum marker, BIP and the mitochondrial marker, COX. VGluRδ2 was detected using an anti-GFP antibody. The red rectangle outlines the "excitatory synaptic" fractions enriched for synaptic markers and pooled for subsequent affinity-purification of PF/PC PSDs.

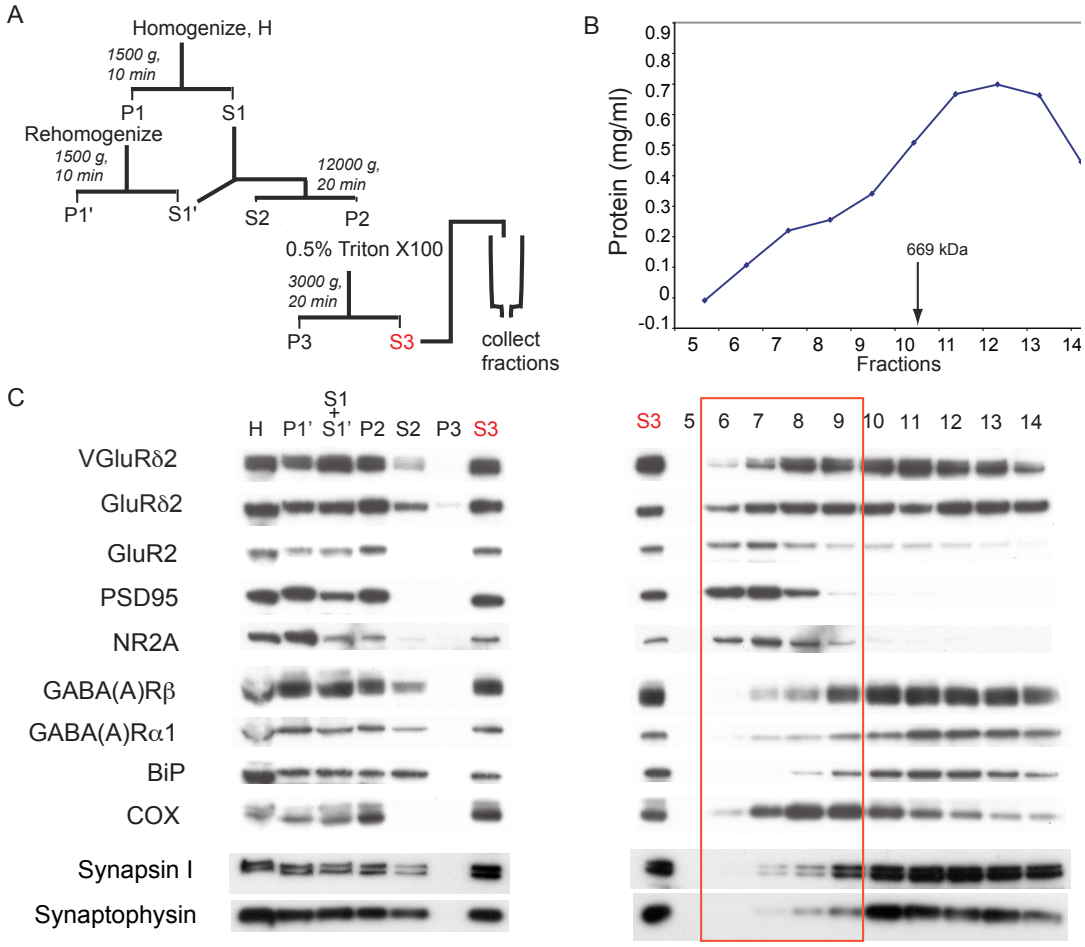

Figure 12. VGluRδ2 is detected in excitatory synaptic fractions using a new purification method.

Homogenization of the cerebella from 10 mice was followed by differential centrifugation to enrich for synaptosomes (Figure 12A). This fraction, P2, was solubilized with Triton X-100 at a final concentration of 0.5% to isolate the large, detergent-insoluble protein complexes, including the PSD. To determine the relative enrichment of synaptic and non-synaptic proteins, each fraction was analyzed by SDS-PAGE and immunoblotting (Figure 12C). The solubilized crude synaptosome fraction (S3) is enriched for synaptic proteins such as neurotransmitter receptors (GluR2, GluRδ2, NR2A, $GABA_AR\beta2$, $GABA_AR\alpha1$), scaffolding proteins (PSD95), and presynaptic markers (synapsin I, synaptophysin). In addition, VGluRδ2 was enriched in S3 like wild-type GluRδ2, suggesting correct trafficking of the fusion protein to the postsynaptic specialization.

Next, the solubilized extract, S3, was fractionated using a Sephacryl S1000 gel filtration column (Figure 12C, right). In this way we were able to separate large protein complexes (>669 kDa), which elute in the early fractions and likely correspond to the PSD, from those that elute later and are at a size consistent with intracellular protein complexes. Protein concentration was measured for each fraction eluted from the column (Figure 12B). Excitatory PSD proteins were selectively enriched in fractions 6-9 (Figure 12C, red triangle), as shown by the distribution of

GluRδ2, GluR2, NR2A and PSD95, as well as the fusion protein, VGluRδ2. On the other hand, inhibitory postsynaptic proteins ($GABA_AR\beta2$, $GABA_AR\alpha1$), presynaptic elements (synapsin I, synaptophysin), and endoplasmic reticulum (ER) marker (BIP) eluted later in the column and were largely excluded from the early, synaptic fractions. In this way we successfully isolated a sample that is selectively enriched for excitatory PSDs from cerebellum.

This pool of PSDs was next subject to affinity purification using a goat anti-GFP antibody, to isolate the tagged parallel fiber to Purkinje cell synapses (Figure 13). Co-immunopurified proteins were collected from the excitatory synaptic fractions of both Pcp2-VGlurδ2 mice and Pcp2-GFP mice, which served as a positive control for affinity purification conditions, and a negative control for co-immunopurification of synaptic proteins. Immunoblot analysis of the purified materials using an anti-GFP antibody indicated successful precipitation of the VGluRδ2 fusion protein or soluble GFP (Figure 13A).

Figure 13. Affinity-purification and protein profiling of the parallel fiber/Purkinje cell PSDs. (A) Synaptic fractions from Pcp2/VGluRδ2 animals were affinity-purified using magnetic beads coated with anti-GFP antibody (VGluRδ2). In parallel, control purifications were performed on preparations from Pcp2/eGFP transgenic mice (GFP). 0.025% of the inputs and flow-throughs (FT) and 25% of the affinity-purified samples (IP) were assayed by Western blot using an anti-GFP antibody and showed immunoprecipitation of both VGluRδ2 and GFP, respectively. **(B)** The same blot was probed for different synaptic markers and the mitochondrial protein COX, showing specific co-purification of synaptic markers localized to the PF/PC synapse. **(C)** Electron microscopy electron dense structures reminiscent of PSDs on the surface of the magnetic beads used for affinity-purification of Pcp2/VGluRδ2 extracts. **(D)** Proteins from the affinity-purified VGluRδ2 PSDs were separated by SDS-PAGE and stained with Coomassie Blue before mass spectrometry analysis. **(E)** Mass spectrometry identified 65 different proteins in the complexes purified from Pcp2/VGluRδ2 mice. These proteins could be classified into 11 functional categories. The number of proteins from each category is indicated in parenthesis.

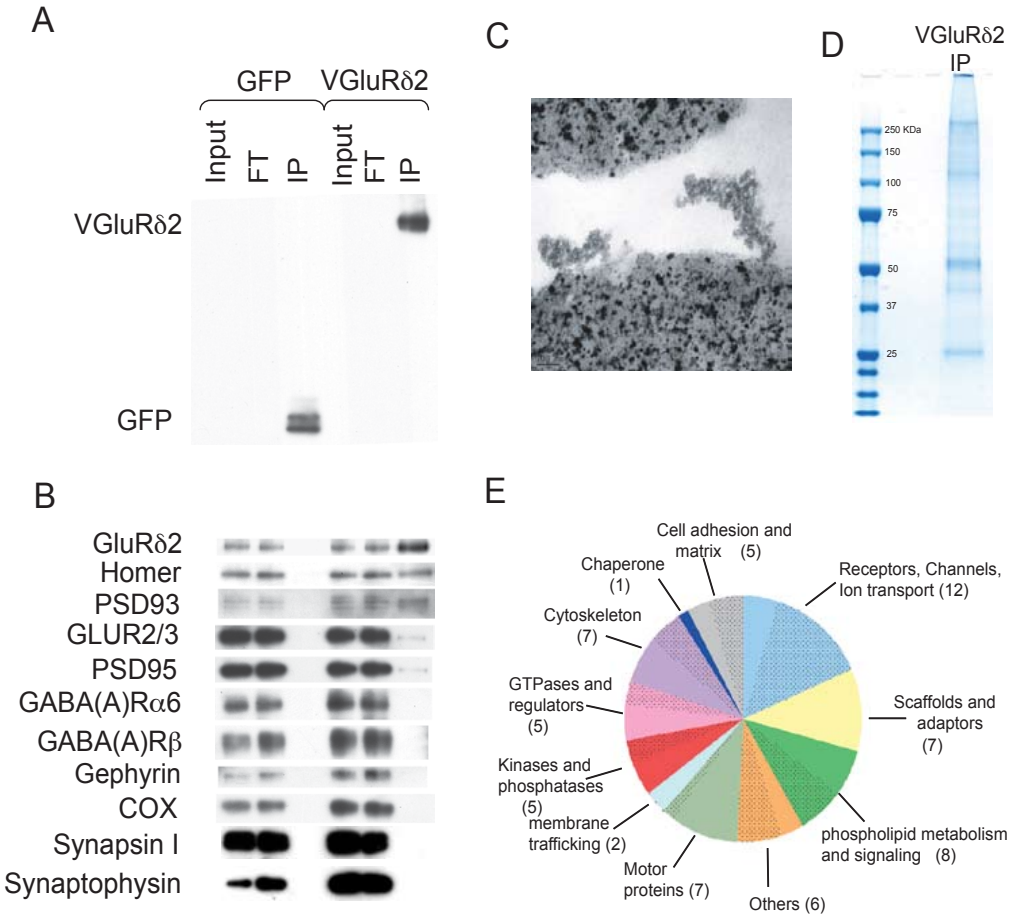

Figure 13. Affinity-purification and protein profiling of the parallel fiber/Purkinje cell PSDs

Analysis by western blot demonstrated the co-immunopurification of several positive makers of the PF/PC synapse (GluRδ2, Homer, PSD93, GluR2/3, and PSD95) as well as the absence of inhibitory synaptic markers ($GABA_AR\alpha6$, $GABA_AR\beta$, gephyrin), presynaptic markers (synapsin I,

synaptophysin) and the mitochondrial marker (COX) (Figure 13B). These results demonstrate the robust and specific isolation of the tagged parallel fiber to Purkinje cell synapse. Furthermore, electron microscopy of the magnetic beads used for affinity purification showed the presence of electron dense structures resembling the PSD in both structure and size (Figure 13C).

Mass spectrometry of the parallel fiber-Purkinje cell synapse

Mass spectrometry (MS) was used to identify the proteins purified from both Pcp2-VGluRδ2 and Pcp2-GFP. The material from several experiments was pooled (30 or 50 cerebella), separated by SDS-PAGE (Figure 13D) and analyzed by MALDI-TOF MS/MS. A total of 65 proteins were identified: 37 proteins were detected with high confidence (Table 3), and 28 were observed at lower levels and identified with less confidence (Table 4). Proteins known to be present at the PF/PC synapse and found by immunoblot analysis to co-purify with VGluRδ2 were confirmed by the MS results. These include the wild-type GluRδ2, AMPAR subunit GluR2 and the scaffolding proteins PSD95, PSD93 and Homer3. Additionally we were able to confirm the absence of presynaptic components and inhibitory neurotransmitter receptors and scaffolding molecules. Also absent were

components of distinct excitatory PSDs, such as NMDA receptor subunits. Finally, we identified several additional scaffolding molecules previously shown to colocalize with GluRδ2, including Shank1 and Shank2, delphilin, and GluRδ2-interacting protein (Grid2ip).

The proteins we identified specifically at the PF/PC synapse could be grouped into eleven functional categories (Figure 13D; Tables 3 and 4). Several of the known markers for the PF/PC PSD were grouped as "scaffolds and adapters", including several members of the Shank family and the PSD family. Other functional categories include proteins important for synapse formation and physiology, like regulators of small GTPases and protein kinases. In addition to proteins of expected functional relevance, eight of the proteins identified in our study can regulate or be regulated by phospholipid metabolism (Itpr1, synaptojanin 1 and 2, phospholipase B, ABCA12, MRCKγ), or contain phospholipid-binding domains (Plekha7, annexin A6, MRCKγ). Proteins in this group were previously unrecognized components of the PF/PC PSD and were thus grouped into a novel category, "phospholipid metabolism and signaling". There is evidence to support the role of phospholipid regulation at this synapse, based on the known role of the metabotropic glutatmate receptor 1 (mGluR1) in regulating LTD through activation of phospholipase C [67]. Another important category of PSD

proteins contained receptors and ion channels, including glutamate receptor subunits and several G protein-coupled receptors (GABA-B and BAI receptors). The BAI receptor, a G protein-coupled receptor, is likely to mediate cell adhesion [163]. Several other proteins identified at the PF/PC synapse in our study are involved in cell adhesion and interaction with the extracellular matrix: receptor protein tyrosine phosphatases [164], delta-catenin-2 [165], and Neph1 [142]. The functional diversity of proteins present at the parallel fiber to Purkinje cell synapse may underlie the need for a multitude of molecules in specifying this synapse.

Table 3. List of proteins identified in the immunoisolates of Venus-tagged GluRδ2. Results are shown of two replicate experiments from either 30 or 50 mice. The detection and confirmation of the proteins through MS and MS/MS analyses are indicated for both experiments. The number of peptides confirmed by MS/MS analysis is shown for each protein. The presence of these proteins in the control experiment, as judged by hypothesis-driven MS/MS analyses, is indicated. Where the presence or absence of the protein could not be judged conclusively, due either to depletion of sample or to inconclusive fragmentation, the entry is marked as not available (n/a).

Table 3. List of proteins identified in the immunoisolates of Venus-tagged GluRδ2.

Proteins isolated via VGluRδ2				MS	MS	MS/MS	MS/MS			
Category	Protein	Description	gi #	30 mice	50 mice	30 mice	50 mice	# peptides	In control	Function
TAG	YFP	Venus		Y	Y	Y	Y	2	Y	
Tagged protein	GluRδ2	glutamate receptor, ionotropic, delta 2	6680091	Y	Y	Y	Y	4	N	Receptors, channels and ion transport
Isolated proteins (Mus Musculus)	Shank2	SH3/ankyrin domain gene 2	28804747	Y	Y	Y	Y	2	N	Scaffolds and adaptors
	Shank1	PREDICTED: SH3 and multiple ankyrin repeat domains 1 isoform 3	82905881		Y		Y	5	N	Scaffolds and adaptors
	Homer3	homer-3	3834613	Y	Y	Y	Y	2	N	Scaffolds and adaptors
	PSD95	Dlgh4 protein	15928679	Y	Y	Y	Y	4	N	Scaffolds and adaptors
	PSD93	chapsyn-110	14518291	Y	Y	Y	Y	3	N	Scaffolds and adaptors
	Jakmip1	gamma-aminobutyric acid (GABA-B) receptor binding protein	30409980	N	Y	N	Y	2	N	Scaffolds and adaptors
	Grid2ip	glutamate receptor, ionotropic delta 2 (Grid2) interacting protein 1	19111166	N	Y	N	Y	7	N	Scaffolds and adaptors
	AMPA2	glutamate receptor, ionotropic, AMPA2 (alpha 2)	85861224	N	Y	N	Y	2	N	Receptors, channels and ion transport
	Gabbr1	GABA B receptor 1	131888529	Y	Y	Y	Y	6	n/a	Receptors, channels and ion transport
	Plekha7	Plekha7 protein [Mus musculus]	54038521	N	Y	N	Y	7	N	Phospholipid metabolism and signaling
	MRCK gamma	CDC42-binding protein kinase gamma (MRCK gamma) (DMPK-like gamma)	81174937	Y	Y	Y	Y	8	N	Phospholipid metabolism and signaling
	Itpr1	inositol 1,4,5-triphosphate receptor 1	146198792	N	Y	N	Y	11	N	Phospholipid metabolism and signaling
	Anxa6	Annexin A6 protein	13542782	Y	Y	N	Y	2	N	Phospholipid metabolism and signaling
	4930407I10Rik	PREDICTED: hypothetical protein	94399886	N	Y	N	Y	5	N	Others
	Ranbp2	Ran-binding protein 2	10442646	N	Y	N	Y	1	N	Others
	Dnahc8	axonemal dynein heavy chain 8	13310482	N	Y	N	Y	16	N	Motor proteins
	Dnahc12	PREDICTED: dynein, axonemal, heavy chain 12	149265372	N	N	N	Y	9	N	Motor proteins
	Cep152	centrosomal protein 152	82885523	N	Y	N	Y	10	N	Motor proteins
	Zwint	SNAP25 interacting protein 30	22028168	N	Y	N	Y	2	N	Membrane trafficking
	P140	PREDICTED: similar to p130Cas-associated protein (p140) (SNAP-25-interacting protein) (SNIP)	94390735	N	Y	N	Y	1	N	Membrane trafficking
	RPTPmam4	brain RPTPmam4 isoform 1	13378306	N	N	N	Y	3	N	Kinases and phosphatases
	Camk2b	Camk2b protein	51480474|	Y	Y	Y	Y	2	N	Kinases and phosphatases
	Camk2a	calcium/calmodulin-dependent protein kinase II alpha isoform 2	28916677	Y	Y	Y	Y	3	N	Kinases and phosphatases

Table 3 (continued).

Proteins isolated via VGluRδ2				MS	MS	MS/MS	MS/MS			
Category	Protein	Description	gi #	30 mice	50 mice	30 mice	50 mice	# peptides	In control	Function
	Synaptopodin isoform 2	PREDICTED: synaptopodin isoform 2	94404501	N	N	N	Y	6	n/a	GTPases and regulators
	Gm941	PREDICTED: hypothetical protein	82995169	Y	Y	Y	Y	5	N	GTPases and regulators
	CAST2 beta	Rab6ip2/CAST2 beta	32478657	N	Y	N	Y	2	N	GTPases and regulators
	Mtap6	neuronal-STOP protein	3171934	N	Y	N	Y	4	N	Cytoskeleton
	Ina	internexin neuronal intermediate filament protein, alpha	17390900	Y	Y	Y	Y	8	N	Cytoskeleton
	HSP 84	Heat shock protein HSP 90-beta (HSP 84) (Tumor-specific transplantation 84 kDa antigen) (TSTA)	123681	N	Y	N	Y	2	n/a	Chaperonne
	Lama1	laminin, alpha 1	117168301	N	Y	N	Y	7	N	Cell adhesion and matrix
	Catenin delta-2	PREDICTED: similar to Catenin delta-2 (Neural plakophilin-related ARM-repeat protein) (NPRAP) (Neurojungin)	94396572	N	N	N	Y	5	N	Cell adhesion and matrix
Likely	Myo18a	Myo18a protein	28436851	Y	Y	Y	Y	3	Y	Motor proteins
Contami-	Myo7b	myosin VIIb	14161694	Y	N	Y	N	2	n/a	Motor proteins
- nants	Cingulin	PREDICTED: similar to Cingulin	94371022	N	N	Y	Y	6	Y	Motor proteins
	Spnb2	spectrin beta 2	56206997	N	Y	N	Y	2	Y	Cytoskeleton
	Actb	actin, beta, cytoplasmic	74213524	Y	Y	Y	Y	3	Y	Cytoskeleton

Table 4. List of proteins identified in the immunoisolates of Venus-tagged GluRδ2 with lower levels of confidence as judged by mass spectrometry. Results are shown from two replicate experiments from either 30 or 50 mice. The detection and confirmation of the proteins through MS and MS/MS analyses is indicated for both experiments. The number of peptides confirmed by MS/MS analyses is shown for each protein. Several proteins were not observed (n/o) at the MS analysis stage, but were identified from MS/MS analyses. The presence of these proteins in the control experiment, as judged by hypothesis-driven MS/MS analyses, is indicated. Where due to either depletion of sample or inconclusive fragmentation, the presence or absence of the protein could not be judged conclusively, the entry is marked as not available (n/a)

Table 4. List of proteins identified in the immunoisolates of Venus-tagged GluRδ2 with lower levels of confidence as judged by mass spectrometry.

Proteins isolated via VGluRδ2				MS	MS	MS/MS	MS/MS			
Category	Protein	Description	gi #	30 mice	50 mice	30 mice	50 mice	# peptides	In control	Function
Isolated proteins Mus Musculus	Grik4	Glutamate receptor, ionotropic, kainate 4	109730793	N	Y	N	Y	1	n/a	Receptors, channels and ion transport
	GluR3	GluR3	84781717	Y	Y	N	N	2	n/a	Receptors, channels and ion transport
	GluR1	Glu receptor 1	227246	Y	Y	Y	Y	3	N	Receptors, channels and ion transport
	Gabbr2	PREDICTED: similar to Gamma-aminobutyric acid type B receptor, subunit 2 precursor (GABA-B receptor 2)	94373276	N	Y	N	Y	1	n/a	Receptors, channels and ion transport
	Bai3	brain-specific angiogenesis inhibitor 3	28628123	Y	N	Y	N	1	n/a	Receptors, channels and ion transport
	Bai2	Brain-specific angiogenesis inhibitor 2 precursor	110278892	N	Y	N	Y	3	n/a	Receptors, channels and ion transport
	Atp6v1a	ATPase, H+ transporting, V1 subunit A	31560731	N	Y	N	Y	1	n/a	Receptors, channels and ion transport
	Atp2a3	ATPase, Ca++ transporting, ubiquitous	31542159	N	Y	N	Y	1	n/a	Receptors, channels and ion transport
	Atp1a1	Atp1a1 protein	16307541	N	N	N	Y	2	N	Receptors, channels and ion transport
	Synj2	Synaptojanin-2 (Synaptic inositol-1,4,5-triphosphate 5-phosphatase 2)	37590481	N	Y	N	Y	1	n/a	Phospholipid metabolism and signalling
	Synj1	Synaptojanin-1 (Synaptic inositol-1,4,5-triphosphate 5-phosphatase 1)	149268231	N	Y	N	Y	1	N	Phospholipid metabolism and signalling
	Plb1	PREDICTED: similar to phospholipase B [Mus musculus]	94376138	N	N	N	Y	1	n/a	Phospholipid metabolism and signalling
	4833417A11Rik	PREDICTED: similar to ATP-binding cassette, sub-family A, member 12 isoform a isoform 2	94363638	N	N	N	Y	4	N	Phospholipid metabolism and signalling
	Setbp1	SETbinding protein	51890215	Y	N	Y	N	2	N	others
	Ncoa7	Ncoa7 protein	50369666	N	Y	N	Y	2	n/a	others
	Ant1	adenine nucleotide translocase-1	902008	N	Y	N	n/a	n/a	n/a	others
	LOC70950	hypothetical protein LOC70950	30794402	N	Y	N	Y	1	n/a	Motor proteins
	R-PTP-mu	Receptor-type tyrosine-protein phosphatase mu precursor (R-PTP-mu)	131570	N	Y	N	N	n/a	N	Kinases and phosphatases
	Mekk3	PREDICTED: similar to Mitogen-activated protein kinase kinase kinase 3 (MEKK 3)	33468949	N	Y	N	Y	1	n/a	Kinases and phosphatases
	Synaptopodin	synaptopodin	46428644	N	Y	N	Y	1	n/a	GTPases and regulators
	Baiap2	Baiap2 protein	13879292	Y	Y	N	Y	1	n/a	GTPases and regulators
	Nesprin 2	similar to nesprin2	145699091	Y	N	Y	N	2	n/a	cytoskeleton
	LAMA2	laminin alpha 2 subunit precursor variant	62087424	N	Y	N	Y	1	n/a	Cell adhesion and matrix
	NEPH1	NEPH1	14572519	N	Y	N	Y	2	N	Cell adhesion and matrix
	BC022980	PREDICTED: similar to periphilin 1 isoform 1	94408554	N	N	N	Y	2	n/a	Cell adhesion and matrix
Likely contami -nants	spectrin alpha 2	PREDICTED: similar to Spectrin alpha chain, brain; (Alpha-II spectrin) (Fodrin alpha chain)	115496850	N	Y	N	n/a	n/a	n/a	cytoskeleton
	mKIAA4061	mKIAA4061 protein = from Blast seacrh, homologue to spectrin domain with coiled-coils 1	60360496	N	N	N	Y	4	n/a	cytoskeleton
	LOC872116	PREDICTED: similar to zinc finger protein 616	94369146	N	N	N	Y	3	Y	others

Confirmation of candidate proteins

To provide additional evidence for the synaptic localization of the novel components that we have identified, we performed immunofluorescence studies on cerebellar sections from wild-type mice. Localization in the molecular layer of the cerebellum, which contains the PF/PC synapses, was evident for MRCKγ, Gm941, BAIAP2, RPTPm, Neph1, and delta2-catenin (Figure 14). Delta2-catenin and Gm941 could also be detected in some cerebellar interneurons. Examination of several *in situ* hybridization databases (www.stjudebgem.org; www.brain-map.org; www.genepaint.org) was used to confirm the expression pattern of candidate proteins. Interpretable data were available for 42 candidates, and all but two were expressed in Purkinje cells, with a majority showing little detectable expression in the granule cell layer (data not shown). These expression data provide additional confirmation that the majority of the proteins identified in our study are components of the PF/PC synapse.

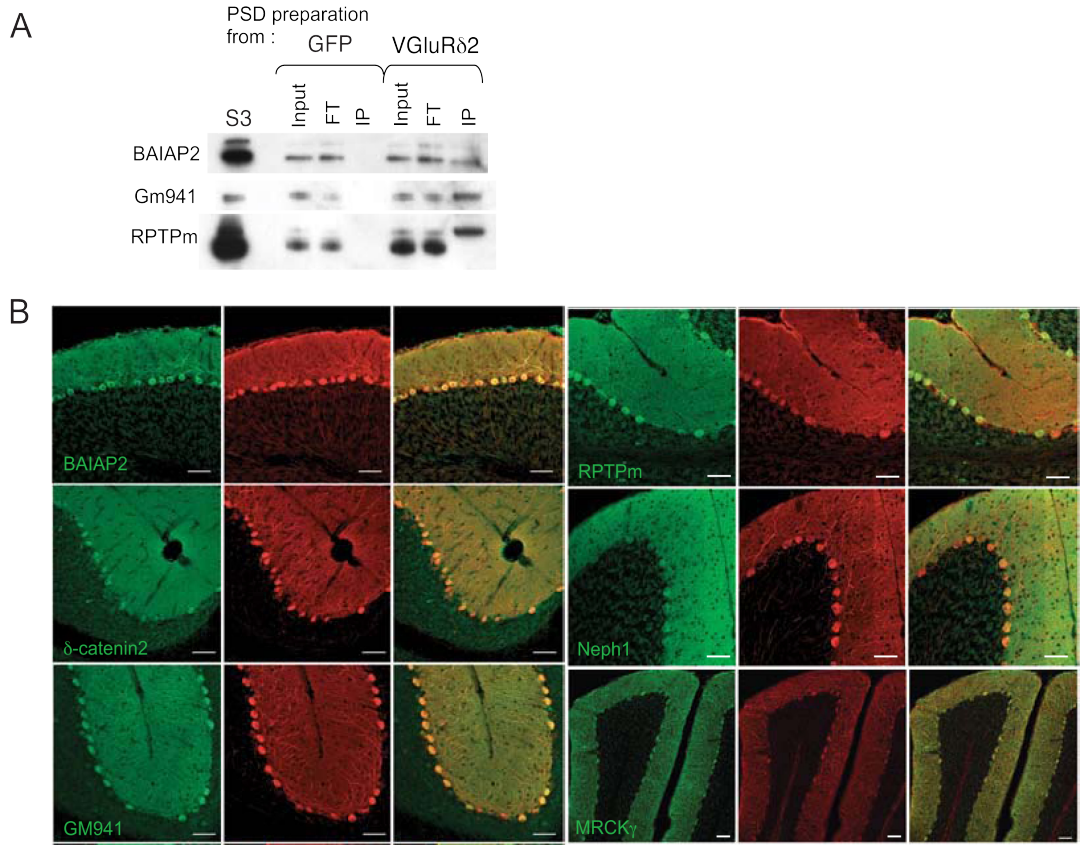

Figure 14. Localization of novel components of PF/PC synapse.

(A) Presence of selected candidates in PF/PC PSDs purified from Pcp2/VGluRδ2 cerebella. 0.025% of the inputs and flow-throughs (FT) and 25% of the affinity-purified samples (IP) obtained from Pcp2-GFP control (GFP) and Pcp2-VGluRδ2 (VGluRδ2) cerebella were assayed by western blot. (B) Analysis of candidate synaptic proteins. Immunofluorescence labeling was performed using antibodies recognizing several candidate proteins identified by mass spectrometry (green) in conjunction with an anti-calbindin antibody specifically labeling Purkinje cells (red). Scale bars: 50 mm.

Summary

We have successfully targeted expression of a Venus-GluRδ2 fusion protein to the parallel fiber-Purkinje cell synapse of the cerebellum using the BAC transgenic approach. The fusion protein displays correct topography in heterologous cells and is present in classically purified synaptic fractions from mouse cerebellum. Purification of the tagged PF/PC synapses was achieved with a novel biochemical method that relies on solubilization of a crude synaptosome fraction followed by gel filtration to enrich for PSDs. The tagged PF/PC synaptic complex was affinity purified from this PSD fraction and analyzed by mass spectrometry. Using this approach we identified approximately 65 proteins, including a novel group of "phospholipid metabolism and signaling" proteins, which are previously unrecognized components of this synapse.

Among the proteins identified were several that represent novel members of this synapse, such as GPM741, RPTPm and BAIAP2. Using immunohistochemistry and immunoblotting we confirmed the Purkinje cell specificity of several candidate proteins identified by mass spectrometry. This work represents the first successful purification of an individual synapse type, and demonstrates the strength of such a strategy in uncovering novel functional components of a particular synapse type.

CHAPTER IV. EXPRESSION OF AN AMPA RECEPTOR FUSION PROTEIN IN CORTICAL PYRAMIDAL NEURONS

Introduction

A study of synaptic specificity, and the potential for uncovering a "synaptic code," is facilitated by the ability to tag and purify multiple synapse types for a comparative study. The GENSAT project has facilitated such an approach, in that we can quickly generate multiple lines of transgenic mice each expressing a synaptic tag in a distinct cell population. We have taken advantage of this in designing a study of AMPA receptor subunit GluR1 containing excitatory synapse types across distinct laminae of the cerebral cortex.

The distribution of AMPA receptor subunits varies across cortical laminae, but the GluR1 subunit is present abundantly in all pyramidal neurons. A comparison of excitatory synaptic protein complexes would validate the known subunit expression patters as well as expand the protein profile of these synapses to include additional molecules important for laminar specificity of excitatory inputs. In addition, it is possible to discover tissue specific markers of excitatory synapses by comparison of GluR1-containing cortical synapses to the GluRδ2-containing Purkinje cell synapses we have previously analyzed.

Results

Cloning and expression of a Venus-GluR1 fusion protein

In order to tag and purify excitatory synapses, we designed a GluR1 fusion protein with an affinity tag, Venus, located extracellularly at the N-terminus (Figure 15A). This fusion protein has proved useful in studying AMPA receptor trafficking and protein interactions in a multitude of experiments both in cultured neurons and *in vivo* [84, 86, 88]. We confirmed expression and membrane trafficking of the Venus-GluR1 fusion protein (VGluR1) in HEK293 cells. Transfected cells were processed for immunochemistry under non-permeabilizing conditions using an anti-GFP antibody, which showed Venus localized extracellularly (data not shown).

We next generated transgenic mice that express the Venus-GluR1 fusion protein under Otx1 gene regulatory elements, using the Otx1 BAC (Figure 15D). This BAC has been shown to drive expression in a subpopulations of cortical layer V pyramidal neurons. Correct modification of the BAC was confirmed by Southern blotting (Figure 15B) and subsequently injected into oocytes for implantation into pseudopregnant females. Transgenic mice were identified by Southern blotting of genomic DNA (Figure 15B).

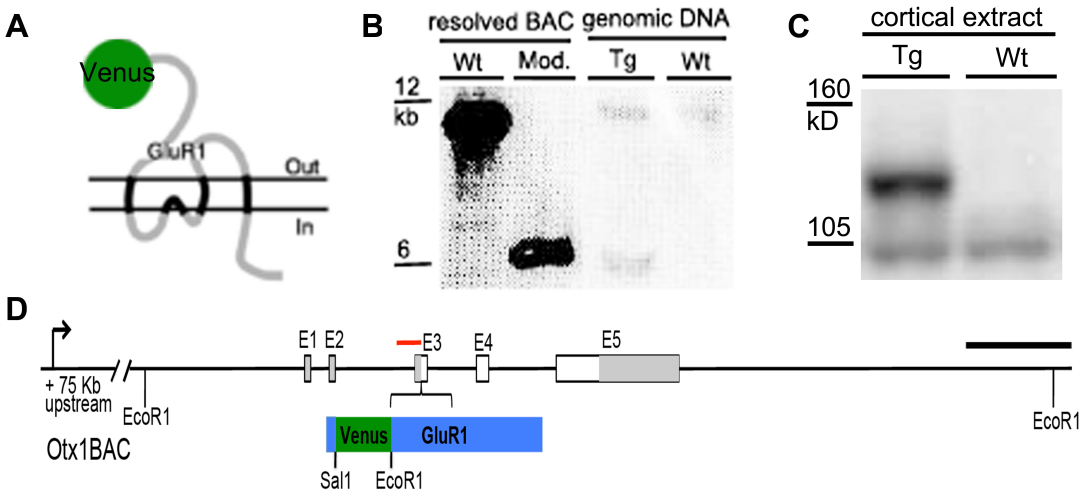

Figure 15. Expression of a Venus-GluR1 fusion protein in mouse cortex. (A) Schematic of AMPA receptor subunit GluR1 N-terminally fused to an affinity tag, Venus. The tag is present extracellularly. (B) Southern blotting confirmed correct modification of an Otx1 BAC with the Venus-GluR1 cDNA. Insertion of the transgene into the wild-type BAC (Wt) introduced an additional EcoR1 restriction site, resulting in hybridization of the probe (red, in D) on a restriction band of smaller size (Mod.). Genomic DNA from a wild-type (Wt) and transgenic (Tg) mouse was analyzed by Southern blotting. The transgenic mouse shows two bands, corresponding to the BAC transgene and the endogenous Otx1 sequence. (C) Whole protein extract was collected from transgenic (Tg) and wild-type (Wt) mouse cortex, separated by SDS page and immunoblotted with an anti-GFP antibody. Extract from the transgenic mouse shows a band corresponding in size to VGluR1. The lower non-specific band is present at equivalent levels in tissue from both animals. (D). Schematic of the Otx1 BAC transgene modified with Venus-GluR1. The VGluR1 was inserted such that it disrupted the Otx1 ATG. Approximately 75 Kb of upstream regulatory sequences is present in the BAC. Scale bar = 2 Kb.

We next tested the transgenic mice for expression of VGluR1 by immunoblotting of cortical protein extract. An anti-GFP antibody detected a band at 130 kDa, which corresponds to VGluR1, in protein extract from transgenic, but not wild-type cortices (Figure 15C).

Expression of Venus-GluR1 in cortical and hippocampal neurons

We next sought to examine the expression pattern of VGluR1 in the mouse cortex using immunohistochemistry with a goat anti-GFP antibody. Tissue from several founder lines was examined, but the fusion protein was not detectable by in the cerebral cortex. However, one founder line (LH-Otx1VGluR1-7) showed robust expression in the hippocampus, specifically in regions CA3 and dentate gyrus (Figure 16A). Hippocampal expression was specific to this particular founder line, suggesting that it is due to the genomic position of the Otx1-VGluR1 BAC transgene. The fusion protein was localized to dendrites (Figure 16A, far right), rather than the soma or axon, corresponding to the correct localization of AMPA receptors. An additional transgenic line, Otx1-GFP, which expresses soluble GFP under the Otx1 BAC regulatory elements was examined in an identical way and showed robust expression in cortical layer V neurons, but not in hippocampus (Figure 16A, left and [146]).

Figure 16. Expression of the Otx1-Venus-GluR1 transgene.

(A) Immunohistochemistry of fixed brain tissue from Otx1-GFP and Otx1-VGluR1 mice using a goat anti-GFP antibody. Robust GFP expression was detectable in brain sections from Otx1-GFP mice in layer V of the cerebral cortex. Brain sections from Otx1-Venus-GluR1 (Otx1VGluR1) showed expression of the VGluR1 fusion protein in hippocampus (CA3 and dentate gyrus). VGluR1 expression was not detectable in the cerebral cortex. A higher magnification image of staining in the hippocampus showed VGluR1 localized to dendrites, and excluded from soma and axons. (B) A crude synaptosome preparation was carried out on cortical and hippocampal tissue from Otx1-VGluR1 mice. Fractions were subject to SDS-PAGE and immunoblotted with anti-GFP and other markers. Synaptic proteins were detectable in the synaptic fraction, S2. S2 was solubilized with 1.0% Triton X-100 to enrich for synaptic protein complexes (S3). This fraction was subject to affinity purification using an anti-GFP antibody. VGluR1 was detected in the immunopurified (IP) material from both cortex and hippocampus. However, no additional synaptic proteins were co-immunopurified with the VGluR1 fusion protein. Scale bars: left and center panels = 200um, right panel = 50um.

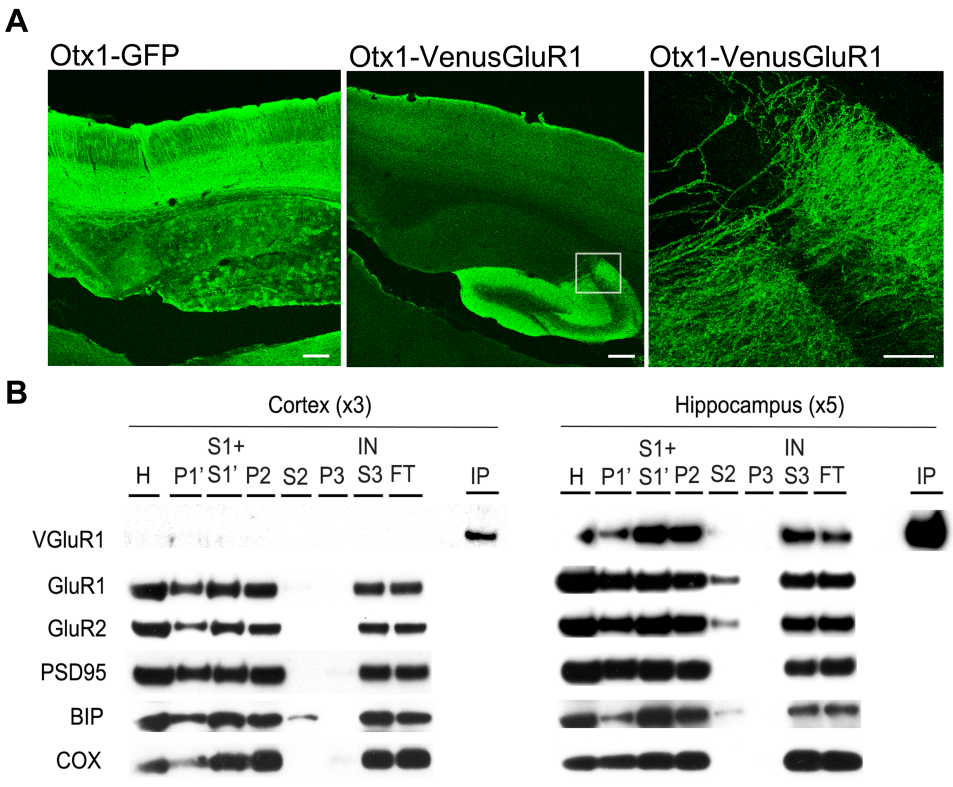

Figure 16. Expression of the Otx1-Venus-GluR1 transgene.

The additional hippocampal expression of the fusion protein in Otx1-VGluR1$_7$ was potentially useful in that it might allow an in-subject comparison between excitatory synapses from two distinct tissues, the hippocampus and cerebral cortex, which could reveal site-specific GluR1 interacting proteins.

Biochemical purification of a crude synaptic fraction was carried out as described [147] for both the hippocampus and cerebral cortex from the Otx1-VGluR1 mice. An aliquot from each step of the purification was separated by SDS-PAGE and immunoblotted with anti-GFP (Figure 16B).

By immunoblotting, it was possible to detect VGluR1 only in the fractions collected from the hippocampal tissue. Although immublotting of whole protein cortical extract showed the presence of VGluR1, it was undetectable after biochemical fractionation.

Next, the crude synaptosome fraction was solubilized with 1.0% Triton X-100 in the case of cortex, and 0.1% Triton X-100 in the case of hippocampus, to enrich for synaptic protein complexes, including the PSD. This fraction, P3, was subject to co-immunopurification using a goat anti-GFP antibody (Figure 16B). The co-immunopurified material was separated by SDS-PAGE and immunoblotted with an anti-GFP antibody as well as additional antibodies for detection of synaptic and non-synaptic markers. While it was possible to detect the fusion protein in the IP from cortical PSDs, it was much less abundant than that found in hippocampal PSDs. In addition, we did not co-immunopurify any additional AMPA receptor subunits, including the endogenous GluR1, nor GluR2. PSD95 was also absent from the IP, as well as BIP and COX. The failure to detect additional AMPA receptor subunits in this fraction can result from a failure of the fusion protein to correctly incorporate into functional AMPA receptors, from the failure of the receptor to traffic to the synapse, or from the method itself,

in which we are attempting to affinity purify from a very crude and complex sample of solubilized protein.

Because of the low expression of VGluR1 in cortex of Otx1-VGluR1$_7$ transgenic mice, we focused our attention on the hippocampus, which robustly expressed VGluR1. In order to better enrich the starting material for affinity purification we relied on gel filtration to separate large protein complexes from smaller, intracellular ones. A percentage of each fraction was separated by SDS-PAGE and analyzed by immunoblotting (Figure 17A). Several markers of excitatory synapses were enriched in the early fractions, and are likely incorporated into large protein complexes. These include Venus-GluR1 and the wild-type GluR1, as well as GluR2, PSD95 and GRIP. GABA$_A$Rα1, a subunit of inhibitory neurotransmitter receptors, was concentrated in later fractions, indicating a separation of excitatory and inhibitory synaptic protein complexes under these conditions. In addition, the endoplasmic reticulum (ER) marker, BIP, was largely excluded from the early fractions and enriched in the later fractions that contain smaller, trafficking protein complexes. Wild-type hippocampal tissue was processed in the same way and immunoblotting of the fractions showed identical distribution of the proteins mentioned above, with the exclusion of VenusGluR1 (data not shown).

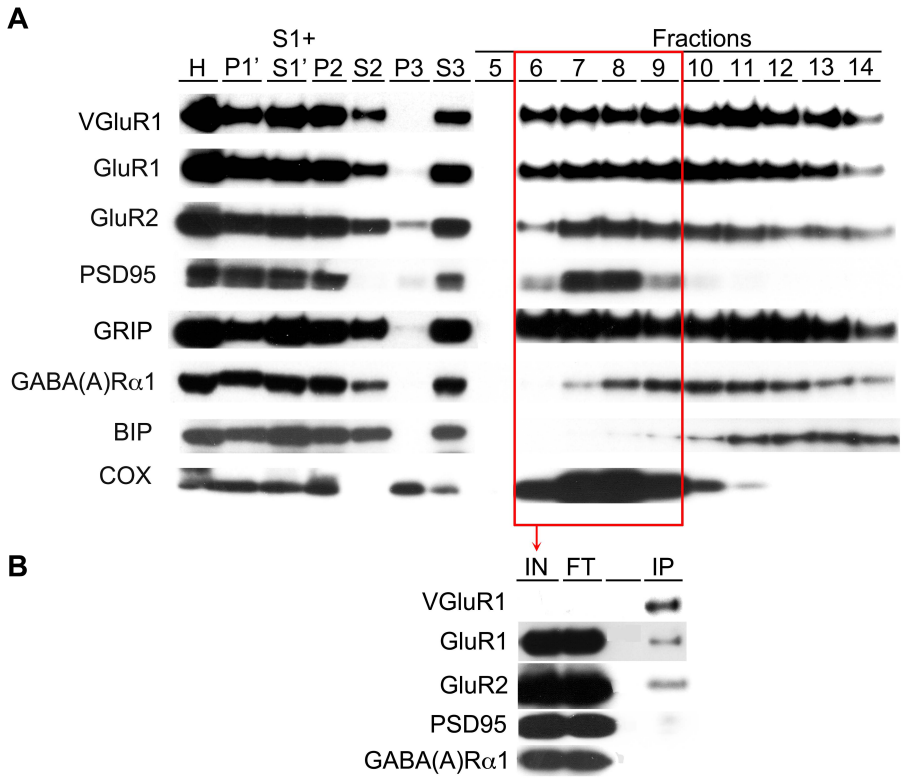

Figure 17. Gel filtration of a solubilized synaptic fraction from Otx1-VGluR1 followed by affinity purification. (A) A crude synaptic fraction prepared from 10 hippocampi was solubilized with 0.1% Triton X-100 and subject to gel filtration. 1.0% in volume of every fraction was separated by SDS-PAGE and assayed for the presence of excitatory synapse markers (PSD95, GluR1, GluR2), inhibitory synapse markers ($GABA_AR\alpha1$), the endoplasmic reticulum marker, BIP and the mitochondrial marker, COX. VGluR1 was detected using an anti-GFP antibody. (B) The early fractions (6-10) were pooled and affinity-purified using a mouse anti-GFP antibody (IP). 0.1% of the inputs and 25% of the affinity-purified samples (IP) were assayed by Western blot using an anti-GFP antibody and showed immunoprecipitation of VGluR1 from the transgenic mouse. The same blot was probed for wild-type GluR1, GluR2 and PSD95, as well as the inhibitory neurotransmitter receptor subunit $GABA_AR\alpha1$.

Next, we pooled the fractions enriched for excitatory synaptic proteins and performed affinity purification with a mouse anti-GFP antibody (Figure 17B). The co-immunopurified material (IP) was separated by SDS-PAGE and immunoblotted with a rabbit anti-GFP antibody, which showed the presence of VGluR1 in the IP from Otx1-VGluR1 hippocampus. The endogenous GluR1 subunit was also present in the IP, as well as an additional AMPA receptor subunit, GluR2, indicating that the VGluR1 fusion protein can assemble with wild-type AMPA receptor subunits. Despite this, we did not detect any additional excitatory synaptic proteins, such as PSD95, indicating that the VGluR1 containing AMPA receptors may not incorporate properly into the synapse.

Generation of transgenic mice expressing Venus-GluR1 in various cortical laminae.

Despite the failure of VGluR1 to successfully co-immunopurify synaptic proteins when expressed under Otx1 regulatory elements, we were not convinced that this fusion protein did not traffic to the synapse. It was possible that the Otx1 driver was simply not sufficient for expression of this fusion protein in cortex, or that the fusion protein was regulated differently in the Otx1-positive layer V pyramidal neurons. In order to test this

hypothesis, and to facilitate a comparative study of GluR1-containing excitatory synapses, we generated multiple lines of transgenic mice, each expressing VGluR1 in a distinct cortical pyramidal cell population (Figure 18).

Each of the BAC drivers was selected for its specificity to pyramidal neurons in a distinct layer of mouse cerebral cortex (Figure 8 and [146]). The BAC modification was carried in a manner similar to Otx1-VGluR1, except that resolution of the intervening shuttle vector sequences was not necessary due to the improvement of the BAC modification technique. Four BAC drivers, Drd4, Glt25d2, March4 and Ntsr1 were modified such that the Venus-GluR1 fusion protein was expressed instead of the endogenous protein (Figure 18A).

Figure 18. Generation of multiple BAC transgenic lines expressing Venus-GluR1. (A) Four BACs, Drd4, Glt25d2, March4 and Ntsr1, were selected based on their expression in distinct cortical pyramidal cell populations. Each was modified such that the Venus-GluR1 cDNA was inserted at the level of the ATG. The amount of upstream regulatory genomic sequences in each BAC is indicated. Insertion of the transgene and shuttle vector (sv) sequences (not illustrated) introduced two additional EcoR1 sites into the BAC. Scale bar = 20 kB. (B) Southern blotting was used to confirm correct co-integration of the shuttle vector-transgene construct into the BAC. The probe (red box in A) corresponded to those sequences used for homologous recombination and hybridizes to two distinct restriction bands in the co-integrate (c). (C) Cortical protein extract was collected from wild-type and transgenic mice and immunoblotted for the presence of Venus-GluR1. All four BAC transgenic lines express the transgene, although the level of expression is not more than that seen for Otx1-VGluR1. Cortical synaptic protein from Glt25d2-VGluR1 was further analyzed by preparation of a solubilized crude synaptic fraction (S3) subject to immunopurification with a mouse

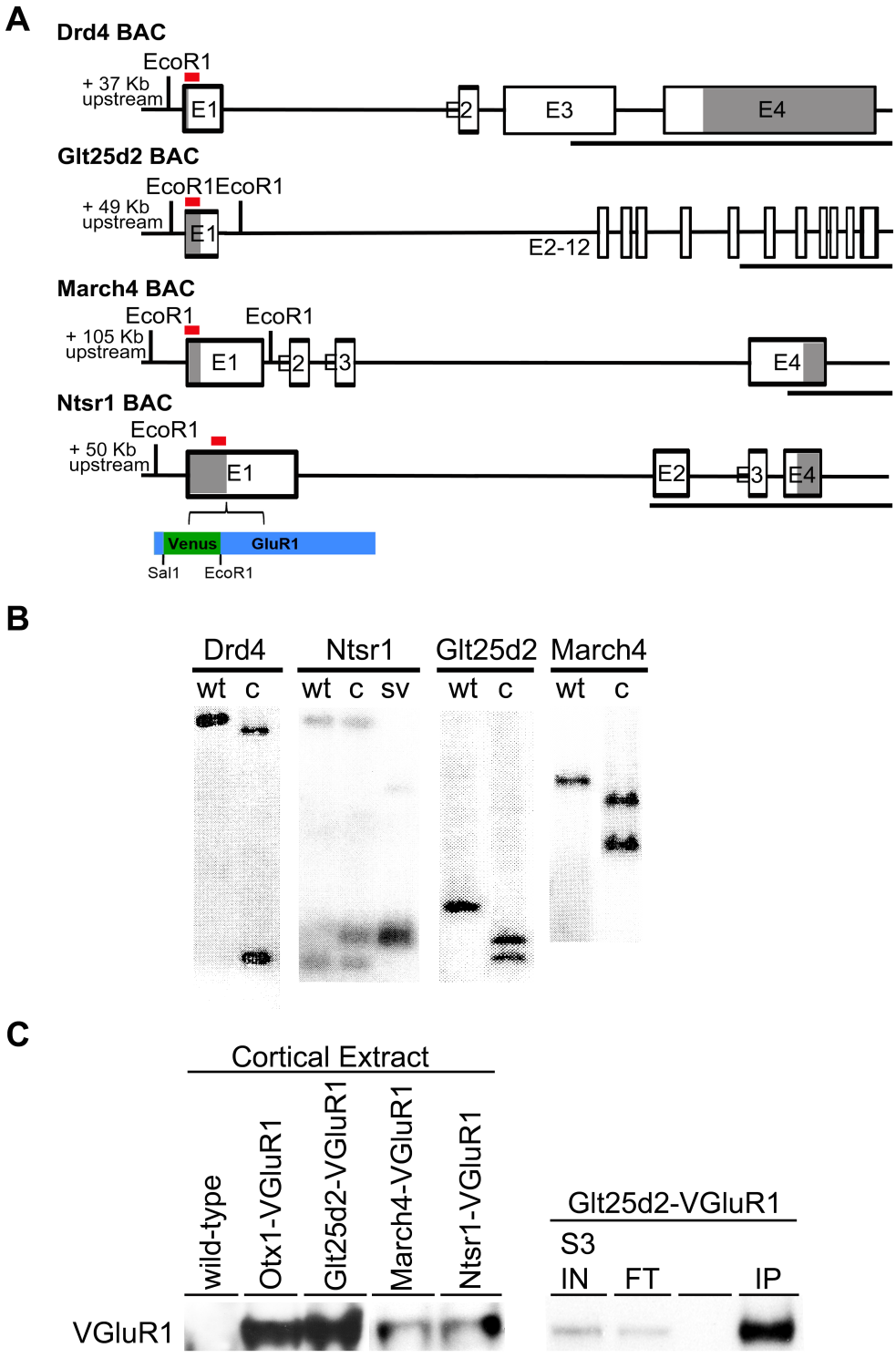

Figure 18. Generation of multiple BAC transgenic lines expressing VGluR1.

Correctly modified BACs were shown by Southern blotting to contain two additional bands, due to the presence of EcoR1 restriction sites introduced with the VGluR1-modified shuttle vector sequences (Figure 18B). Each modified BAC was purified and injected into oocytes, which were surgically implanted into pseudopregnant females. Successful incorporation of the transgene was confirmed by dot blotting and PCR genotyping of genomic DNA (data not shown).

To confirm expression of VGluR1 in the cortex of each BAC transgenic line, we collected cortical protein extract and immunoblotted with an anti-GFP antibody (Figure 18C, left panel). The fusion protein was present in Glt25d2-VGluR1 cortical protein extract at a similar level to the previously analyzed line, Otx1-VGluR1. Immunoblots of cortical extract from Ntsr1-VGluR1 and March4-VGluR1 also detected VGluR1, but at considerably lower levels. Cortical extract from Drd4-VGluR1 did not contain any detectable VGluR1 protein (data not shown). These results were consistent across several founder lines for each BAC. Furthermore, immunoblotting detected the VGluR1 fusion protein in a solubilized, PSD-enriched fraction (S3) from cortices of Glt25d2-VGluR1 mice (Figure 18C, right panel). We were able to immunopurify VGluR1 from this fraction using a mouse anti-GFP antibody, as shown by immunoblotting the IP

material with a rabbit anti-GFP antibody. We attempted to further analyze the expression of the transgene in these cortical expression lines by immunohistochemistry of fixed brain tissue. However, as in the case of Otx1-VGluR1 (Figure 16A), the fusion protein was undetectable in cortex by immunohistochemistry for all of the lines (data not shown).

Because of the relatively high level of expression of VGluR1 under the Glt25d2 BAC regulatory elements, this line was subject to further biochemical analysis. A crude synaptic fraction was prepared from five cortices and solubilized with 1.0% Triton X-100, followed by size exclusion chromatography on a Sephacryl S1000 column. A percentage of each fraction collected was separated by SDS-PAGE and immunoblotted for various proteins (Figure 19A). The early fractions, which contain large protein complexes, were enriched in excitatory synaptic proteins (GluR1, GluR2, PSD95, GRIP) and the mitochondrial marker, COX. The smaller, likely intracellular protein complexes were enriched in later fractions and contained makers of inhibitory synapses ($GABA_AR$ $\alpha1$, $GABA_AR\beta2/3$) and the ER marker, BIP. Because of the low level of expression of VGluR1, it was not possible to detect the fusion protein in the dilute fractions collected after gel filtration. In order to confirm the presence of the fusion protein in the various fractions, and to assess its distribution, we performed

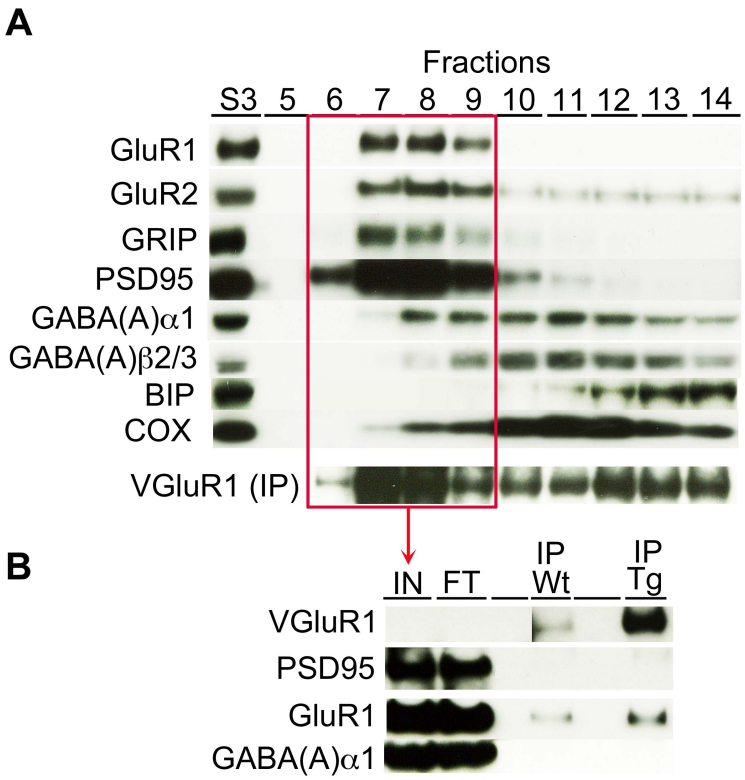

Figure 19. Gel filtration of a solubilized synaptic fraction from Glt25d2-VGluR1 transgenic mice followed by affinity purification. (A) A crude synaptic fraction was prepared from 5 cortices, solubilized with 1.0% Triton X-100 and subject to gel filtration. Each fraction was assayed for the presence of excitatory synapse markers (PSD95, GluR1, GluR2, GRIP), inhibitory synapse markers (GABA(A)Rα1, GABA(A)R β2/3), the endoplasmic reticulum marker, BIP and the mitochondrial marker, COX. VGluR1 was immunopurified from each fraction using a mouse anti-GFP antibody and detected via immunoblotting with a rabbit anti-GFP antibody. (B) Fractions 6-10 were pooled and affinity-purified using a mouse anti-GFP antibody and showed immunoprecipitation of VGluR1 from the transgenic mouse (IP Tg) but not wild-type (IP Wt). The same blot was probed for wild-type GluR1 and PSD95, as well as the inhibitory neurotransmitter receptor subunit $GABA_AR\alpha1$.

immunopurification of each fraction using a mouse anti-GFP antibody (Figure 19A, bottom). The immunopurified material from each fraction was immunoblotted with an anti-GFP antibody, which detected VGluR1 in each fraction, however, the distribution of the fusion receptor differed from that of the endogenous GluR1 subunit. While both the fusion and wild-type GluR1 subunits were enriched in the early fractions, which contain large protein complexes, Venus-GluR1 was also enriched in the later fractions, presumably in other intracellular compartments. Tissue from wild-type cortex was processed simultaneously and showed identical distribution of wild-type proteins in the biochemical fractions as well as the absence of VGluR1 (data not shown).

Next, we pooled the early fractions (6-9) from both Glt25d2-VGluR1 and wild-type cortices and performed affinity purification using a mouse anti-GFP antibody (Figure 19B). VGluR1 was detected by immunoblotting in the IP from transgenic but not wild-type cortex. The endogenous GluR1 was only slightly enriched in the IP from Glt25d2-VGluR1, compared to wild-type. PSD95, the major excitatory synaptic scaffolding protein, and the AMPA receptor subunit GluR2 (not shown) were absent from the IP, as was the inhibitory neurotransmitter receptor subunit $GABA_AR\alpha1$. As in the case of Otx1-VGluR1, it appears that VGluR1 expressed under control of

Glt25d2 regulatory elements does not traffic properly to excitatory synapses, and perhaps does not form functional receptors.

Summary

Protein profiling in the mouse central nervous system necessitates that one compare multiple synapse types. Using the BAC transgenic approach we generated multiple transgenic lines each expressing a Venus-GluR1 fusion protein in a distinct pyramidal cell population. We intended to purify GluR1-containing PSDs from each of these five pyramidal cell populations and analyze the components by mass spectrometry for a comparative study. Included in our study was Otx1-VGluR1, which would provide a useful comparison to Otx1-VGABA$_A$Rα1, a transgenic line that contains affinity tagged inhibitory synapses.

The fusion protein showed correct topography in non-neuronal cells, was successfully integrated into each BAC and was expressed by multiple founder mice for each transgenic line generated. Unfortunately, the expression levels of this fusion protein in cortex were relatively low, and not detectable by immunohistochemical methods. Nevertheless, we were able to detect protein in cortical protein extract, demonstrating that the fusion

protein was expressed under the control of the various BAC regulatory sequences.

One Otx1-VGluR1 founder line expressed the fusion protein at robust levels in CA3 and dentate gyrus of hippocampus. We further analyzed the hippocampus from this line and the cortex of an additional line, Glt25d2-VGluR1, for biochemical enrichment of VGluR1 in large protein complexes that contain other markers of excitatory synapses. VGluR1 was present in a crude synaptic fraction and in large protein complexes separated by gel filtration, but at extremely low levels and in a distribution that differed from wild-type GluR1. In addition, affinity purification of these pooled fractions showed that VGluR1 did not co-immunopurify PSD95, an abundant constituent of the excitatory postsynaptic specialization. Endogenous GluR1 was only minimally enriched in the IP from these transgenic lines. Together these results suggest that Venus-GluR1 does not successfully incorporate into synapses when expressed at physiological levels in both hippocampus and cortex of adult mice.

CHAPTER V. PROTEIN PROFILE OF INHIBITORY SYNAPSES IN CEREBRAL CORTEX

Introduction

Synaptic activity in the central nervous system is defined as being either excitatory or inhibitory, depending on the resulting change in postsynaptic membrane potential. The two types of input are morphologically, biochemically and functionally distinct. Fast synaptic inhibition in the brain and spinal cord is mediated largely by ionotropic GABA receptors, which are pentameric chloride ion channels [24]. $GABA_A$ receptors also represent a major site of action of clinically relevant drugs, such as benzodiazepines, barbiturates, ethanol, and general anesthetics. The precise subunit composition of a given $GABA_A$ receptor determines its expression pattern, subcellular localization and ligand affinities [2, 166-168]. The most common composition consists of two alpha, two beta and one gamma subunit, with the $\alpha 1$ subunit expressed most abundantly in the central nervous system [2, 3].

Excitatory synapses are easily enriched and purified biochemically due to the presence of a detergent insoluble post-synaptic density (PSD), thus the molecular architecture of these synapses is described in great detail in the literature [25, 68, 169]. Inhibitory synapses, on the other hand, lack a

large PSD and have not been purified or defined biochemically. Several known protein constituents of inhibitory synapses were described in the introduction. A key component, gephyrin, is thought to be the major scaffolding protein of this synapse. However, it has not been shown to bind directly to GABA receptors, and is not necessary for clustering of all GABA receptor subunits [28]. Because many of the proteins thought to colocalize at inhibitory synapses are gephyrin-binding proteins, the list of inhibitory synaptic elements is not conclusive. Furthermore, many of these interactions have been shown exclusively *in vitro* [170].

We have designed a novel *in vivo* method to biochemically purify and analyze synaptic protein complexes and have applied this to $GABA_AR\alpha1$ containing synapses in a specific class of layer V cortical pyramidal neurons.

Results

Tagging inhibitory synapses in layer V cortical pyramidal neurons

In order to specifically purify inhibitory synapses from layer V cortical neurons, we took advantage of the BAC transgenic approach for transgene expression. We selected the Otx1 BAC, which drives expression in a specific population of layer V pyramidal neurons. The Otx1 BAC was modified to express a fusion protein consisting of the $GABA_A$ receptor $\alpha 1$ subunit N-terminally fused to an affinity tag, Venus (Figure 20A). We first transfected Venus-$GABA_A R\alpha 1$ (V$GABA_A R\alpha 1$) cDNA into HEK293 cells. SDS-PAGE followed by immunoblotting with an anti-GFP antibody showed that the protein was expressed and migrated at the expected size of 75 kDa (data not shown). In addition, immunocytochemistry of non-permeabilized HEK293 cells showed that the fusion protein was inserted into the plasma membrane with the correct topographical organization, that is, with the affinity tag, Venus, localized extracellularly (data not shown).

We then went on to modify the Otx1 BAC such that the Otx1 ATG was disrupted by insertion of the Venus-$GABA_A R\alpha 1$ cDNA (Figure 20D). Successful modification of the BAC was checked by Southern blot (Figure 20B). The insertion of the cDNA introduces an additional EcoR1 restriction

Figure 20. Tagging inhibitory synapses in a population of cortical layer V pyramidal neurons. (A) The $GABA_A$ receptor α1 subunit was N-terminally fused to an affinity tag, Venus. The topography of the receptor positions Venus extracellularly, to allow for efficient purification of the synaptic complex. (B) Correct modification of the Otx1 BAC with the Venus-$GABA_A$Rα1 fusion construct was confirmed with Southern blot (EcoRI digest, probe shown as red bar in (D)), before injection into mouse oocytes. (C) Immunoblot analysis of cortical extract from both wild-type (Wt) and transgenic (Tg) mice, using an anti-GFP antibody, confirmed expression of Venus-$GABA_A$Rα1. The fusion protein migrates at the expected size of 75 kDa and is present only in extract from the transgenic mouse. A nonspecific band is present in both extracts at 50 kDa. (D) Schematic diagram of the modification of the Otx1 BAC with the Venus-$GABA_A$Rα1 construct. Otx1 is expressed specifically in a subpopulation of cortical layer V pyramidal neurons. Otx1 expression was disrupted by introduction of the fusion construct at the level of the Otx1 atg. The red bar indicates the probe used in (A). The arrow denotes the likely start of regulatory sequences, based on the presence of upstream coding region for an unrelated gene. Scale bar = 2 kB.

(E) Immunohistochemistry using an anti-GFP antibody confirmed the expression of Venus-$GABA_A$Rα1 in cortical layer V pyramidal neurons. Brain sections from wild-type mice showed no detectable expression of GFP, while the Otx1-Venus-$GABA_A$Rα1 transgenic mice showed robust, and specific layer V cortical expression. A magnified view shows the expression of the fusion protein in pyramidal cell soma (arrows) and dendrites (arrowheads), in accordance with the known location of inhibitory synaptic input.

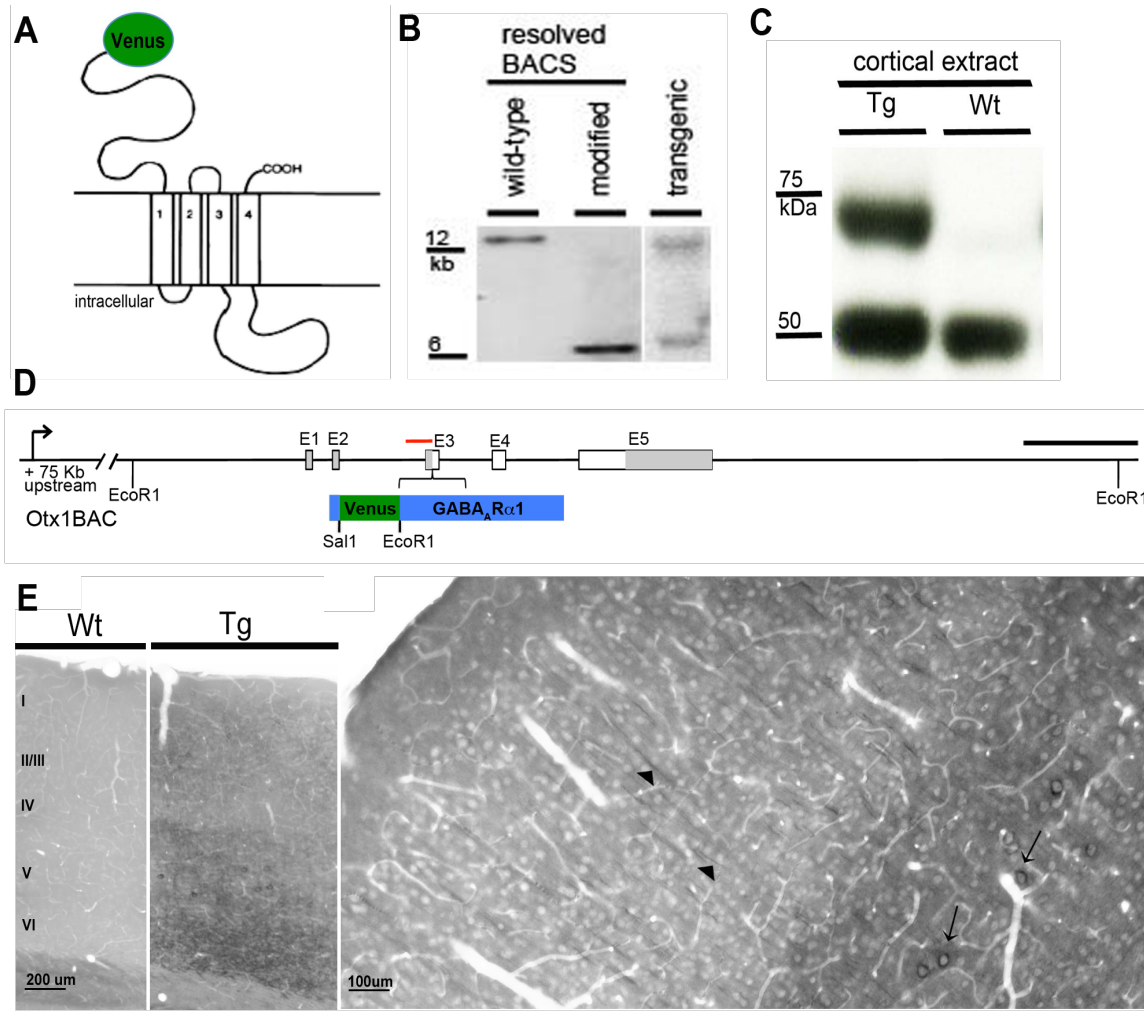

Figure 20. Tagging inhibitory synapses in a population of cortical layer V pyramidal neurons.

site into the BAC, causing the modified BAC to hybridize the probe on a restriction fragment of smaller size.

The correctly modified Otx1-Venus-GABA$_A$Rα1 BAC was then injected into oocytes, which were surgically implanted into pseudopregnant females. Genomic DNA was purified from founder mice and analyzed by

PCR (data not shown) and Southern blotting for successful insertion of the transgene (Figure 20B, right). Southern blotting of genomic DNA from the transgenic mouse shows hybridization at restriction bands of two sizes, the larger band corresponds to wild-type Otx1, while the smaller band corresponds to the Otx1-Venus-$GABA_AR\alpha1$ transgene.

Expression of the transgene *in vivo* was confirmed by collecting cortical protein extract. Proteins were separated by SDS-PAGE and immunoblotted with a rabbit anti-GFP antibody (Figure 20C). Extract from transgenic mice contained a band corresponding to the $VGABA_AR\alpha1$ fusion protein, while wild-type extract lacked the fusion protein. A nonspecific band (50 kDa) was present at equivalent levels in both extracts. Otx1-$VGABA_AR\alpha1$ transgenic mice were further analyzed by immunohistochemistry of fixed brain sections using a rabbit anti-GFP antibody (Figure 20E). $VGABA_AR\alpha1$ was detected specifically in layer V pyramidal neurons in the brain sections from transgenic mice, while no signal was detected in wild-type brain sections (Figure 20E, far left). The fusion protein was detected in the cell body as well as the proximal and distal dendrites, which corresponds to the known localization of inhibitory synaptic inputs (Figure 20E, right).

To further demonstrate the correct subcellular localization of $VGABA_AR\alpha1$, we performed immuno-electron microscopy on fixed brain sections (Figure 21). We detected $VGABA_AR\alpha1$ at the synaptic membrane apposed to inhibitory terminals, which were visualized by immunostaining with an anti-GAD65/67 antibody. These synapses were found on the cell body of layer V pyramidal neurons (Figure 21A, C) and dendrites (Figure 21B, D). The inhibitory terminals were identified by the presence of GAD, the shape and size of the synaptic vesicles, and the lack of PSD (symmetric synapse). $VGABA_AR\alpha1$ was not present at excitatory terminals except in cases where a single spine head was innervated by both excitatory and inhibitory terminals (Figure 21D). $VGABA_AR\alpha1$ was also found prominently in subcellular compartments (Figure 21A, inset), most likely as part of trafficking complexes.

Figure 21. Immuno-electron microscopy confirms Venus-GABA$_A$Rα1 localizes to inhibitory synapses. VGABA$_A$Rα1 immunolabeling is revealed by the SIG procedure in figures (A), (B), and (D) and by the DAB procedure in figure (C). Inhibitory terminals are immunoreactive for GAD65/67, which is revealed with the DAB procedure. (A) A GAD immunoreactive terminal, indicated by an asterisk, contacts the soma of a layer V pyramidal neuron and colocalizes with Venus-GABA$_A$Rα1, indicated by an arrow. VGABA$_A$Rα1 immunoreactivity is also seen intracellularly (arrowhead and inset). Asymmetric synapses are immunonegative for both GAD and VGABA$_A$Rα1 (dashed arrows). (B) A GAD immunoreactive terminal (asterisk) colocalizes with Venus-GABA$_A$Rα1 (arrow) on the dendritic shaft. (C) A layer V pyramidal cell expresses VGABA$_A$Rα1 intracellularly (arrowhead) and on the plasma membrane. The expression colocalizes with a GAD immunoreactive terminal (asterisk). (D) A GAD immunoreactive terminal (asterisk) makes a symmetric synapse onto a spine head that is immunopositive for VGABA$_A$Rα1 (arrow). The same spine also forms an asymmetric synapse (dashed arrow) that is immunonegative for GAD. An additional spine (upper left corner, dashed arrow) makes only an asymmetric synapse and is immunonegative for VGABA$_A$Rα1. Scale bars: A-C = 500μm; D = 100 μm. Cy: cytoplasm. Nu : nucleus. Sh: spine head. De: dendrite.

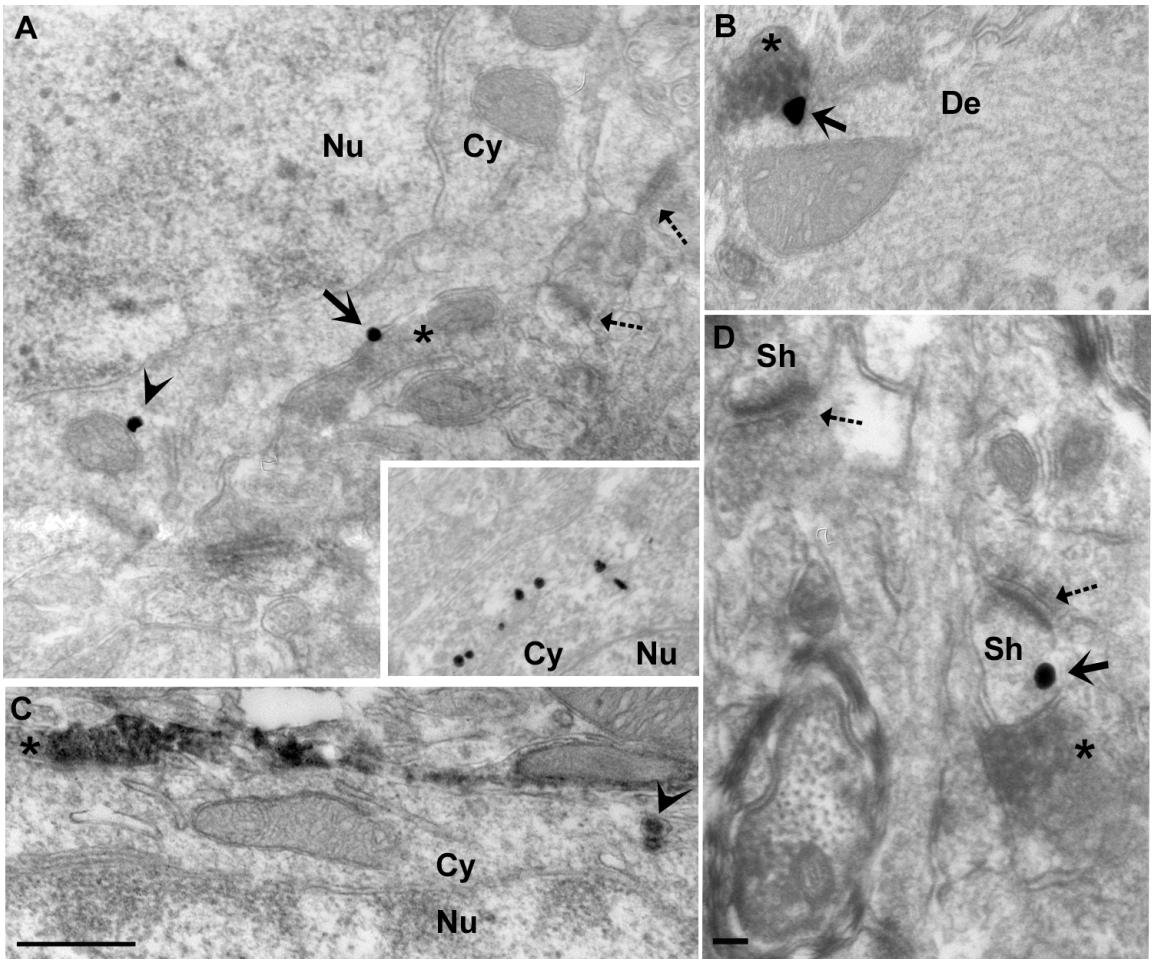

Figure 21. Immuno-electron microscopy confirms Venus-GABA$_A$Rα1 localizes to inhibitory synapses.

Biochemical purification of inhibitory synaptic protein complexes

After confirming the correct subcellular localization of the Venus-$GABA_AR\alpha1$ fusion protein we went on to biochemically purify the tagged synapses. Several methods for purification of GABA receptors have relied on detergent solubilization of a synaptic fraction, most frequently using the detergent sodium deoxycholate [171]. While these methods are useful for purifying intact receptors, we were not able to purify synaptic protein complexes in this way (data not shown). Instead, we made several modifications to the novel method we devised to purify tagged parallel fiber-Purkinje cell synapses of the cerebellum (Figure12A). Optimization of this method for enrichment of $VGABA_AR\alpha1$ tagged synapses proved successful.

Cortices from five mice were homogenized and a crude synaptosome fraction was obtained by differential centrifugation. Solubilization of this fraction in a final concentration of 0.1% Triton X-100 proved sufficient to purify intact inhibitory synaptic complexes. Sodium deoxycholate and CHAPS were also tested for their ability to solubilize Venus-$GABA_AR\alpha1$. Sodium deoxycholate was efficient in solubilizing the GABA receptor but it disrupted receptor-protein interactions, while CHAPS was inefficient (data not shown).

After solubilization, the S3 fraction was separated by size-exclusion chromatography using the gel filtration resin, Sephacryl S1000. In this way, it was possible to separate large protein complexes containing VGABA$_A$Rα1 from those that were smaller, and likely corresponding to intracellular protein complexes. Protein from each fraction was separated by SDS-PAGE and subject to immunoblotting for known markers of inhibitory and excitatory synapses, as well as the endoplasmic reticulum (ER) marker, BIP, and the mitochondrial marker, COX (Figure 22A). The early fractions (6-10) were enriched for synaptic and mitochondrial proteins, while the ER marker was selectively enriched in the later fractions (11-14), further validating their distinct subcellular localization. VGABA$_A$Rα1 was detected using a rabbit anti-GFP antibody and segregated in the gel filtration fractions similarly to wild-type GABA$_A$Rα1. The GABA receptor subunits α1, β2/3 and γ2, as well as the scaffolding protein, gephyrin, were distributed throughout the fractions, suggesting their incorporation in protein complexes of both large and small size. GABA$_A$Rα2, on the other hand, showed selective enrichment in the earlier fractions, more closely resembling the excitatory synaptic components, such as PSD95 and GluR2. The difference in fractionation of the GABA$_A$Rα1 and -α2 subunits correlates to known differences in their immunocytochemical localization and clustering [97].

Figure 22. Enrichment of inhibitory synaptic fractions followed by affinity purification of VGABA$_A$Ra1 tagged synapses. (A) We prepared a crude synaptosome fraction, P2, which was solubilized in 0.1% Triton X-100 and centrifuged to prepare a fraction, S3, enriched in inhibitory synaptic complexes. The extract was then separated on a Sephacryl S1000 gel filtration column. 0.1% in volume of every fraction was analyzed by immunoblotting for the presence of inhibitory synapse markers (GABA(A)Rα1, GABA(A)Rα2, GABA(A)Rβ2/3, GABA(A)R γ2, gephyrin), excitatory synapse markers (PSD95, GluR2), the endoplasmic reticulum marker, BIP and the mitochondrial marker, COX. VGABA$_A$Ra1 was detected using an anti-GFP antibody. The red rectangle outlines the "synaptic" fractions enriched for synaptic markers and pooled for subsequent affinity-purification of VGABA$_A$Ra1 tagged synapses. Protein dosage was performed on every fraction collected. The void volume was determined by the elution of Dextran blue sulfate.

(B) Synaptic fractions (Input 6-10) from Otx1-VGABA$_A$Ra1 mice were pooled and affinity-purified using a mouse anti-GFP antibody (IP VGABA$_A$Ra1). In parallel, control purifications were performed on preparations from Otx1-GFP transgenic mice (IP GFP). 1.0% of the inputs and 10% of the affinity-purified samples (IP) were assayed by Western blot using an anti-GFP antibody and showed immunoprecipitation of both VGluRδ2 and GFP, respectively. The same blot was probed for different synaptic markers and the mitochondrial protein COX, showing specific co-immunopurification of inhibitory synaptic markers.

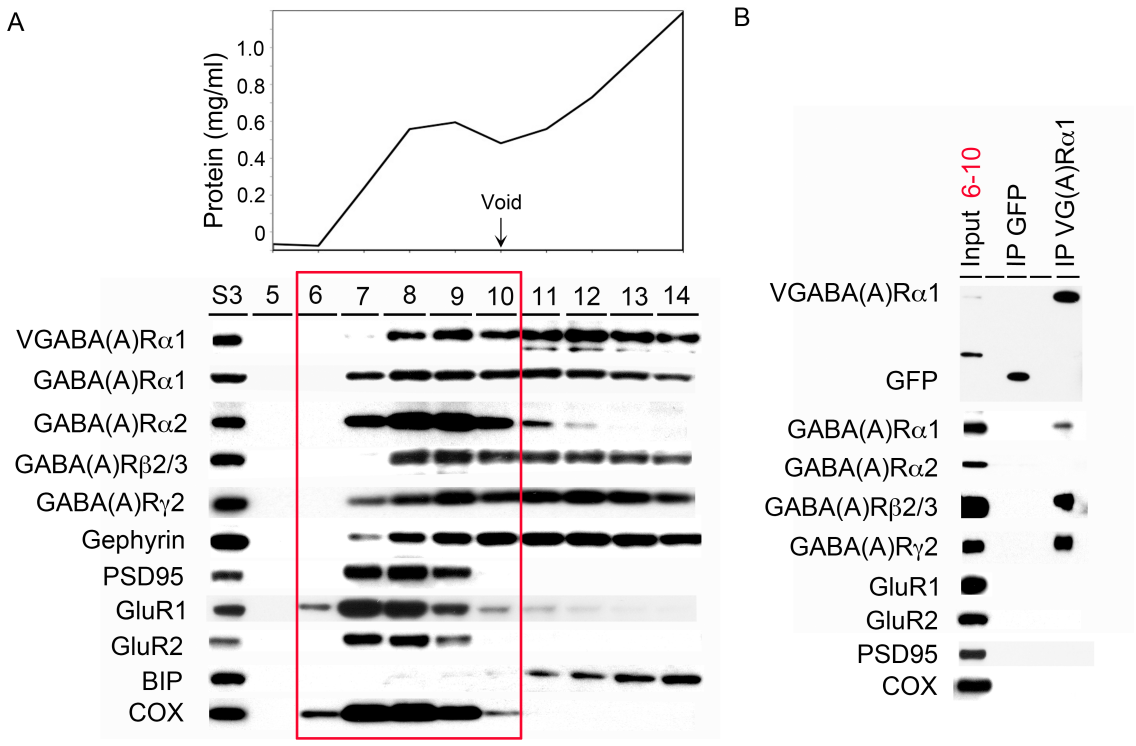

Figure 22. Enrichment of inhibitory synaptic fractions followed by affinity purification of VGABA$_A$Ra1 tagged synapses.

The same purification scheme was used to enrich for inhibitory synaptic proteins from an Otx1-GFP transgenic mouse, which expresses soluble GFP in the equivalent population of pyramidal neurons, and serves as a control for affinity purification. The distribution of proteins was identical in fractions purified from the Otx1-GFP cortices (not shown).

Next, synaptic fractions 6-10 from Otx1-GFP or Otx1-VGABA$_A$Rα1 were pooled and subject to affinity purification using a mouse monoclonal

anti-GFP antibody. The affinity-purified proteins were separated by SDS-PAGE and immunoblotted for both synaptic and nonsynaptic proteins (Figure 22B). We detected either GFP or VGABA$_A$Rα1 in the immunopurified (IP) material using an anti-GFP antibody. The wild-type GABA$_A$ receptors α1, β2/3 and γ2 were detected in the IP from the Otx1-VGABA$_A$Rα1 mouse, confirming that the fusion protein incorporates correctly with the endogenous GABA$_A$R subunits. Alternatively, GABA$_A$ receptor α2 was absent from the IP lane. Excitatory synaptic components, such as PSD95, GluR1 and GluR2 were also absent from the IP, as well as the ER marker, BIP, and the mitochondrial marker, COX. Material from the Otx1-GFP control mouse lacked any co-immunopurified proteins, confirming the specificity of our affinity purification technique. Standard amounts of soluble GFP were also run on the gel, to allow approximation of the quantity of fusion protein. This was useful in determining the amount of protein to pool for analysis by mass spectrometry.

Mass spectrometry of cortical inhibitory synapses

Affinity purified synaptic material was pooled from 25 cortices from either Otx1-Venus-GABA$_A$Rα1 or Otx1-GFP and analyzed by mass spectrometry. Proteins were alkylated and denatured, separated by SDS-

PAGE and stained with zinc. Excised bands were digested with trypsin and the resulting peptides subject to liquid chromatography-tandem mass spectrometry (LC-MS/MS). Using this method we have so far generated a list of 12 proteins found specifically in the material immunopurified via VGABA$_A$Rα1, and absent from the material purified via GFP (Table 5).

Mass spectrometry identified several wild-type GABA$_A$R subunits, including α1, α2, α3, β1, β2, β3 and γ2, all of which are expressed in inhibitory cortical pyramidal cells. It is noteworthy that GABA$_A$Rα2 subunit was present, as this subunit was not detectable by immunoblotting of the same material. This is likely due to the difference in abundance of the immunopurified material in the two types of analysis. Absent from our co-IP were several non-cortical GABA$_A$R subunits, including α6, which is exclusively expressed in cerebellar granule cells and the cochlea, and the γ1 subunit, which is enriched in the amygdala, pallidal areas, the substantia nigra and the inferior olive [3].

Table 5. Proteins uniquely immunopurified via Venus-GABA$_A$Rα1

	Protein name (a)	ensemble # (b)	MW(kDa)	log(e)+ (c)	sequence coverage(%) (d)	peptide # (e)	unique peptide # (f)
Isolated proteins (mus musculus)	GABA(A) receptor subunit alpha-1	00000020707	51.7	-107.6	29.4	17	8
	GABA(A) receptor subunit alpha-2	000000572	51.1	-61.9	19.5	8	3
	GABA(A) receptor subunit alpha-3	00000062638	55.4	-36.3	9.5	5	2
	GABA(A) receptor subunit beta-2	00000007797	54.6	-74.1	27.4	10	4
	GABA(A) receptor subunit beta-1	00000031122	54.1	-46.9	19.2	7	2
	GABA(A) receptor subunit beta-3	00000038051	54.1	-46.7	22.2	9	2
	GABA(A) receptor subunit gamma-2	00000063812	55.1	-13.9	7.8	3	
	Synaptic vesicle glycoprotein 2B	00000065495	77.4	-6.2	3.2	2	
	Gephyrin	00000054064	80.7	-20.4	6.1	4	
	Neuroligin-2	00000053097	90.9	-143.3	21	16	
	Glutamate receptor ionotropic, AMPA 2	00000074787	98.7	-18.9	5	5	
	Homer protein homolog 1 (VASP/Ena-related gene)	00000079026	41.6	-19.9	10	4	
Likely contaminants	Alpha-actinin-1	00000021554	103	-44.5	8	6	
	Alpha-actinin-2	00000067708	103.8	-7.8	2.6	2	

Table 5. Proteins uniquely immunopurified via Venus-GABA$_A$Rα1 were determined by subtracting proteins immunoisolated via GFP. (a) Proteins were identified by the GPM protein sequence database search program using data from LC-MS/MS experiments. (b) Ensemble # is the protein accession number in Ensemble Mouse database. (c) Log(e) is the base-10 log of the expectation that an assignment is stochastic.

(d) Sequence coverage shows the percentage of protein sequence covered by the identified peptides. (e) Peptide # shows the number of identified peptides. (f) Unique peptide # shows the number of peptide matches that are unique to the homologue, when more than one homologues are reported.

In addition to $GABA_A$ receptor subunits, we found two additional inhibitory synaptic proteins in the immunopurified material, gephyrin and neuroligin-2 (NL-2). Gephyrin, a microtubule binding protein, is a known component of inhibitory synapses [108, 172] and may be important for clustering of these receptors [107]. Neuroligin-2 is a cell adhesion molecule with known specificity for inhibitory synapses [138], which likely plays a role in synaptogenesis and maintenance of these contacts. The presence of gephyrin and NL-2 in the IP was confirmed by immunoblotting (Figure 23).

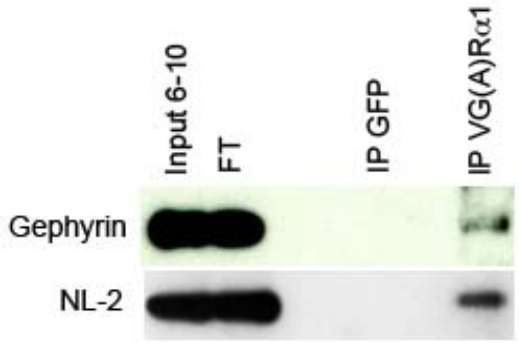

Figure 23. Immunoblot analysis confirms the presence of gephyrin and neuroligin-2 in immunopurified material. Inhibitory synaptic complexes were biochemically enriched from 5 cortices and affinity purified using a monoclonal mouse anti-GFP antibody against soluble GFP (IP GFP) or Venus-$GABA_A$Rα1 (IP VG(A)Rα1). The total amount of IP was separated by SDS-PAGE and analyzed by immunoblotting for gephyrin and neuroligin-2 (NL-2).

Excitatory synaptic components are almost entirely excluded from the IP, with the exception of the AMPA receptor subunit, GluR2. The presence of GluR2 was surprising given the absence of GluR2 on immunoblots, but might be relevant as it appeared in the absence of additional excitatory proteins, including additional AMPA receptor subunits and PSD95.

Two potentially novel members of inhibitory synapses were identified by mass spectrometry, Homer protein homolog 1 (Homer1) and Synaptic vesicle glycoprotein 2B (SV2B). Homer is known to cluster components of the excitatory postsynaptic density [75], and may play a similar role at inhibitory synapses. SV2B is located presynaptically and, together with SNAP-25 and synaptotagmin, functions in neurotransmitter release [173]. Further work will be necessary to clarify whether SV2B is a contaminant or is localized postsynaptically at cortical inhibitory synapses.

Summary.

We have successfully generated transgenic mice that express a Venus-$GABA_AR\alpha1$ fusion protein in layer V cortical pyramidal neurons. Light and electron microscopy confirmed the presence of the tagged receptor at inhibitory synapses in the targeted cell type. A novel approach to the biochemical enrichment of inhibitory synaptic protein complexes followed

by affinity purification via the tagged receptor, proved efficient in isolating the inhibitory synaptic protein complex. Mass spectrometry of this complex revealed twelve proteins, including several $GABA_AR$ subunits expressed in cortical pyramidal neurons. We also identified two specific inhibitory synaptic clustering proteins, gephyrin and neuroligin-2, thus demonstrating the efficacy of our method for the *in vivo* biochemical purification of inhibitory synaptic complexes.

Mass spectrometry also identified several components whose functions are not readily apparent. The presence of excitatory AMPA receptor GluR2 subunit as well as Homer protein homolog 1, coupled with the absence of additional AMPA receptor subunits or the major excitatory scaffolding protein, PSD95, suggests a novel function or localization of these synaptic proteins. Further analysis of this complex, including additional affinity purification experiments, will be required to determine the specificity of these proteins to inhibitory synapses in mouse cerebral cortex.

DISCUSSION

Activity at the synapse, a discrete site of contact between the pre- and post-synaptic neurons, is the basis for neurotransmission in the central nervous system. Synapses are complex and dynamic structures, composed of a multitude of proteins, such as neurotransmitter receptors, scaffolding proteins, and signaling molecules. Given that an individual neuron receives thousands of synaptic inputs, there likely exists a molecular mechanism for defining and maintaining unique synapse types. To determine the protein specification for individual synapses it is necessary to purify and analyze the protein content of only a single class of synapse. A comparative analysis of multiple synapse types could lead to valuable insights into the molecular mechanisms of synapse specification. Such a comprehensive approach is possible due to the availability of hundreds of BAC vectors for neuronal cell-type specific expression of a transgene (www.gensat.org). We have taken advantage of this approach to target individual cell types for expression of a synaptic affinity tag, which was then used to purify synaptic protein complexes. Mass spectrometric analysis was used to generate a protein profile of each purified synapse type and to identify novel and functionally relevant synaptic proteins.

We first targeted the parallel fiber to Purkinje cell (PF/PC) excitatory synapse of the cerebellum for purification and mass spectrometry analysis. The PF/PC synapse is unique in that it contains the orphan receptor, GluRδ2, which is genetically defined as being between NMDA and non-NMDA receptor types. Although the precise function of GluRδ2 is not completely understood, is required for correct motor development and function, and has also been implicated in several neurological diseases [162]. It is also necessary for long-term depression in the cerebellum, and motor learning dependant on this structure [80]. A second excitatory input to the Purkinje cell is from climbing fibers (CF/PC), but these synapses do not contain GluRδ2 [65]. Proteomic analysis is likely to provide insight into the unique molecular and functional properties of the PF/PC synapse.

To analyze only the PF/PC synapse, we targeted expression of a Venus-GluRδ2 fusion protein to Purkinje cells of the cerebellum. This fusion protein enabled affinity purification of the PF/PC synaptic protein complex using an anti-GFP antibody to recognize Venus. A major advantage of employing a synaptic affinity tag is that it allowed comparison of the immunopurified proteins to those contaminants immunopurified via soluble GFP expressed in the same cell type. In order to maximize recovery of synaptic proteins for analysis by mass spectrometry, we employed a novel

method of PSD purification that relied on gel filtration of a solubilized crude synaptic fraction. Gel filtration resulted in a a pool of large protein complexes, enriched in excitatory synaptic proteins, including Venus-GluRδ2, relative to trafficking and inhibitory synaptic proteins. Affinity purification with an anti-GFP antibody was successful in purifying a large protein complex that contained GluRδ2 and other markers of excitatory synapses, such as GluR2 and PSD95, while components of inhibitory synapses and ER were absent.

Mass spectrometric analysis of this complex identified 65 proteins, which were organized into 11 functional categories. Most of these categories have previously been included in descriptions of the postsynaptic specialization [174], but one category, "phospholipid metabolism and signaling" contained several members newly associated with the PF/PC synapse. This group included eight proteins that can regulate or be regulated by phospholipid metabolism (Iptr1, synaptojanin 1 and 2, phospholipase B, ABCA12, MRCKγ) or contain phospholipid binding domains (Plekha7, annexin A6, MRCKγ). This suggests that phospholipid regulation is a major feature of the PF/PC synapse, in accordance with the major role of the metabotropic glutamate receptor 1 (mGluR1) in regulating the physiology of the PF/PC synapse [67]. mGluR1 exerts its action by inducing

phosphatidylinositol-4,5-P2 (PIP2) hydrolysis [175, 176]. Two of the proteins we identified, MRCKγ and Itpr1, respond to the metabolites of PIP2 hydrolysis (DAG and IP3, respectively) and may be key components of the molecular pathway by which mGluR1 functions at this synapse.

Phosholipid metabolism has been strongly implicated in presynaptic functions, such as vesicle recycling [177], and our results show that it also likely plays a role in postsynaptic regulation of the synapse. In particular, two proteins we identified at PF/PC synapses, synaptojanin-1 and -2, are PIP2-metabolizing enzymes that are found both pre- and post-synaptically [174]. Another interesting member of this category, MRCKγ, has not previously been shown at PF/PC synapses and is known to modulate actin cytoskeleton and cell morphology [178]. This is interesting since deficiencies in spine length and spine morphology of Purkinje cells may play a role in neurodevelopmental diseases such as mental retardation and Angelman syndrome [145, 159].

The diversity of proteins present at the PF/PC synapse demonstrates the complexity of the PSD and suggests the possibility of a "synaptic code" to define individual synapse types. Proteins that contain classical adhesion domains are commonly found at synapses and targeting of particular adhesion molecules could specify synapse types. For example, our study

identified Neph1 and the receptor tyrosine phophatase, RPTPmu. Given the known role of the C. elegans Neph1 homolog, SYG1, in specifying synapses *in vivo*, it is possible that Neph1 may play a role in specifying the PF/PC synapse as distinct from the CF/PC synapse. Receptor tyrosine phosphatases play important roles in axon guidance, and have also been shown to control synapse formation [179].

The majority of proteins identified in this study are specifically expressed in Purkinje cells. This conforms with previous studies of expression analysis of proteins identified in bulk synapse preparations, which show that receptors and other upstream signaling molecules have a highly variable expression pattern in the vertebrate brain [180]. Furthermore, the diversity of excitatory inputs within the Purkinje cells may suggest that quite distinct sets of proteins are necessary for specifying an individual class of synapse.

Our initial approach to the study of such specificity employed the expression of Venus-GluRδ2 fusion protein in the Purkinje cell, which is localized specifically to the PF/PC synapse. In order to identify synaptic proteins enriched at other excitatory inputs to Purkinje cells, we sought to express a Venus-GluR2 fusion protein under the same BAC regulatory control elements. Since GluR2 is present at both PF/PC and CF/PC

synapses [65], a subtraction method could be used to define a class of proteins differentially expressed at each synapse type. Although it was possible to express Venus-GluR2 in HEK293T cells (not shown) this fusion protein was not expressed *in vivo* in the cerebellum (Pcp2-VGluR2) or in the cortex (Otx1-VGluR2).

An instructive comparison to identify regulators of synaptic specificity is between excitatory synapses in distinct brain regions and/or cell types. We took advantage of the available BAC vectors for cortical pyramidal cell expression to localize a Venus-GluR1 fusion protein to excitatory synapses in distinct cortical cell types. Although VGluR1 was expressed with correct topography in HEK293 cells, only low levels were detectable in the cortex *in vivo* under control of several BAC vector sequences (Otx1, March4, Ntsr1, Drd4, Glt25d2). One transgenic line, Otx1-VGluR1$_7$ expressed VGluR1 in CA3 and DG of hippocampus due to a positional effect of transgene insertion. VGluR1 was highly expressed and appeared by immunofluorescence to localize to dendrites. However, affinity purification of VGluR1 from hippocampus and cortex of Otx1-VGluR1$_7$, and from cortex of an additional line (Glt25d2-VGluR1) showed that this fusion protein did not likely traffic to synapses.

Our findings that Venus-GluR2 and Venus-GluR1 are not correctly

localized to excitatory synapses *in vivo* are contrast with a number of studies that utilize these fusion proteins to examine AMPA receptor function [84, 86-88, 181]. GFP-GluR1 fusion protein expressed *in vitro* mainly forms homomeric receptors that are distinguished electrophysiologically by alterations in their rectification properties [86, 87]. In one study, GPF tagged GluR2 was expressed in cultured hippocampal neurons, efficiently inserted into the synapse and was shown to interact with GRIP and NSF, known regulators of AMPA receptor trafficking [181]. In another study, GFP-GluR1 was introduced into neurons with the Sindbis virus expression system to levels three times that of endogenous GluR1 and trafficked efficiently to synapses [86]. In both experiments, recombinant GluR1 subunits were distributed similarly to the endogenous GluR1 subunit and delivered to the synapse.

There are several potential explanations for the differences in expression of tagged glutamate receptors in our BAC transgenic animals compared to those published in the literature. First, there are likely greater regulatory constraints on glutamate receptor expression and trafficking in the intact brain than in dissociated neurons or organotypic slice cultures. These differences may manifest by cell type, as exemplified by the higher level of expression of VGluR1 in hippocampus than in cortex, and the fact that most

studies of these recombinant receptors were carried out in dissociated hippocampal neurons or hippocampal slice cultures. Tissue specific regulation of AMPA receptor trafficking is supported by the expression of distinct transmembrane AMPA receptor regulatory protein (TARP) isoforms in hippocampus and cortex, which interact with AMPA receptors at the post-synaptic density and are required for their surface expression [182]. Second, most expression systems result in levels of AMPA receptor fusion protein those are much higher than endogenous levels. If only a small percentage of GFP-GluR1 is properly assembled into synaptic protein complexes, it would be possible to detect this protein at synapses only when expressed at extremely high levels. Third, homomeric GFP-GluR1 receptors may not be efficiently trafficked to the synapse *in vivo* at physiological levels of expression.

Finally, the fact that Venus-GluR2 was not expressed at all in our transgenic mice points to differences in the regulation and trafficking of the various AMPA receptor subunits [183, 184]. AMPARs assembled as GluR2 homomers or GluR2/GluR3 heteromers cycle in and out of the synaptic membrane in a constitutive manner, which does not require synaptic activity [185, 186]. This constitutive trafficking requires GluR2-specific interactions with NSF [187]. In contrast, AMPARs containing the GluR1 subunit

translocate into spines and are inserted into synapses in response to NMDA-receptor activation during LTP [84]. The constitutive nature of GluR2 trafficking may indicate differences in regulation of assembly and insertion of this subunit and preclude the expression of a Venus-tagged GluR2 subunit at physiological levels *in vivo*.

Because we could not co-immunopurify any excitatory synaptic proteins via Venus-GluR1 or Venus-GluR2, it was not possible to profile additional excitatory synapses. Improvements in the design of affinity tagged AMPA receptor subunits may facilitate their proper insertion into synapses and enable future studies.

In addition to excitatory synapses, we undertook a study of inhibitory synaptic protein complexes. Because inhibitory synapses lack a detergent insoluble PSD, they have not been biochemically purified with classical methods. Our alternative method relied on size exclusion chromatography rather than density centrifugation to enrich for large protein complexes. This approach enabled the purification of a complex of inhibitory synaptic proteins. Using the BAC transgenic approach, we expressed a Venus-$GABA_A\alpha1$ subunit in a subpopulations of pyramidal neurons of mouse cerebral cortex and showed that this receptor was similar to the endogenous $GABA_A\alpha1$ subunit in the various purification steps. Interestingly, gel

filtration revealed differences in the subcellular distribution of $GABA_A\alpha1$ and $\alpha2$ subunits. The $\alpha2$ subunit was concentrated in the early fractions, which contained large protein complexes, and its distribution resembled markers of insoluble excitatory PSDs. By contrast, the $\alpha1$ subunit was distributed throughout the fractions, in both large and small protein complexes. These observations correlate with published differences in $GABA_A$ receptor subunit distribution in neurons. For example, hippocampal pyramidal neurons cluster receptors containing $\alpha2$ subunits at synapses on the axon initial segment and dendrites, whereas receptors containing $\alpha1$ subunits are more uniformly expressed [10, 96]. In addition, a diffuse $GABA_A$ receptor subunit immunoreactivity can be seen throughout the brain in addition to clusters, suggesting the presence of a sizable pool of extrasynaptic receptors [95, 108], as shown by postembedding immuno-electron microscopy [96]. We also saw a large population of extrasynaptic Venus-$GABA_A\alpha1$ subunit by electron microscopy, and saw both the tagged and wild-type $\alpha1$ subunits distributed across both large- and small-protein-complex fractions during gel filtration. The distribution of $GABA_A$ receptor subunits may be indicative of differences in their subcellular localization or unique trafficking properties. A better understanding of such differences could be gained by subunit-specific proteomic analysis of $GABA_A$ receptor

interacting proteins.

We used affinity purification to explore the proteins present at Venus-$GABA_A\alpha1$ tagged inhibitory synapses. By pooling the purified material from an equivalent of twenty-five cortices, we were able to identify twelve proteins specifically immunopurified with Venus-$GABA_A\alpha1$. This list is preliminary, as we have not yet replicated the mass spectrometry analysis. Of these twelve proteins, most were additional $GABA_A$ receptor subunits, including $\alpha1$, $\alpha2$, $\alpha3$, $\beta1$, $\beta2$, $\beta3$, and $\gamma2$, all of which are expressed in inhibitory cortical pyramidal cells. This result indicates that the tagged $\alpha1$ receptor assembles properly into mature $GABA_A$ receptors. The $\alpha2$ subunit is likely present in this complex at lower levels than wild-type $\alpha1$, $\beta2$, $\beta3$ and $\gamma2$, as it was not initially identified by immunoblotting of a small percentage of the purified material. As described above, the $\alpha1$ and $\alpha2$ subunits are thought to segregate into distinct receptor pools *in vivo*. Perhaps they only colocalize in a fraction of synapses, and this interaction is detectable only by the very sensitive methods of mass spectrometry for detection of proteins in a complex sample.

In addition to the various receptor subunits, mass spectrometry positively identified gephyrin, a multidomain protein that likely provides a scaffold for postsynaptic proteins and an anchor to the cytoskeleton [28]. A

recent study has identified a 10-amino-acid sequence within the major intracellular domain of the α2 subunit that regulates the accumulation of $GABA_A$ receptors at postsynaptic specializations, in a process dependent on gephyrin [107]. Studies of the retina have shown that $GABA_A$ receptors containing the α1 subunit were not colocalized with gephyrin, suggesting that gephyrin was associated only with certain receptor subtypes [188]. However, recent results indicate that in brain gephyrin does in fact colocalize with $GABA_A$ receptor subunits α1, α2, and α3, as well as the γ2 subunit [98]. Our results provide further evidence that gephyrin is indeed present at $GABA_A$α1 containing synapses.

The precise function and localization of gephyrin in clustering of $GABA_A$ receptors remains elusive, as many studies have provided contrasting results. Whereas removal of gephyrin by gene targeting or mRNA expression interference strongly affects $GABA_A$ receptor clustering [189], some $GABA_A$ receptor clusters can still form in neurons lacking gephyrin [110]. Furthermore, the subsynaptic localization of gephyrin in GABAergic synapses depends on $GABA_A$ receptor clustering. That is, when $GABA_A$ receptor postsynaptic clusters are disrupted by targeted deletion of the gene encoding the γ2 subunit, gephyrin clusters disappear and the receptors disperse in the cell membrane [190, 191]. The distribution of

gephyrin in our gel filtration fractions to both large and small protein complexes may underlie its divergent functions. Inconsistencies in the data on the role of gephyrin at inhibitory synapses suggest the presence of additional clustering and scaffolding molecules that regulate inhibitory synaptic structure.

One potential regulatory protein is neuroligin-2, a cell adhesion molecule involved in synapse formation [122, 192, 193] and localized specifically to inhibitory synapses *in vivo* [138]. Studies have shown that neuroligins are capable of inducing both excitatory and inhibitory presynaptic contact formation, and that the precise synapse formed depends on interactions of the appropriate neuroligin with scaffolding molecules, such as neurexin1-β and PSD95 [194]. For example, enhanced expression of PSD-95 induces clustering of NL-2 and NL-3 and shifts endogenous NL-2 from inhibitory to excitatory synapses [195]. These findings provided evidence that assembly of specific postsynaptic elements can regulate a balance between excitatory and inhibitory synapses. Thus, abnormalities in the expression of and/or interactions between these molecules may result in aberrant synapse formation and a change in the ratio of excitatory to inhibitory inputs. An upset in the balance of excitatory and inhibitory synapses is thought to underlie complex psychiatric disorders [196-198].

The identification by mass spectrometry of NL-2, and the absence of NL-1, demonstrates the specificity and efficacy of our approach to purifying inhibitory synaptic protein complexes.

In addition to specific markers of inhibitory synapses, mass spectrometry of Venus-$GABA_A$ α1 tagged protein complexes identified two proteins that are typically found at excitatory receptors, AMPA receptor subunit GluR2 and Homer protein homolog 1. It is noteworthy that the GluR2 subunit alone was localized to our tagged inhibitory synapses, since it is typically found as part of heteromeric receptors that contain either GluR1 or GluR3 [199]. The GluR2 subunit of AMPA receptors interacts with NSF and this interaction has been shown to cause differences in intracellular sorting and trafficking of GluR2 compared to the other AMPA receptor subunits [184]. GABARAP, a $GABA_A$ receptor binding protein, also binds NSF and is involved in trafficking of receptors to the synapse [170, 200]. Further analysis will be required to determine if AMPA receptor GluR2 subunits are in fact localized to inhibitory synapses, and if this is mediated by GABARAP via their common interaction with NSF.

Homer protein homolog 1 (Homer1) is a member of the Homer family of adaptor proteins, which are predominantly localized to the PSD in mammalian neurons. Each Homer protein has several variants, which are

classified primarily into the long and short forms. The long Homer forms, which include Homer1, are constitutively expressed and consist of two major domains: the amino-terminal target-binding domain, which includes an Enabled/vasodilator-stimulated phosphoprotein (Ena/VASP) homology 1 (EVH1) domain, and the carboxy-terminal self-assembly domain containing a coiled-coil structure and leucine-zipper motif [75]. The EVH1 domain is homologous to that of mENA/VASP, a microfilament binding protein known to be involved in the structural organization of inhibitory synapses [111, 201]. Perhaps Homer1 also plays a role in the structural integrity of these synapses via its interaction with additional adapter molecules, although immunohistochemical analysis of Homer1 localization in cortical pyramidal neurons is necessary to confirm its presence at inhibitory synapses. Evidence for the presence of postsynaptic scaffolding proteins common to both inhibitory and excitatory receptors is supported by the identification of an isoform of GRIP1 that colocalizes with GABA receptor in cultured hippocampal neurons [112]. It is possible that we have identified a unique isoform of Homer in inhibitory synaptic protein complexes.

Our ability to tag and purify individual synapse types was facilitated by the use of BAC transgenesis for expression of synaptic tags in a multitude of cell types. We have shown here that it is indeed possible to analyze an

individual class of synapse and generate a list of specific and functionally interesting synaptic proteins. The value of such an approach lies in the ability to compare multiple synapse types across various brain regions. Already we can observe a striking difference in the molecular complexity of excitatory and inhibitory synaptic protein complexes. This difference is expected, as the simpler, symmetric structure of inhibitory synapses suggests that they contain vastly fewer molecules. In the case of both excitatory and inhibitory synapses we have identified novel potential synaptic components whose functional relevance will be assayed in future experiments.

REFERENCES

1. Fritschy, J.M. and H. Mohler, *GABAA-receptor heterogeneity in the adult rat brain: differential regional and cellular distribution of seven major subunits.* J Comp Neurol, 1995. **359**(1): p. 154-94.

2. Pirker, S., et al., *GABA(A) receptors: immunocytochemical distribution of 13 subunits in the adult rat brain.* Neuroscience, 2000. **101**(4): p. 815-50.

3. Sieghart, W. and G. Sperk, *Subunit composition, distribution and function of GABA(A) receptor subtypes.* Curr Top Med Chem, 2002. **2**(8): p. 795-816.

4. Wisden, W., et al., *The distribution of 13 GABAA receptor subunit mRNAs in the rat brain. I. Telencephalon, diencephalon, mesencephalon.* J Neurosci, 1992. **12**(3): p. 1040-62.

5. *The Gene Expression Nervous System Atlas (GENSAT) Project*, NINDS Contracts N01NS02331 & HHSN271200723701C to The Rockefeller University (New York, NY).

6. Heintz, N., *BAC to the future: the use of bac transgenic mice for neuroscience research.* Nat Rev Neurosci, 2001. **2**(12): p. 861-70.

7. Kwok, K.H., et al., *Cellular localization of GluR1, GluR2/3 and GluR4 glutamate receptor subunits in neurons of the rat neostriatum.* Brain Res, 1997. **778**(1): p. 43-55.

8. Martin, L.J., et al., *AMPA glutamate receptor subunits are differentially distributed in rat brain.* Neuroscience, 1993. **53**(2): p. 327-58.

9. Vissavajjhala, P., et al., *Synaptic distribution of the AMPA-GluR2 subunit and its colocalization with calcium-binding proteins in rat cerebral cortex: an immunohistochemical study using a GluR2-specific monoclonal antibody.* Exp Neurol, 1996. **142**(2): p. 296-312.

10. Kittler, J.T., K. McAinsh, and S.J. Moss, *Mechanisms of GABAA receptor assembly and trafficking: implications for the modulation of inhibitory neurotransmission.* Mol Neurobiol, 2002. **26**(2-3): p. 251-68.

11. Kittler, J.T. and S.J. Moss, *Modulation of GABAA receptor activity by phosphorylation and receptor trafficking: implications for the efficacy of synaptic inhibition.* Curr Opin Neurobiol, 2003. **13**(3): p. 341-7.

12. Harris, K.M. *Synapse Web*. 1999; Available from: http://synapses.clm.utexas.edu/.

13. Douglas, R. and K. Martin, *Neocortex*, in *The synaptic organization of the brain*, G.M. Shepherd, Editor. 1998, Oxford University Press: New York. p. 459-510.

14. Wikipedia. *Diagram of the cerebellar circuitry.* 2002; Available from: http://en.wikipedia.org/wiki/File:CerebCircuit.png.

15. Shepherd, G.M., *The Synaptic Organization of the Brain*. 4th ed. 1998, New York: Oxford University Press.

16. Hollmann, M. and S. Heinemann, *Cloned glutamate receptors.* Annu Rev Neurosci, 1994. **17**: p. 31-108.

17. Somogyi, P., et al., *Salient features of synaptic organisation in the cerebral cortex.* Brain Res Brain Res Rev, 1998. **26**(2-3): p. 113-35.

18. Lisman, J., *A mechanism for the Hebb and the anti-Hebb processes underlying learning and memory.* Proc Natl Acad Sci U S A, 1989. **86**(23): p. 9574-8.

19. Malenka, R.C. and R.A. Nicoll, *Long-term potentiation--a decade of progress?* Science, 1999. **285**(5435): p. 1870-4.

20. Scannevin, R.H. and R.L. Huganir, *Postsynaptic organization and regulation of excitatory synapses.* Nat Rev Neurosci, 2000. **1**(2): p. 133-41.

21. Skutella, T. and R. Nitsch, *New molecules for hippocampal development.* Trends Neurosci, 2001. **24**(2): p. 107-13.

22. Kim, E. and M. Sheng, *PDZ domain proteins of synapses.* Nat Rev Neurosci, 2004. **5**(10): p. 771-81.

23. Ponomarev, I., et al., *Transcriptional signatures of cellular plasticity in mice lacking the alpha1 subunit of GABAA receptors.* J Neurosci, 2006. **26**(21): p. 5673-83.

24. Enna, S.J. and H. Mohler, *The GABA Receptors*. 3rd ed. The Receptors, ed. K.A. Neve. 1997, Totowa, New Jersey: Humana Press.

25. Sheng, M., *Molecular organization of the postsynaptic specialization.* Proc Natl Acad Sci U S A, 2001. **98**(13): p. 7058-61.

26. Kasai, H., et al., *Structure-stability-function relationships of dendritic spines.* Trends Neurosci, 2003. **26**(7): p. 360-8.

27. Breukel, A.I., E. Besselsen, and W.E.J.M. Ghijsen, *Synaptosomes: A model system to study release of multiple classes of neurotransmitters.*, in *Neurotransmitter Methods*, R. Rayne, Editor. 1997, Humana Press: Totowa. p. 33-48.

28. Fritschy, J.M., R.J. Harvey, and G. Schwarz, *Gephyrin: where do we stand, where do we go?* Trends Neurosci, 2008. **31**(5): p. 257-64.

29. Moss, S.J. and T.G. Smart, *Constructing inhibitory synapses.* Nat Rev Neurosci, 2001. **2**(4): p. 240-50.

30. Carlin, R.K., et al., *Isolation and characterization of postsynaptic densities from various brain regions: enrichment of different types of postsynaptic densities.* J Cell Biol, 1980. **86**(3): p. 831-45.

31. Cho, K.O., C.A. Hunt, and M.B. Kennedy, *The rat brain postsynaptic density fraction contains a homolog of the Drosophila discs-large tumor suppressor protein.* Neuron, 1992. **9**(5): p. 929-42.

32. Husi, H., et al., *Proteomic analysis of NMDA receptor-adhesion protein signaling complexes.* Nat Neurosci, 2000. **3**(7): p. 661-9.

33. Walikonis, R.S., et al., *Identification of proteins in the postsynaptic density fraction by mass spectrometry.* J Neurosci, 2000. **20**(11): p. 4069-80.

34. Husi, H. and S.G. Grant, *Proteomics of the nervous system.* Trends Neurosci, 2001. **24**(5): p. 259-66.

35. Dosemeci, A., et al., *Preparation of postsynaptic density fraction from hippocampal slices and proteomic analysis.* Biochem Biophys Res Commun, 2006. **339**(2): p. 687-94.

36. Jordan, B.A., et al., *Identification and verification of novel rodent postsynaptic density proteins.* Mol Cell Proteomics, 2004. **3**(9): p. 857-71.

37. Satoh, K., et al., *Identification of activity-regulated proteins in the postsynaptic density fraction.* Genes Cells, 2002. **7**(2): p. 187-97.

38. Yoshimura, Y., et al., *Molecular constituents of the postsynaptic density fraction revealed by proteomic analysis using multidimensional liquid chromatography-tandem mass spectrometry.* J Neurochem, 2004. **88**(3): p. 759-68.

39. Chen, X., et al., *Mass of the postsynaptic density and enumeration of three key molecules.* Proc Natl Acad Sci U S A, 2005. **102**(32): p. 11551-6.

40. Petersen, J.D., et al., *Distribution of postsynaptic density (PSD)-95 and Ca2+/calmodulin-dependent protein kinase II at the PSD.* J Neurosci, 2003. **23**(35): p. 11270-8.

41. Sheng, M. and C.C. Hoogenraad, *The postsynaptic architecture of excitatory synapses: a more quantitative view.* Annu Rev Biochem, 2007. **76**: p. 823-47.

42. Ramon y Cajal, S., *Cajal on the cerebral cortex: an annotated translation of the complete writings.* History of Neuroscience, ed. J. DeFelipe and E.G. Jones. 1988, New York: Oxford University Press. 654.

43. Somogyi, P. and T. Klausberger, *Defined types of cortical interneurone structure space and spike timing in the hippocampus.* J Physiol, 2005. **562**(Pt 1): p. 9-26.

44. Toyama, K., et al., *An intracellular study of neuronal organization in the visual cortex.* Exp Brain Res, 1974. **21**(1): p. 45-66.

45. Castro-Alamancos, M.A. and B.W. Connors, *Thalamocortical synapses.* Prog Neurobiol, 1997. **51**(6): p. 581-606.

46. Dantzker, J.L. and E.M. Callaway, *Laminar sources of synaptic input to cortical inhibitory interneurons and pyramidal neurons.* Nat Neurosci, 2000. **3**(7): p. 701-7.

47. Feldmeyer, D. and B. Sakmann, *Synaptic efficacy and reliability of excitatory connections between the principal neurones of the input (layer 4) and output layer (layer 5) of the neocortex.* J Physiol, 2000. **525 Pt 1**: p. 31-9.

48. Hevner, R.F., et al., *Beyond laminar fate: toward a molecular classification of cortical projection/pyramidal neurons.* Dev Neurosci, 2003. **25**(2-4): p. 139-51.

49. Wu, S.X., et al., *Pyramidal neurons of upper cortical layers generated by NEX-positive progenitor cells in the subventricular zone.* Proc Natl Acad Sci U S A, 2005. **102**(47): p. 17172-7.

50. Guillemot, F., et al., *Molecular mechanisms of cortical differentiation.* Eur J Neurosci, 2006. **23**(4): p. 857-68.

51. Molnar, Z. and A.F. Cheung, *Towards the classification of subpopulations of layer V pyramidal projection neurons.* Neurosci Res, 2006. **55**(2): p. 105-15.

52. Kasper, E.M., et al., *Pyramidal neurons in layer 5 of the rat visual cortex. III. Differential maturation of axon targeting, dendritic morphology, and electrophysiological properties.* J Comp Neurol, 1994. **339**(4): p. 495-518.

53. Feng, G., et al., *Imaging neuronal subsets in transgenic mice expressing multiple spectral variants of GFP.* Neuron, 2000. **28**(1): p. 41-51.

54. Frantz, G.D., et al., *Regulation of the POU domain gene SCIP during cerebral cortical development.* J Neurosci, 1994. **14**(2): p. 472-85.

55. Weimann, J.M., et al., *Cortical neurons require Otx1 for the refinement of exuberant axonal projections to subcortical targets.* Neuron, 1999. **24**(4): p. 819-31.

56. Llinas, R. and K. Walton, *Cerebellum*, in *The synaptic organization of the brain*, G.M. Shepherd, Editor. 1998, Oxford University Press: New York. p. 255-288.

57. Braitenberg, V. and R.P. Atwood, *Morphological observations on the cerebellar cortex.* J Comp Neurol, 1958. **109**(1): p. 1-33.

58. Bayer, S.A., *Hippocampal region.*, in *The Rat Nervous System*, G. Paxinos, Editor. 1985, Academic Press: San Diego. p. 335-352.

59. Gaarskjaer, F.B., *The organization and development of the hippocampal mossy fiber system.* Brain Res, 1986. **396**(4): p. 335-57.

60. Markakis, E.A. and F.H. Gage, *Adult-generated neurons in the dentate gyrus send axonal projections to field CA3 and are surrounded by synaptic vesicles.* J Comp Neurol, 1999. **406**(4): p. 449-60.

61. Petralia, R.S. and R.J. Wenthold, *Light and electron immunocytochemical localization of AMPA-selective glutamate receptors in the rat brain.* J Comp Neurol, 1992. **318**(3): p. 329-54.

62. Geiger, J.R., et al., *Relative abundance of subunit mRNAs determines gating and Ca2+ permeability of AMPA receptors in principal neurons and interneurons in rat CNS.* Neuron, 1995. **15**(1): p. 193-204.

63. Yamazaki, M., et al., *Molecular cloning of a cDNA encoding a novel member of the mouse glutamate receptor channel family.* Biochem Biophys Res Commun, 1992. **183**(2): p. 886-92.

64. Araki, K., et al., *Selective expression of the glutamate receptor channel ?2 subunit in cerebellar Purkinje cells.* Biochemical and Biophysical Research Communications, 1993. **197**(3): p. 1267-1276.

65. Landsend, A.S., et al., *Differential localization of delta glutamate receptors in the rat cerebellum: coexpression with AMPA receptors in parallel fiber-spine synapses and absence from climbing fiber-spine synapses.* J Neurosci, 1997. **17**(2): p. 834-42.

66. Kashiwabuchi, N., et al., *Impairment of motor coordination, Purkinje cell synapse formation, and cerebellar long-term depression in GluR delta 2 mutant mice.* Cell, 1995. **81**(2): p. 245-52.

67. Ito, M., *Cerebellar long-term depression: characterization, signal transduction, and functional roles.* Physiol Rev, 2001. **81**(3): p. 1143-95.

68. Kennedy, M.B., *The postsynaptic density at glutamatergic synapses.* Trends Neurosci, 1997. **20**(6): p. 264-8.

69. Dong, H., et al., *GRIP: a synaptic PDZ domain-containing protein that interacts with AMPA receptors.* Nature, 1997. **386**(6622): p. 279-84.

70. Wyszynski, M., et al., *Association of AMPA receptors with a subset of glutamate receptor-interacting protein in vivo.* J Neurosci, 1999. **19**(15): p. 6528-37.

71. Srivastava, S., et al., *Novel anchorage of GluR2/3 to the postsynaptic density by the AMPA receptor-binding protein ABP.* Neuron, 1998. **21**(3): p. 581-91.

72. Tomita, S., et al., *Dynamic interaction of stargazin-like TARPs with cycling AMPA receptors at synapses.* Science, 2004. **303**(5663): p. 1508-11.

73. Letts, V.A., et al., *The mouse stargazer gene encodes a neuronal Ca2+-channel gamma subunit.* Nat Genet, 1998. **19**(4): p. 340-7.

74. Chen, L., et al., *Stargazin regulates synaptic targeting of AMPA receptors by two distinct mechanisms.* Nature, 2000. **408**(6815): p. 936-43.

75. Shiraishi-Yamaguchi, Y. and T. Furuichi, *The Homer family proteins.* Genome Biol, 2007. **8**(2): p. 206.

76. Bottai, D., et al., *Synaptic activity-induced conversion of intronic to exonic sequence in Homer 1 immediate early gene expression.* J Neurosci, 2002. **22**(1): p. 167-75.

77. Brakeman, P.R., et al., *Homer: a protein that selectively binds metabotropic glutamate receptors.* Nature, 1997. **386**(6622): p. 284-8.

78. Boeckers, T.M., et al., *C-terminal synaptic targeting elements for postsynaptic density proteins ProSAP1/Shank2 and ProSAP2/Shank3.* J Neurochem, 2005. **92**(3): p. 519-24.

79. Uchino, S., et al., *Direct interaction of post-synaptic density-95/Dlg/ZO-1 domain-containing synaptic molecule Shank3 with GluR1 alpha-amino-3-hydroxy-5-methyl-4-isoxazole propionic acid receptor.* J Neurochem, 2006. **97**(4): p. 1203-14.

80. Uemura, T., H. Mori, and M. Mishina, *Direct interaction of GluRdelta2 with Shank scaffold proteins in cerebellar Purkinje cells.* Mol Cell Neurosci, 2004. **26**(2): p. 330-41.

81. Lim, S., et al., *Characterization of the Shank family of synaptic proteins. Multiple genes, alternative splicing, and differential expression in brain and development.* J Biol Chem, 1999. **274**(41): p. 29510-8.

82. Xiao, B., et al., *Homer regulates the association of group 1 metabotropic glutamate receptors with multivalent complexes of homer-related, synaptic proteins.* Neuron, 1998. **21**(4): p. 707-16.

83. Lissin, D.V., et al., *Activity differentially regulates the surface expression of synaptic AMPA and NMDA glutamate receptors.* Proc Natl Acad Sci U S A, 1998. **95**(12): p. 7097-102.

84. Shi, S.H., et al., *Rapid spine delivery and redistribution of AMPA receptors after synaptic NMDA receptor activation.* Science, 1999. **284**(5421): p. 1811-6.

85. Sheng, M. and S. Hyoung Lee, *AMPA receptor trafficking and synaptic plasticity: major unanswered questions.* Neurosci Res, 2003. **46**(2): p. 127-34.

86. Hayashi, Y., et al., *Driving AMPA receptors into synapses by LTP and CaMKII: requirement for GluR1 and PDZ domain interaction.* Science, 2000. **287**(5461): p. 2262-7.

87. Shi, S., et al., *Subunit-specific rules governing AMPA receptor trafficking to synapses in hippocampal pyramidal neurons.* Cell, 2001. **105**(3): p. 331-43.

88. Takahashi, T., K. Svoboda, and R. Malinow, *Experience strengthening transmission by driving AMPA receptors into synapses.* Science, 2003. **299**(5612): p. 1585-8.

89. Henley, J., *Proteins involved in the synaptic organization of AMPA (alpha-amino-3-hydroxy-5-methylisoxazolepropionate) receptors.* Biochem Soc Trans, 2001. **29**(Pt 4): p. 485-8.

90. Braithwaite, S.P., G. Meyer, and J.M. Henley, *Interactions between AMPA receptors and intracellular proteins.* Neuropharmacology, 2000. **39**(6): p. 919-30.

91. Simon, J., et al., *Analysis of the set of GABA(A) receptor genes in the human genome.* J Biol Chem, 2004. **279**(40): p. 41422-35.

92. Chen, S., et al., *Benzodiazepine-mediated regulation of alpha1, alpha2, beta1-3 and gamma2 GABA(A) receptor subunit proteins in the rat brain hippocampus and cortex.* Neuroscience, 1999. **93**(1): p. 33-44.

93. Barnard, E.A., et al., *International Union of Pharmacology. XV. Subtypes of gamma-aminobutyric acidA receptors: classification on the basis of subunit structure and receptor function.* Pharmacol Rev, 1998. **50**(2): p. 291-313.

94. Farrant, M. and Z. Nusser, *Variations on an inhibitory theme: phasic and tonic activation of GABA(A) receptors.* Nat Rev Neurosci, 2005. **6**(3): p. 215-29.

95. Fritschy, J.M., et al., *Independent assembly and subcellular targeting of GABA(A)-receptor subtypes demonstrated in mouse hippocampal and olfactory neurons in vivo.* Neurosci Lett, 1998. **249**(2-3): p. 99-102.

96. Nusser, Z., et al., *Differential synaptic localization of two major gamma-aminobutyric acid type A receptor alpha subunits on hippocampal pyramidal cells.* Proc Natl Acad Sci U S A, 1996. **93**(21): p. 11939-44.

97. Nusser, Z., W. Sieghart, and P. Somogyi, *Segregation of different GABAA receptors to synaptic and extrasynaptic membranes of cerebellar granule cells.* J Neurosci, 1998. **18**(5): p. 1693-703.

98. Sassoe-Pognetto, M., et al., *Colocalization of multiple GABA(A) receptor subtypes with gephyrin at postsynaptic sites.* J Comp Neurol, 2000. **420**(4): p. 481-98.

99. Brickley, S.G., S.G. Cull-Candy, and M. Farrant, *Single-channel properties of synaptic and extrasynaptic GABAA receptors suggest differential targeting of receptor subtypes.* J Neurosci, 1999. **19**(8): p. 2960-73.

100. Wang, H., et al., *GABA(A)-receptor-associated protein links GABA(A) receptors and the cytoskeleton.* Nature, 1999. **397**(6714): p. 69-72.

101. Kittler, J.T., et al., *The subcellular distribution of GABARAP and its ability to interact with NSF suggest a role for this protein in the intracellular transport of GABA(A) receptors.* Mol Cell Neurosci, 2001. **18**(1): p. 13-25.

102. O'Sullivan, G.A., et al., *GABARAP is not essential for GABA receptor targeting to the synapse.* Eur J Neurosci, 2005. **22**(10): p. 2644-8.

103. Kneussel, M., et al., *The gamma-aminobutyric acid type A receptor (GABAAR)-associated protein GABARAP interacts with gephyrin but is not involved in receptor anchoring at the synapse.* Proc Natl Acad Sci U S A, 2000. **97**(15): p. 8594-9.

104. Kittler, J.T., I.L. Arancibia-Carcamo, and S.J. Moss, *Association of GRIP1 with a GABA(A) receptor associated protein suggests a role for GRIP1 at inhibitory synapses.* Biochem Pharmacol, 2004. **68**(8): p. 1649-54.

105. Prior, P., et al., *Primary structure and alternative splice variants of gephyrin, a putative glycine receptor-tubulin linker protein.* Neuron, 1992. **8**(6): p. 1161-70.

106. Sassoe-Pognetto, M. and J.M. Fritschy, *Mini-review: gephyrin, a major postsynaptic protein of GABAergic synapses.* Eur J Neurosci, 2000. **12**(7): p. 2205-10.

107. Tretter, V., et al., *The clustering of GABA(A) receptor subtypes at inhibitory synapses is facilitated via the direct binding of receptor alpha 2 subunits to gephyrin.* J Neurosci, 2008. **28**(6): p. 1356-65.

108. Essrich, C., et al., *Postsynaptic clustering of major GABAA receptor subtypes requires the gamma 2 subunit and gephyrin.* Nat Neurosci, 1998. **1**(7): p. 563-71.

109. Jacob, T.C., et al., *Gephyrin regulates the cell surface dynamics of synaptic GABAA receptors.* J Neurosci, 2005. **25**(45): p. 10469-78.

110. Kneussel, M., et al., *Gephyrin-independent clustering of postsynaptic GABA(A) receptor subtypes.* Mol Cell Neurosci, 2001. **17**(6): p. 973-82.

111. Giesemann, T., et al., *Complex formation between the postsynaptic scaffolding protein gephyrin, profilin, and Mena: a possible link to the microfilament system.* J Neurosci, 2003. **23**(23): p. 8330-9.

112. Charych, E.I., et al., *A four PDZ domain-containing splice variant form of GRIP1 is localized in GABAergic and glutamatergic synapses in the brain.* J Biol Chem, 2004. **279**(37): p. 38978-90.

113. Kanematsu, T., et al., *Role of the PLC-related, catalytically inactive protein p130 in GABA(A) receptor function.* EMBO J, 2002. **21**(5): p. 1004-11.

114. Bedford, F.K., et al., *GABA(A) receptor cell surface number and subunit stability are regulated by the ubiquitin-like protein Plic-1.* Nat Neurosci, 2001. **4**(9): p. 908-16.

115. Beck, M., et al., *Identification, molecular cloning, and characterization of a novel GABAA receptor-associated protein, GRIF-1.* J Biol Chem, 2002. **277**(33): p. 30079-90.

116. Keller, C.A., et al., *The gamma2 subunit of GABA(A) receptors is a substrate for palmitoylation by GODZ.* J Neurosci, 2004. **24**(26): p. 5881-91.

117. Rathenberg, J., J.T. Kittler, and S.J. Moss, *Palmitoylation regulates the clustering and cell surface stability of GABAA receptors.* Mol Cell Neurosci, 2004. **26**(2): p. 251-7.

118. Kittler, J.T., et al., *Constitutive endocytosis of GABAA receptors by an association with the adaptin AP2 complex modulates inhibitory synaptic currents in hippocampal neurons.* J Neurosci, 2000. **20**(21): p. 7972-7.

119. Kittler, J.T., et al., *Phospho-dependent binding of the clathrin AP2 adaptor complex to GABAA receptors regulates the efficacy of inhibitory synaptic transmission.* Proc Natl Acad Sci U S A, 2005. **102**(41): p. 14871-6.

120. Smith, K.R., et al., *Regulation of inhibitory synaptic transmission by a conserved atypical interaction of GABA(A) receptor beta- and gamma-subunits with the clathrin AP2 adaptor.* Neuropharmacology, 2008. **55**(5): p. 844-50.

121. Dalva, M.B., A.C. McClelland, and M.S. Kayser, *Cell adhesion molecules: signalling functions at the synapse.* Nat Rev Neurosci, 2007. **8**(3): p. 206-20.

122. Brose, N., *Synaptic cell adhesion proteins and synaptogenesis in the mammalian central nervous system.* Naturwissenschaften, 1999. **86**(11): p. 516-24.

123. Bellocchio, E.E., et al., *Uptake of glutamate into synaptic vesicles by an inorganic phosphate transporter.* Science, 2000. **289**(5481): p. 957-60.

124. Chaudhry, F.A., et al., *The vesicular GABA transporter, VGAT, localizes to synaptic vesicles in sets of glycinergic as well as GABAergic neurons.* J Neurosci, 1998. **18**(23): p. 9733-50.

125. Crump, F.T., R.T. Fremeau, and A.M. Craig, *Localization of the brain-specific high-affinity l-proline transporter in cultured hippocampal neurons: molecular heterogeneity of synaptic terminals.* Mol Cell Neurosci, 1999. **13**(1): p. 25-39.

126. Dumoulin, A., et al., *Presence of the vesicular inhibitory amino acid transporter in GABAergic and glycinergic synaptic terminal boutons.* J Cell Sci, 1999. **112 (Pt 6)**: p. 811-23.

127. Esclapez, M., et al., *Comparative localization of two forms of glutamic acid decarboxylase and their mRNAs in rat brain supports the concept of functional differences between the forms.* J Neurosci, 1994. **14**(3 Pt 2): p. 1834-55.

128. Minelli, A., et al., *GAT-1, a high-affinity GABA plasma membrane transporter, is localized to neurons and astroglia in the cerebral cortex.* J Neurosci, 1995. **15**(11): p. 7734-46.

129. Ribak, C.E. and R.C. Roberts, *GABAergic synapses in the brain identified with antisera to GABA and its synthesizing enzyme, glutamate decarboxylase.* J Electron Microsc Tech, 1990. **15**(1): p. 34-48.

130. Nusser, Z., W. Sieghart, and I. Mody, *Differential regulation of synaptic GABAA receptors by cAMP-dependent protein kinase in mouse cerebellar and olfactory bulb neurones.* J Physiol, 1999. **521 Pt 2**: p. 421-35.

131. Ango, F., et al., *Ankyrin-based subcellular gradient of neurofascin, an immunoglobulin family protein, directs GABAergic innervation at purkinje axon initial segment.* Cell, 2004. **119**(2): p. 257-72.

132. Nusser, Z., et al., *Cell type and pathway dependence of synaptic AMPA receptor number and variability in the hippocampus.* Neuron, 1998. **21**(3): p. 545-59.

133. Takumi, Y., et al., *Different modes of expression of AMPA and NMDA receptors in hippocampal synapses.* Nat Neurosci, 1999. **2**(7): p. 618-24.

134. Racca, C., et al., *NMDA receptor content of synapses in stratum radiatum of the hippocampal CA1 area.* J Neurosci, 2000. **20**(7): p. 2512-22.

135. Liao, D., et al., *Regulation of morphological postsynaptic silent synapses in developing hippocampal neurons.* Nat Neurosci, 1999. **2**(1): p. 37-43.

136. Scheiffele, P., et al., *Neuroligin expressed in nonneuronal cells triggers presynaptic development in contacting axons.* Cell, 2000. **101**(6): p. 657-69.

137. Graf, E.R., et al., *Neurexins induce differentiation of GABA and glutamate postsynaptic specializations via neuroligins.* Cell, 2004. **119**(7): p. 1013-26.

138. Varoqueaux, F., S. Jamain, and N. Brose, *Neuroligin 2 is exclusively localized to inhibitory synapses.* Eur J Cell Biol, 2004. **83**(9): p. 449-56.

139. Levinson, J.N. and A. El-Husseini, *Building excitatory and inhibitory synapses: balancing neuroligin partnerships.* Neuron, 2005. **48**(2): p. 171-4.

140. Chubykin, A.A., et al., *Activity-dependent validation of excitatory versus inhibitory synapses by neuroligin-1 versus neuroligin-2.* Neuron, 2007. **54**(6): p. 919-31.

141. Sperry, R.W., *CHEMOAFFINITY IN THE ORDERLY GROWTH OF NERVE FIBER PATTERNS AND CONNECTIONS.* Proc Natl Acad Sci U S A, 1963. **50**: p. 703-10.

142. Shen, K. and C.I. Bargmann, *The immunoglobulin superfamily protein SYG-1 determines the location of specific synapses in C. elegans.* Cell, 2003. **112**(5): p. 619-30.

143. Donoviel, D.B., et al., *Proteinuria and perinatal lethality in mice lacking NEPH1, a novel protein with homology to NEPHRIN.* Mol Cell Biol, 2001. **21**(14): p. 4829-36.

144. Barletta, G.M., et al., *Nephrin and Neph1 co-localize at the podocyte foot process intercellular junction and form cis hetero-oligomers.* J Biol Chem, 2003. **278**(21): p. 19266-71.

145. Koekkoek, S.K., et al., *Deletion of FMR1 in Purkinje cells enhances parallel fiber LTD, enlarges spines, and attenuates cerebellar eyelid conditioning in Fragile X syndrome.* Neuron, 2005. **47**(3): p. 339-52.

146. Gong, S., et al., *A gene expression atlas of the central nervous system based on bacterial artificial chromosomes.* Nature, 2003. **425**(6961): p. 917-25.

147. Dunkley, P.R., et al., *A rapid Percoll gradient procedure for isolation of synaptosomes directly from an S1 fraction: homogeneity and morphology of subcellular fractions.* Brain Res, 1988. **441**(1-2): p. 59-71.

148. Allen, T.E., et al., *Association of guide RNA binding protein gBP21 with active RNA editing complexes in Trypanosoma brucei.* Mol Cell Biol, 1998. **18**(10): p. 6014-22.

149. Worlock, A.J., et al., *The use of paramagnetic beads for the detection of major histocompatibility complex class I and class II antigens.* Biotechniques, 1991. **10**(3): p. 310-5.

150. Link, A.J., et al., *Direct analysis of protein complexes using mass spectrometry.* Nat Biotechnol, 1999. **17**(7): p. 676-82.

151. de Hoffman, E. and V. Stroobant, *Mass Spectrometry. Principles and applications.* 2 ed. 2002, New York: John Wiley & Sons, LTD.

152. Gong, S., et al., *Highly efficient modification of bacterial artificial chromosomes (BACs) using novel shuttle vectors containing the R6Kgamma origin of replication*, in *Genome Res*. 2002. p. 1992-8.

153. Cristea, I.M., et al., *Fluorescent proteins as proteomic probes.* Mol Cell Proteomics, 2005. **4**(12): p. 1933-41.

154. Aoki, C., S. Rodrigues, and H. Kurose, *Use of electron microscopy in the detection of adrenergic receptors.* Methods Mol Biol, 2000. **126**: p. 535-63.

155. Cristea, I.M., S.J. Gaskell, and A.D. Whetton, *Proteomics techniques and their application to hematology.* Blood, 2004. **103**(10): p. 3624-34.

156. Krutchinsky, A.N., W. Zhang, and B.T. Chait, *Rapidly switchable matrix-assisted laser desorption/ionization and electrospray quadrupole-time-of-flight mass spectrometry for protein identification*, in *J Am Soc Mass Spectrom*. 2000. p. 493-504.

157. Coon, J.J., et al., *Tandem mass spectrometry for peptide and protein sequence analysis.* Biotechniques, 2005. **38**(4): p. 519, 521, 523.

158. Ito, M., *Control of mental activities by internal models in the cerebellum.* Nat Rev Neurosci, 2008. **9**(4): p. 304-13.

159. Dindot, S.V., et al., *The Angelman syndrome ubiquitin ligase localizes to the synapse and nucleus, and maternal deficiency results in abnormal dendritic spine morphology.* Hum Mol Genet, 2008. **17**(1): p. 111-8.

160. Polleux, F. and J.M. Lauder, *Toward a developmental neurobiology of autism.* Ment Retard Dev Disabil Res Rev, 2004. **10**(4): p. 303-17.

161. Vogel, M.W., et al., *The Lurcher mouse: fresh insights from an old mutant.* Brain Res, 2007. **1140**: p. 4-18.

162. Yuzaki, M., *The delta2 glutamate receptor: 10 years later.* Neurosci Res, 2003. **46**(1): p. 11-22.

163. Adams, J.C. and R.P. Tucker, *The thrombospondin type 1 repeat (TSR) superfamily: diverse proteins with related roles in neuronal development.* Dev Dyn, 2000. **218**(2): p. 280-99.

164. Sallee, J.L., E.S. Wittchen, and K. Burridge, *Regulation of cell adhesion by protein-tyrosine phosphatases: II. Cell-cell adhesion.* J Biol Chem, 2006. **281**(24): p. 16189-92.

165. Kosik, K.S., et al., *Delta-catenin at the synaptic-adherens junction.* Trends Cell Biol, 2005. **15**(3): p. 172-8.

166. Hutcheon, B., J.M. Fritschy, and M.O. Poulter, *Organization of GABA receptor alpha-subunit clustering in the developing rat neocortex and hippocampus.* Eur J Neurosci, 2004. **19**(9): p. 2475-87.

167. Maric, D., et al., *GABAA receptor subunit composition and functional properties of Cl- channels with differential sensitivity to zolpidem in embryonic rat hippocampal cells.* J Neurosci, 1999. **19**(12): p. 4921-37.

168. McKernan, R.M., et al., *GABAA receptor subtypes immunopurified from rat brain with alpha subunit-specific antibodies have unique pharmacological properties.* Neuron, 1991. **7**(4): p. 667-76.

169. Boeckers, T.M., *The postsynaptic density.* Cell Tissue Res, 2006. **326**(2): p. 409-22.

170. Chen, L., et al., *The gamma-aminobutyric acid type A (GABAA) receptor-associated protein (GABARAP) promotes GABAA receptor clustering and modulates the channel kinetics.* Proc Natl Acad Sci U S A, 2000. **97**(21): p. 11557-62.

171. Duggan, M.J., S. Pollard, and F.A. Stephenson, *Immunoaffinity purification of GABAA receptor alpha-subunit iso-oligomers. Demonstration of receptor populations containing alpha 1 alpha 2, alpha 1 alpha 3, and alpha 2 alpha 3 subunit pairs.* J Biol Chem, 1991. **266**(36): p. 24778-84.

172. Sassoe-Pognetto, M., et al., *Postsynaptic colocalization of gephyrin and GABAA receptors.* Ann N Y Acad Sci, 1999. **868**: p. 693-6.

173. Benussi, L., et al., *Progranulin Leu271LeufsX10 is one of the most common FTLD and CBS associated mutations worldwide*, in *Neurobiol Dis*. 2009. p. 379-385.

174. Collins, M.O., et al., *Molecular characterization and comparison of the components and multiprotein complexes in the postsynaptic proteome.* J Neurochem, 2006. **97 Suppl 1**: p. 16-23.

175. Cotman, C.W., M. Nieto-Sampedro, and E.W. Harris, *Synapse replacement in the nervous system of adult vertebrates.* Physiol Rev, 1981. **61**(3): p. 684-784.

176. Jorntell, H. and C. Hansel, *Synaptic memories upside down: bidirectional plasticity at cerebellar parallel fiber-Purkinje cell synapses.* Neuron, 2006. **52**(2): p. 227-38.

177. Di Paolo, G. and P. De Camilli, *Phosphoinositides in cell regulation and membrane dynamics.* Nature, 2006. **443**(7112): p. 651-7.

178. Leung, T., et al., *Myotonic dystrophy kinase-related Cdc42-binding kinase acts as a Cdc42 effector in promoting cytoskeletal reorganization.* Mol Cell Biol, 1998. **18**(1): p. 130-40.

179. Dunah, A.W., et al., *LAR receptor protein tyrosine phosphatases in the development and maintenance of excitatory synapses.* Nat Neurosci, 2005. **8**(4): p. 458-67.

180. Emes, R.D., et al., *Evolutionary expansion and anatomical specialization of synapse proteome complexity.* Nat Neurosci, 2008. **11**(7): p. 799-806.

181. Braithwaite, S.P., H. Xia, and R.C. Malenka, *Differential roles for NSF and GRIP/ABP in AMPA receptor cycling.* Proc Natl Acad Sci U S A, 2002. **99**(10): p. 7096-101.

182. Tomita, S., et al., *Functional studies and distribution define a family of transmembrane AMPA receptor regulatory proteins.* J Cell Biol, 2003. **161**(4): p. 805-16.

183. Harms, K.J., K.R. Tovar, and A.M. Craig, *Synapse-specific regulation of AMPA receptor subunit composition by activity.* J Neurosci, 2005. **25**(27): p. 6379-88.

184. Lee, S.H., A. Simonetta, and M. Sheng, *Subunit rules governing the sorting of internalized AMPA receptors in hippocampal neurons.* Neuron, 2004. **43**(2): p. 221-36.

185. Passafaro, M., V. Piech, and M. Sheng, *Subunit-specific temporal and spatial patterns of AMPA receptor exocytosis in hippocampal neurons.* Nat Neurosci, 2001. **4**(9): p. 917-26.

186. Panicker, S., K. Brown, and R.A. Nicoll, *Synaptic AMPA receptor subunit trafficking is independent of the C terminus in the GluR2-lacking mouse*, in *Proc Natl Acad Sci USA*. 2008. p. 1032-7.

187. Nishimune, A., et al., *NSF binding to GluR2 regulates synaptic transmission.* Neuron, 1998. **21**(1): p. 87-97.

188. Sassoe-Pognetto, M., et al., *Colocalization of gephyrin and GABAA-receptor subunits in the rat retina.* J Comp Neurol, 1995. **357**(1): p. 1-14.

189. Yu, W. and A.L. De Blas, *Gephyrin expression and clustering affects the size of glutamatergic synaptic contacts.* J Neurochem, 2008. **104**(3): p. 830-45.

190. Fritschy, J.M., et al., *Pre- and post-synaptic mechanisms regulating the clustering of type A gamma-aminobutyric acid receptors (GABAA receptors).* Biochem Soc Trans, 2003. **31**(Pt 4): p. 889-92.

191. Schweizer, C., et al., *The gamma 2 subunit of GABA(A) receptors is required for maintenance of receptors at mature synapses.* Mol Cell Neurosci, 2003. **24**(2): p. 442-50.

192. Sudhof, T.C., *Neuroligins and neurexins link synaptic function to cognitive disease.* Nature, 2008. **455**(7215): p. 903-11.

193. Rao, A., K.J. Harms, and A.M. Craig, *Neuroligation: building synapses around the neurexin-neuroligin link.* Nat Neurosci, 2000. **3**(8): p. 747-9.

194. Ichtchenko, K., et al., *Neuroligin 1: a splice site-specific ligand for beta-neurexins.* Cell, 1995. **81**(3): p. 435-43.

195. Levinson, J.N., et al., *Neuroligins mediate excitatory and inhibitory synapse formation: Involvement of PSD-95 and neurexin-1beta in neuroligin induced synaptic specificity.* J Biol Chem, 2005.

196. Kehrer, C., et al., *Altered Excitatory-Inhibitory Balance in the NMDA-Hypofunction Model of Schizophrenia.* Front Mol Neurosci, 2008. **1**: p. 6.

197. Rippon, G., et al., *Disordered connectivity in the autistic brain: challenges for the "new psychophysiology"*, in *International journal of psychophysiology : official journal of the International Organization of Psychophysiology*. 2007. p. 164-72.

198. Fritschy, J.M., *Epilepsy, E/I Balance and GABA(A) Receptor Plasticity.* Front Mol Neurosci, 2008. **1**: p. 5.

199. Fukata, Y., et al., *Molecular constituents of neuronal AMPA receptors.* J Cell Biol, 2005. **169**(3): p. 399-404.

200. Leil, T.A., et al., *GABAA receptor-associated protein traffics GABAA receptors to the plasma membrane in neurons.* J Neurosci, 2004. **24**(50): p. 11429-38.

201. Bausen, M., et al., *The state of the actin cytoskeleton determines its association with gephyrin: role of ena/VASP family members.* Mol Cell Neurosci, 2006. **31**(2): p. 376-86.